uOttawa

L'Université canadienne
Canada's university

FACULTÉ DES ÉTUDES SUPÉRIEURES ET POSTOCTORALES

uOttawa

L'Université canadienne
Canada's university

FACULTY OF GRADUATE AND POSDOCTORAL STUDIES

Omer Salem Ahmed Yagob

AUTEUR DE LA THÈSE / AUTHOR OF THESIS

M.A.Sc. (Civil Engineering)

GRADE / DEGREE

Department of Civil Engineering

FACULTÉ, ÉCOLE, DÉPARTEMENT / FACULTY, SCHOOL, DEPARTMENT

Vulnerability of Buildings to Blast Loads and Progressive Collapse

TITRE DE LA THÈSE / TITLE OF THESIS

Dr. N. Naumoski

DIRECTEUR (DIRECTRICE) DE LA THÈSE / THESIS SUPERVISOR

Dr. M. Saatcioglu

CO-DIRECTEUR (CO-DIRECTRICE) DE LA THÈSE / THESIS CO-SUPERVISOR

EXAMINATEURS (EXAMINATRICES) DE LA THÈSE / THESIS EXAMINERS

Dr. B. Isgor

Dr. B. Martin-Perez

Dr. D. Palermo

Gary W. Slater

Le Doyen de la Faculté des études supérieures et postdoctorales / Dean of the Faculty of Graduate and Postdoctoral Studies

Vulnerability of Buildings to Blast Loads and Progressive Collapse

By

Omer Salem Ahmed Yagob

Thesis submitted to the Faculty of the Graduate and Postdoctoral Studies
in partial fulfillment of the requirements for the M.A.Sc. degree
in Civil Engineering

Department of Civil Engineering
Faculty of Engineering
University of Ottawa

April 2007

Your file Votre référence
ISBN: 978-0-494-32489-9
Our file Notre référence
ISBN: 978-0-494-32489-9

Dedicated to my parents

Acknowledgements

I would like to thank Allah SWT that finally this thesis could be completed. With a deep sense of gratitude, I wish to express my sincere thanks to my supervisor, Dr. Nove Naumoski for his great help, support, understanding and supervising this work. His patience, stimulating suggestions and encouragement helped me to finish this thesis. I also thank my co-supervisor Dr. Murat Saatcioglu for his suggestions, comments and valuable advice that were very helpful in my research.

Thanks to 7th April University (Faculty of Engineering / Sabratha, Libya) and the Libyan Embassy (Libyan Culture Section in Ottawa) for the financial support during my study in Canada. I also want to thank the faculty members and the other employees of the Department of Civil Engineering, University of Ottawa, for their generosity during my studies.

Sincere thanks to Mr. Mohammed Hjaji, Mr. Fathalla Shalouf, Mr. Bona Murty, Mr. Alain Boisvenue, Mr. Mohammad Shooshtari Mr. Shehab Ahmed and Mr. Mohammad Ghorbanie for their help and support. Also, I would like to thank my friends Khalid Tarmissi, Abidallah Albaruni, Basem Elbarouni, and Osama Elaghy for their efforts to help me when needed.

Finally, I owe my special thanks to my parents and my brothers for their faith in me, moral support, and understanding throughout my study. Their love and trust have always inspired me, and their sacrifices will never be forgotten.

Abstract

This study is intended to contribute to the understanding of the behaviour of buildings when subjected to blast loads, and to assess the potential for progressive collapse when columns are lost or severely damaged due to blasts. The objective of the study is twofold, i.e., (i) to investigate the performance of reinforced concrete frame buildings subjected to blast loads, and (ii) to assess the vulnerability of such buildings to progressive collapse.

Two buildings designed for Ottawa in accordance with the 2005 edition of the National Building Code of Canada were used to achieve these objectives. One of the buildings was designed as a moderately ductile, and the other one as a ductile frame building. For the purpose of the first objective, nonlinear time history analyses were conducted to the moderately ductile building for a number of bomb blast scenarios. Blast loads resulting from detonations of 125 kg, 250 kg, and 500 kg TNT at distances of 5, 10, 15, 20, 25 and 30 m from the building were used in the analysis. The performance of the building was assessed by considering the interstorey drifts, displacement ductilities, and curvature ductilities obtained from the analysis. The results from the analyses showed that the building could be severely damaged and even could collapse when subjected to blast loads due to bomb detonations at distances smaller than 15 m from the building.

Regarding the second objective, both the moderately ductile and the ductile buildings were analysed following the guidelines for progressive collapse analysis and design, prepared by the U.S. General Services Administration (GSA). Columns were removed at the first storey of each building. The following three cases were considered: (i) exterior column removed, (ii) corner column removed, and (iii) interior column removed. Elastic static analysis was conducted for each of these cases using 3-D models, and applying loads as required by the GSA guidelines. The demand/capacity ratios obtained from the analysis, and the GSA criteria were used for the assessment of the vulnerability to progressive collapse. The results showed that the ductile building is much more vulnerable to progressive collapse than the moderately ductile building.

Table of Contents

Acknowledgements i

Abstract ii

Table of Contents iii

List of Tables v

List of Figures vi

Chapter 1: Introduction **1**

1.1 Background 1
1.2 Objective and Scope of the Study 2
1.3 Outline of the Thesis 3

Chapter 2: Literature Review **5**

2.1 Literature Related to Blast Load Effects 5
2.2 Literature Related to Progressive Collapse 6

Chapter 3: Blast Loads **9**

3.1 The Blast Process 9
3.2 General Characteristics of Overpressure and Dynamic Pressure 10
3.3 Blast Wave Parameters for Blast Loading 11
3.4 Reference Blast Wave Parameters 12
3.5 Loads on Buildings due to Bomb Explosions 13

Chapter 4: Description and Modelling of Building **21**

4.1 Description of Building 21
4.2 Design of Building 21
4.3 Modeling of the Building for Blast Analysis 24

Chapter 5: Analysis for Blast Loading..... 32

5.1 Blast Load Cases and Load Computation..... 32
5.2 Nonlinear Dynamic Analysis..... 33
5.3 Performance Parameters..... 34
5.4 Computation of Displacement Ductility..... 35
5.5 Computation of Curvature Ductility..... 36
5.6 Discussion of Results..... 37
5.6.1 Interstorey Drifts and Displacement Ductilities..... 37
5.6.2 Column Curvature Ductilities..... 38
5.6.3 Beam Curvature Ductilities..... 39
5.7 Summary..... 40

Chapter 6: Progressive Collapse analysis..... 69

6.1 Introduction..... 69
6.2 Guidelines for Progressive Collapse Prevention..... 70
6.2.1 Structural Configurations for Progressive Collapse Analysis..... 70
6.2.2 Analysis Methods..... 71
6.2.3 Acceptance Criteria..... 71
6.3 Progressive Collapse Analysis..... 72
6.4 Discussion of Results..... 73
6.4.1 Results for Moderately Ductile Frame Building..... 73
6.4.2 Results for Ductile Frame Building..... 74
6.5 Summary..... 75

Chapter 7: Discussion and Conclusions..... 87

7.1 Discussion..... 87
7.2 Observations and Conclusions..... 88
7.2.1 Blast Load Effects..... 88
7.2.2 Progressive Collapse..... 90
7.3 Recommendations for Future Research..... 90

References..... 92

List of Tables

Table 4.1 Gravity loads and properties of concrete and reinforcing steel used in the design..... 26

Table 4.2 Seismic forces on frames..... 26

Table 4.3 Reinforcement in the transverse frames of the moderately ductail building..... 27

Table 4.4 Reinforcement in the transverse frames of the ductail building..... 27

Table 5.1 Overpressures at floor levels of the building for detonation of 125 kg TNT..... 43

Table 5.2 Overpressures at floor levels of the building for detonation of 250 kg TNT..... 43

Table 5.3 Overpressures at floor levels of the building for detonation of 500 kg TNT..... 43

Table 5.4 Duration of overpressures for different detonations and distances..... 44

List of Figures

Figure 1.1 Collapse of Alfred P. Murrah Federal Building, Oklahoma City, due to bomb blast (from the National Academy of Science 1995)..... 4

Figure 1.2 Partial progressive collapse of the Ronan Point Building in London, England (from Shankar 2004)..... 4

Figure 3.1 Variation of pressure with distance at successive times (from ASCE 1985)..... 15

Figure 3.2 Schematic for the variation of overpressure and dynamic pressure with time at a point (from ASCE 1985)..... 15

Figure 3.3 Idealized function of blast overpressure vs. time..... 16

Figure 3.4 Schematic for angles of incidence of blast waves striking a building structure..... 16

Figure 3.5 Variation of reflection coefficient with incident angle and Pressure (from TM5-1300 manual)..... 17

Figure 3.6 Positive phase shock wave parameters for hemispherical TNT detonation on the surface at see level (from TM5-1300 manual)..... 18

Figure 3.7 Blast loading to a rectangular building (From ASCE 1997)..... 19

Figure 3.8 Front façade loading; (a) for $t_c < t_d$ and (b) for $t_c > t_d$ (from ASCE 1997)..... 20

Figure 4.1 Plan of floors and elevation of transverse frames of the building..... 28

Figure 4.2 Seismic design spectrum for Ottawa, for site class C..... 29

Figure 4.3 Design details for interior transverse frame members of The moderately ductile building..... 30

Figure 4.4 Hysteretic moment-rotation model used in DRAIN-2DX..... 31

Figure 5.1 Plan of the building and location of explosion..... 45

Figure 5.2 Blast loads at floor levels..... 45

Figure 5.3 Reflected overpressures, P_r, for detonations of 250 kg TNT at different distances. 46

Figure 5.4 Response time history of roof displacement due to 500 kg TNT detonation at distance of 10 m..... 47

Figure 5.5 Variation of interstorey drift with distance for 500 kg TNT detonation..... 48

Figure 5.6 Moment response of the first storey interior column due to 500 kg TNT detonation at distance of 10 m; (a) time history of the base moment and (b) base moment vs. storey displacement..... 49

Figure 5.7 Schematic for distributions of moments and curvatures in reinforced concrete structural members (from Paulay and Priestley 1992)..... 50

Figure 5.8 Maximum interstorey drifts and displacement ductilities for 125 kg TNT detonation; (a) interstorey drifts and (b) displacement ductilities..... 51

Figure 5.9 Maximum interstorey drifts and displacement ductilities for 250 kg TNT detonation; (a) interstorey drifts and (b) displacement ductilities..... 52

Figure 5.10 Maximum interstorey drifts and displacement ductilities for 500 kg TNT detonation; (a) interstorey drifts and (b) displacement ductilities..... 53

Figure 5.11 Column curvature ductilities for 125 kg TNT detonation at R=5 m..... 54

Figure 5.12 Column curvature ductilities for 250 kg TNT detonation; (a) R=5 m and(b) R=10 m..... 55

Figure 5.13 Column curvature ductilities for 500 kg TNT detonation; (a) R= 5 m and(b) R=10 m..... 56

Figure 5.14 Beam curvature ductilities for 125 kg TNT detonation at R=5 m; (a) exterior beams and (b) interior beams..... 57

Figure 5.15 Beam curvature ductilities for 125 kg TNT detonation at R=10 m; (a) exterior beams and (b) interior beams..... 58

Figure 5.16 Beam curvature ductilities for 250 kg TNT detonation at R=5 m;(a) exterior beams and (b) interior beams..... 59

Figure 5.17 Beam curvature ductilities for 250 kg TNT detonation at R=10 m;(a) exterior beams and (b) interior beams..... 60

Figure 5.18 Beam curvature ductilities for 250 kg TNT detonation at R=15 m; (a) exterior beams and (b) interior beams..... 61

Figure 5.19 Beam curvature ductilities for 250 kg TNT detonation at R=20 m; (a) exterior beams and (b) interior beams..... 62

Figure 5.20 Beam curvature ductilities for 500 kg TNT detonation at R=5 m; (a) exterior beams and (b) interior beams..... 63

Figure 5.21 Beam curvature ductilities for 500 kg TNT detonation at R=10 m; (a) exterior beams and (b) interior beams..... 64

Figure 5.22 Beam curvature ductilities for 500 kg TNT detonation at R=15 m; (a) exterior beams and (b) interior beams..... 65

Figure 5.23 Beam curvature ductilities for 500 kg TNT detonation at R=20 m; (a) exterior beams and (b) interior beams..... 66

Figure 5.24 Beam curvature ductilities for 500 kg TNT detonation at R=25 m;(a) exterior beams and (b) interior beams..... 67

Figure 5.25 Beam curvature ductilities for 500 kg TNT detonation at R=30 m; (a) exterior beams and (b) interior beams..... 68

Figure 6.1 Cases considered in the progressive collapse analysis: (a) exterior column removed, (b) corner column removed, and (c) interior column removed..... 76

Figure 6.2 Schematic for the loads for Case 3 of the progressive collapse analysis..... 77

Figure 6.3 Demand/capacity ratios for Case 1 of the progressive collapse analysis of the moderately ductile building: (a) longitudinal frame and (b) transverse frame..... 78

Figure 6.4 Demand/capacity ratios for Case 2 of the progressive collapse analysis of the moderately ductile building: (a) longitudinal frame and (b) transverse frame..... 79

Figure 6.5 Demand/capacity ratios for Case 3 of the progressive collapse analysis of the moderately ductile building: (a) longitudinal frame and (b) transverse frame..... 80

Figure 6.6 Displacements for Case 1 of the progressive collapse analysis:
(a) longitudinal frame and (b) transverse frame..... 81

Figure 6.7 Displacements for Case 2 of the progressive collapse analysis:
(a) longitudinal frame and (b) transverse frame..... 82

Figure 6.8 Displacements for Case 3 of the progressive collapse analysis:
(a) longitudinal frame and (b) transverse frame..... 83

Figure 6.9 Demand/capacity ratios for Case 1 of the progressive collapse
analysis of the ductile building: (a) longitudinal frame and (b) transverse frame..... 84

Figure 6.10 Demand/capacity ratios for Case 2 of the progressive collapse
analysis of the ductile building: (a) longitudinal frame and (b) transverse frame..... 85

Figure 6.11 Demand/capacity ratios for Case 3 of the progressive collapse
analysis of the ductile building: (a) longitudinal frame and (b) transverse frame..... 86

Chapter 1

Introduction

1.1 Background

Terrorist attacks by bombs have been conducted many times in the past, worldwide. However, the number of such attacks has grown dramatically in recent years. Many embassies, commercial centres, governmental buildings, industrial facilities, and residential buildings have been attacked during the last decade. Various explosive devices have been used during these attacks. The biggest devastations have been caused by explosive devices loaded on vehicles (i.e., car bombs). The most notable attacks in North America using car bombs were those on the World Trade Centre Tower in New York City on February 26, 1993, and on the Alfred P. Murrah Federal Building in Oklahoma City on April 19, 1995 (Fig. 1.1) (National Academy of Science 1995). During the bomb detonation in the underground garage of the World Trade Centre, six people were killed and many other were injured. The devastation was much bigger in Oklahoma City, where the bombing resulted in 168 deaths and hundreds of injuries. The bomb was placed about five meters away from the building and caused a collapse of one side of the building.

The effects of a bomb explosion on a given structure depend on many factors, including:

- the type and size of the bomb,
- location of the explosion centre relative to the structure (e.g. internal or external explosion),
- distance between the explosion centre and the structure,

- location of the explosion centre within the building, for internal explosions (basement or at higher floors, close to walls or columns, etc),
- type of the structure (reinforced concrete, steel, or masonry structure),
- type of the structural system (moment resisting, shear wall, or combined frame-shear wall structural system, reinforced or unreinforced masonry, infill masonry wall system, etc.),
- height of the structure, and
- design considerations for blast and/or other dynamic effects during the design or strengthening of the structure.

Each of these factors separately and in combination with the other factors has a significant effect on the performance of the structure during a bomb blast.

Another issue related to blast loads is the progressive collapse. Bomb blast can cause damage to a critical member of the structural system, that can result in a progressive failure of other members, and to partial or total collapse of the structure. One of the first cases for progressive collapse was the partial collapse of the Ronan Point apartment building in London, England (Fig. 1.2) which is considered as an important case in the consideration of the progressive collapse.

1.2 Objective and Scope of the Study

The objective of this study is twofold:

- to investigate the performance of reinforced concrete frame buildings subjected to blast loads, and
- to assess the vulnerability of such buildings to progressive collapse.

Two buildings designed for Ottawa in accordance with the National Building Code of Canada (NBCC 2005) were used to achieve these objectives. One of the buildings was designed as a moderately ductile, and the other one as a ductile frame building. For the purpose of the first objective, nonlinear time history analyses were conducted to the moderately ductile building for a number of bomb blast scenarios. The performance of the building was assessed by considering the interstorey drifts, displacement ductilities, and curvature ductilities obtained from the analyses.

Regarding the second objective, both the moderately ductile and the ductile building were analysed following the General Services Administration guidelines (GSA 2003) for progressive collapse analysis and design of new federal office buildings. The vulnerability of the buildings to progressive collapse was assessed by considering the demand/capacity ratios for the structural members, as required by the GSA guidelines.

1.3 Outline of the Thesis

The material from the study is presented in six chapters. Chapter 2 reviews the available literature related to blast loads and progressive collapse.

The major characteristic of blast waves and the overpressures resulting from blasts are discussed in Chapter 3. This chapter also discusses the calculation of blast loads for use in the analysis of building structures.

Chapter 4 describes the design of the moderately ductile and the ductile building used in the analysis. Modelling of the buildings for use in the nonlinear analysis program DRAIN-2DX (Prakash et al. 1993) is described in this chapter. The main features of the DRAIN-2DX program are also presented.

Chapter 5 presents the method for nonlinear dynamic analysis of buildings subjected to blast loads. The different detonation scenarios used in the analysis are also discussed. The results from the nonlinear dynamic analysis of the moderately ductile building are described in details.

Chapter 6 provides an overview of the existing guidelines for progressive collapse analysis. The analysis for progressive collapse of the moderately ductile and the ductile buildings are discussed. The results from the analysis are presented.

Finally, Chapter 7 presents the major observations and conclusions based on the results for the study.

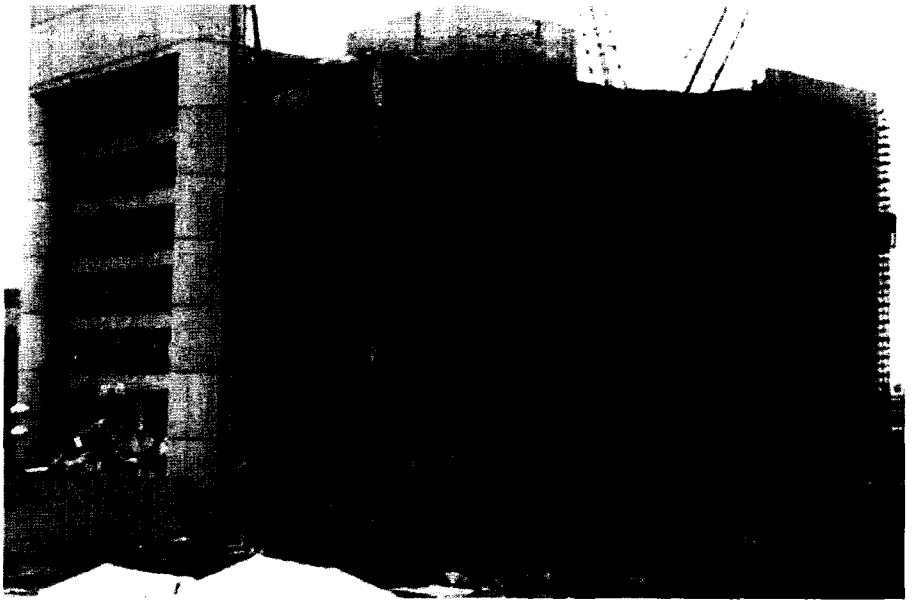

Figure 1.1 Collapse of Alfred P. Murrah Federal Building, Oklahoma City, due to bomb blast (from the National Academy of Science 1995).

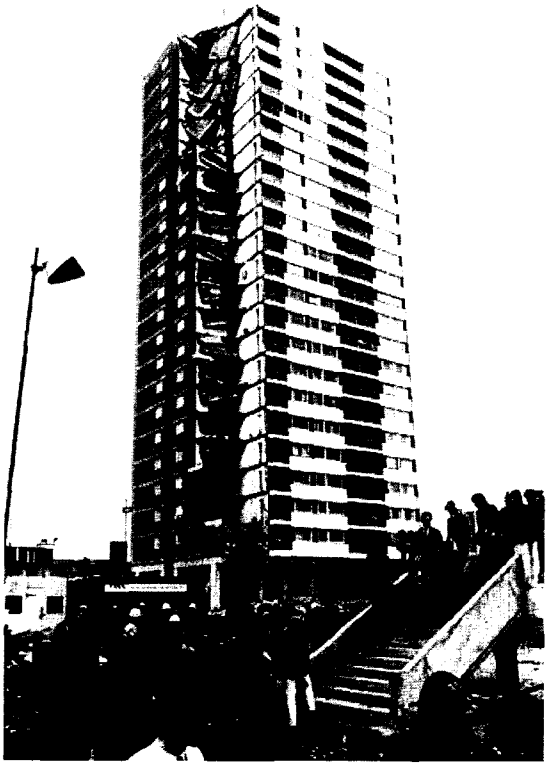

Figure 1.2 Partial progressive collapse of the Ronan Point Building in London, England (from Shankar 2004).

Chapter 2

Literature Review

2.1 Literature Related to Blast Load Effects

There are numerous references on the blast and the blast loads on building structures. The most important references on these issues are presented briefly hereafter.

One of the most useful documents related to the design of blast loads is the TM5-1300 Manual entitled "Structures to resist the effects of accidental explosions" (NAVFAC 1990). This manual was jointly prepared by the U.S. Departments of Army, Navy and Air Force. It represents a state-of-the-art document and provides guidelines for the design of different types of structures subjected to blast loads. Various charts for determining the blast loads, and for the design of structures subjected to such loads are included in this document.

Biggs (1964) provides the basis for the dynamic behaviour of structural members subjected to blast loads. The design of structural components (beams, slabs, and columns) subjected to blast loads is discussed in detail. This represents the basis for the so-called "member by member" design approach, that is the most suitable for practical design.

Baker (1973) describes the most important characteristics of blast waves, which are important to be understood in the design of structures under blast loads.

Longinow and Mniszewski (1996) discuss the protection of buildings against bomb attacks. They describe the damage mechanisms manifested by solid phase explosions and provide suggestions on steps to reduce damage and casualties in buildings subjected to such attacks. The authors suggest the use of redundant framing systems, e.g., steel and concrete moment resistant frame structural systems, to redistribute the loads when a part of the structure (beam or a column) is damaged by the blast and to prevent progressive collapse.

They also suggest that the floor system should be properly designed to resist upward blast loads.

Corley at al. (1998) summarize the findings of a team of engineers that investigated the damage caused by the bombing of Alfred P. Murrah Federal Building in Oklahoma City. They also provide recommendations for the design and construction of new federal buildings. It is suggested that special moment frame detailing would be more effective against blast loading than would an ordinary moment frame. The authors also provide suggestions for preventing progressive collapse. It is emphasized that the redundancy is the most important feature to prevent progressive collapse due to bomb blast. It is also noted that the seismic detailing requirements for regions of high seismic risk in the structural design could provide blast protection.

In addition to the foregoing literature, there are several manuals prepared by the American Society of Civil Engineers (ASCE). The most important of these are the ASCE Manual No. 42 – "Design of Structures to Resist Nuclear Weapons Effects" (ASCE 1985), the manual "Design of blast resistant buildings in petrochemical facilities" (ASCE 1997), and the manual "Structural design for physical security – state of the practice" (ASCE 1999).

A review of the available manuals for blast load design is given in the report entitled "Protecting buildings from bomb damage" (National Academy Press, 1995). This report also summarizes the major subjects of each manual.

2.2 Literature Related to Progressive Collapse

The issue on progressive collapse was triggered by the partial collapse of a 23 storey apartment building in eastern London, England (known as Ronan Point) as a result of explosion at the 18^{th} floor. The explosion was considered as a relatively small accidental explosion that resulted from a build up of gas from a family cooker. However, it was sufficient to blow outwards the outer panels of the kitchen (i.e., the panels on the façade, on the corner of the building) (Shankar 2004). As a result of this, the continuity of the load path (vertically) was lost, which caused collapse of the entire corner of the building.

There are numerous technical papers regarding to progressive collapse. A number of these papers deal with specific cases for progressive collapse such as the Ronan Point collapse, and the collapse of the Alfred P. Murrah Building in Oklahoma City.

Corley et al. (1998) summarize the findings of the Building Performance Assessment Team that investigated the damage caused by the bombing of the Alfred P. Murah Building. The authors also provide recommendations for the design and construction of new federal buildings. They suggest that special moment frame detailing would be more effective against blast loading (and progressive collapse) than would be an ordinary moment resisting frame.

Shankar (2004) also discusses the progressive collapse of the Ronnan Point apartment building and the Alfred P. Murrah building. The author reviews various U.S. codes and standards for the reduction of the risks from progressive collapse.

McGuire (1974) discusses the problem of progressive collapse and measures for its prevention. Differences between traditional and newer structures, and the existing state of design codes (in 1970's) are reviewed with specific reference to the collapse of the Ronan Point apartment building. The changes in the United Kingdom code following the incident and the criteria adopted thereafter to the design to resist progressive collapse also are discussed.

Burnett (1975) studied the provisions related to progressive collapse including those of the United Kingdom, Sweden, Denmark, Germany, Netherland, Canada, France and Eastern Europe. The various provisions are discussed individually for their content, background, and interpretation. A discussion is given on the problems in the implementation of both the building provisions and the design for prevention of progressive collapse.

One of the most important documents related to progressive collapse is prepared by the U.S. General Services Administration, entitled "Progressive collapse analysis and design guidelines" (GSA 2003). These guidelines are specifically prepared for new federal office buildings and major modernization projects. This document describes in detail the methods for the analysis for progressive collapse, the loads for use in the analysis, and the acceptance criteria for progressive collapse. The issues related to the prevention of progressive collapse are discussed for reinforced concrete and steel building structures. In general, this is a very useful document for the design of new buildings to resist progressive collapse, and for the evaluation of the risk from progressive collapse for existing buildings.

The U.S. Department of Defence published a document entitled "Design of buildings to resist progressive collapse" in the frame of the Unified Facilities Criteria (UFC). This document was jointly prepared by the U.S. Army Corps of Engineers, the Naval facilities

Engineering Command, and the Air Force Civil Engineer Support Agency. While it was prepared for military facilities, it is very useful for the design of civilian structures. As the GSA guidelines, the UFC document provides specifications for the loading, analysis, and design of building structures to resist progressive collapse.

Chapter 3

Blast Loads

3.1 The Blast Process

An explosion is caused by a sudden and rapid release of a large amount of energy. Explosions can be categorized as physical, nuclear, or chemical events. An example of a physical explosion is the failure of a tank with compressed gas. Nuclear explosions result from the release of energy due to nuclear reactions.

The chemical explosion, which is primarily used in terrorist attacks, involves chemical reaction of flammable materials (i.e. the explosive materials) that are parts of the explosive compound. The explosive materials in chemical explosions, that are used in terrorist bombings are usually high explosives, and are either solids or liquids. In general, only a portion of the total mass of the explosive is involved in the detonation process. The remainder of the mass is usually consumed by deflagration resulting in a large amount of the material's chemical energy being dissipated as thermal energy, which in turn may cause fires.

When a high explosive is detonated, the following sequence of events occurs. First, the explosion reaction generates a hot gas which can be at a pressure of 100 to 300 kilobar (kb) and with a temperature of about 3000 to 4000°C (Mays and Smith 1995) [1 bar = 100 kPa]. A violent expansion of this gas then occurs and the surrounding air is pushed out of the volume it occupies. As a consequence, a layer of compressed air, that is called the shock or blast wave, forms in front of this gas containing most of the energy released by the explosion. The blast wave propagates outward in all directions from the explosion centre. The front of the wave, called the shock front, is like a wall of highly compressed air, and moves outward from the explosion centre at a very high speed. The pressure of the air of the shock front

(called *incident* pressure) is much greater than that in the region behind it. The velocity and the peak pressure of the shock front decrease very rapidly as the shock front propagates outward (Fig. 3.1).

3.2 General Characteristics of Overpressure and Dynamic Pressure

The transient pressure greater than the ambient (surrounding atmospheric) pressure is defined as the *overpressure*. As the shock front arrives at a given point, the overpressure at that point rapidly increases from zero to the peak (i.e., maximum) overpressure. If nothing interferes with the blast wave, the rise time to peak overpressure will be less than a microsecond. The magnitude of the peak overpressure and the variation of the overpressure with time depend on the type and amount of explosive, the height of the explosion above the ground surface, and the distance from the explosion.

As the blast wave moves outward from the explosion, the flow of the mass air behind the shock front produces a wind. The resulting pressure is called *dynamic pressure*. It depends on the incident pressure (i.e., the quantity of the explosive), the density of the air through which the blast wave passes, and the wind velocity behind the shock front.

Figure 3.2 shows qualitatively the variations with time of the overpressure and the dynamic pressure. A finite time elapses between the detonation and the arrival of the shock front at a given location. This time of arrival depends on the type and quantity of the explosive, and the distance from the explosion centre.

As can be seen in Fig. 3.2, the duration of the blast wave is characterized by two distinct phases, the positive and the negative. During the first (i.e., the positive) phase, the overpressure rises very rapidly from the ambient (atmospheric) pressure to the peak value, and then decreases slowly reaching the ambient pressure once again. In the second (i.e., the negative) phase, a vacuum is created and the air is sucked in, resulting in underpressure (i.e., smaller pressure than the normal atmospheric pressure). Consequently, the wind blows toward the point of the detonation during the negative phase. The peak value of the underpressure is much smaller than that of the overpressure.

Given the uncertainties in the estimation of the overpressure, the overpressure function is approximated in this study as shown in Fig. 3.3. The negative phase is neglected

because its effects are very small compared to those of the positive phase. The load function illustrated in Fig. 3.3 was used in all the analyses conducted in this study.

3.3 Blast Wave Parameters for Blast Loading

Some of the parameters of a blast wave are shown in Fig. 3.2. The parameters that are used in the estimation of the blast loading are as follows:

- Peak positive overpressure, P_{so} (also called peak *side-on* overpressure, or incident overpressure); this is the maximum overpressure when the shock front approaches a given location.
- Positive phase impulse, I_o; it is the area under the positive overpressure-time curve (Fig. 3.2)
- Duration of the positive phase, t_d
- Peak dynamic (blast wind) overpressure, q_o
- Peak reflected overpressure, P_r
- Shock front velocity, U
- Blast wave length, L_w; for low overpressures, $L_w = U\ t_d$.

All these parameters can be determined from standard charts available in the literature that are discussed in Section 3.4. Among these parameters, the peak reflected overpressure, P_r, is of special importance when blast loads are considered, and this parameter is discussed in more details hereafter.

The blast wave travels as an incident wave until it strikes a solid surface or an object. Upon striking such a surface, a reflection of the incident wave occurs, and the surface experiences much higher overpressure than that of the incident wave. This overpressure is called *reflected overpressure* because it is due to the reflection of the blast wave. The reflection of blast waves is a very complex problem. However, for the purpose of determining the loads due to blast effects, only the basic features of the blast wave reflection are needed, and these are discussed hereafter. Detailed discussions on the reflection of blast waves are given in Baker (1973).

The biggest effect on the reflected overpressure has the *angle of incidence*. Figure 3.4 shows schematically the angles of incidence of blast waves striking a building structure. As

shown in the figure, the angle of incidence represents the angle between the line from the centre of explosion to the point on the surface considered, and the line through the centre of the explosion perpendicular to the surface. This is the same as the angle between the reflective surface and the tangent of the blast wave at the point considered.

For simplicity, the angle of incidence, α, is assumed 0^o for the front façade, and 90^o for the side façade. The largest reflected overpressures are associated with angles of incidence of about zero degrees. The peak overpressure of the reflected wave for an angle of incidence of 0^o is called *normally reflected* peak overpressure or *face-on* overpressure. There is no reflection for an angle of incidence of 90^o, and the overpressure on the surface is that of the incident overpressure, i.e., the side-on overpressure. Regular reflections occur for angles of incidence of 0^o to approximately 40^o. For angles of incidence larger than 40^o, the so-called Mach reflection occurs, which is a very complex phenomenon (Baker 1973). The peak reflected overpressures, P_r, are calculated by amplifying the peak overpressure, P_{so}, i.e.

$$P_r = C_r P_{so} \tag{3.1}$$

where C_r represents the reflection coefficient of the blast wave. This coefficient depends on the peak overpressure and the angle of incidence of the wave front. Diagrams for determining reflection coefficients are available in the literature. Figure 3.5 shows curves for reflection coefficients for angles of incidence from 0^o to 90^o, and for different peak overpressures.

3.4 Reference Blast Wave Parameters

Based on experimental and theoretical investigations, diagrams for determining the values of all foregoing parameters are available in the literature. These diagrams are usually given in terms of a scaled weight of TNT (tri-nitro-toluene). The diagrams for TNT explosive represent *reference diagrams* and can be used for determining blast wave parameters for other types of explosives. Figure 3.6 illustrates reference diagrams for an explosion on the surface at see level. A separate curve is given for each blast wave parameter as a function of the scaled distance $Z = R/W^{1/3}$, where R is the distance from the explosion in ft, and W is the mass of TNT in lb (mass). The units of the parameters are shown at the figure. Note that only the curves for the positive overpressure, P_{so}, the reflected overpressure, P_r, and the shock

front velocity, U, are not scaled. The curves for all other parameters are scaled to $W^{1/3}$. It is also important to mention that the curve for P_r represents normally reflected overpressure (i.e., reflected overpressure for angle of incidence of 0^o (see Figs. 3.4 and 3.5).

To determine the blast wave parameters for another type of explosive, it is necessary to convert the mass of that explosive into a TNT equivalent mass. This can be done by multiplying the mass of the explosive by a corresponding conversion factor. For a given explosive, the conversion factor represents the ratio of the specific energy of that explosive to the specific energy of TNT. Conversion factors for different types of explosives are available in the literature (e.g. ASCE 1999; Mays and Smith 1995).

3.5 Loads on Buildings due to Bomb Explosions

When an explosion blast wave strikes a building, the building is loaded by the overpressure and drag forces of the blast wave. The interaction between the blast wave and a building structure is very complex. For practical applications, the blast loading is simplified as illustrated in Fig. 3.7.

Methods are available for determining blast loads acting on a building for a specified location of explosion. The magnitudes and time histories of the loads depend on the orientation of the building relative to the detonation centre. The loads are usually referred to as the front facade, side facade, rear façade, and roof loads (ASCE 1997). Among these loads, of interest for this study is the front façade load and it is discussed hereafter. Details for the other loadings are given in ASCE (1997).

When a blast wave strikes the front façade of a building, normal reflection occurs and the entire front façade is instantly subjected to reflected overpressure. The reflected overpressure is substantially larger than the overpressure in the immediate surroundings. Consequently, there is a flow of air from the region of high pressure to the one at low pressure. For practical applications, the load per unit area of the front face of a building structure is simplified as illustrated in Fig. 3.8(a). It can be seen in the figure that the reflected overpressure decreases from the peak reflected overpressure at time zero, to the so-called "stagnation" overpressure at time t_c that is known as "clearing time" (see Fig. 3.7). The expression for the stagnation overpressure, P_s, (according to ASCE 1997) is as follows:

$$P_s = P_{so} + C_d q_o \tag{3.2}$$

where P_{so} is the incident (side-on) overpressure, q_o is the peak dynamic wind overpressure, and C_d is the drag coefficient. For the front façade of a building, the drag coefficient $C_d = 1$ (ASCE 1997; Mays and Smith, 1995; ASCE manual No. 42, 1985). The expression for the time t_c (according to ASCE (1997) and ASCE manual No. 42 (1985)) is as follows:

$$t_c = 3S / U < t_d \tag{3.3}$$

where,

S = clearing distance (the smaller of H or B/2; see Fig. 3.7),

H = height of the building, and

B = width of the building.

If t_c is larger than t_d, then the front wall load is a triangular load as shown in Fig. 3.8(b).

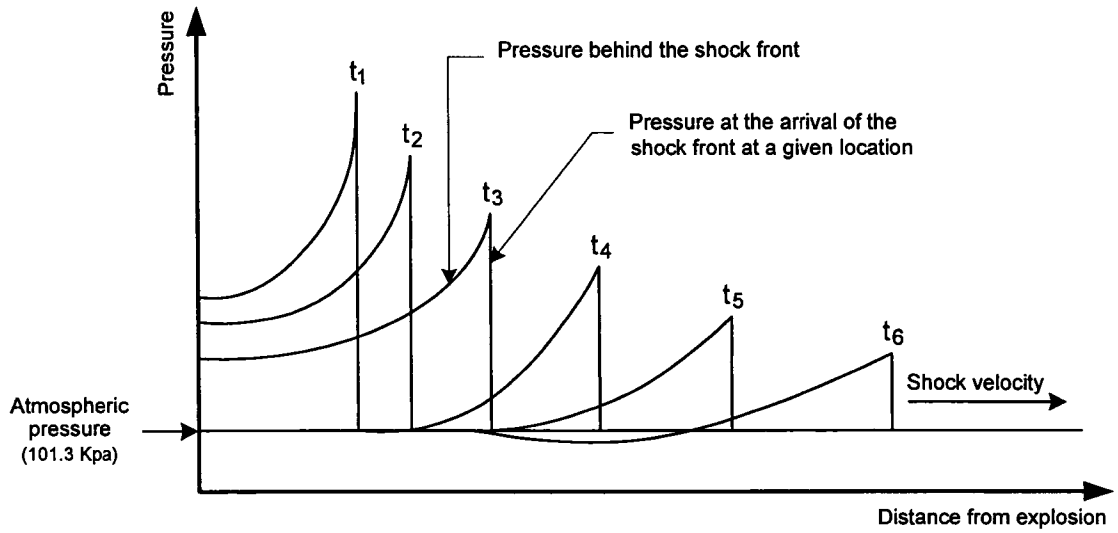

Figure 3.1 Variation of pressure with distance at successive times (from ASCE 1985).

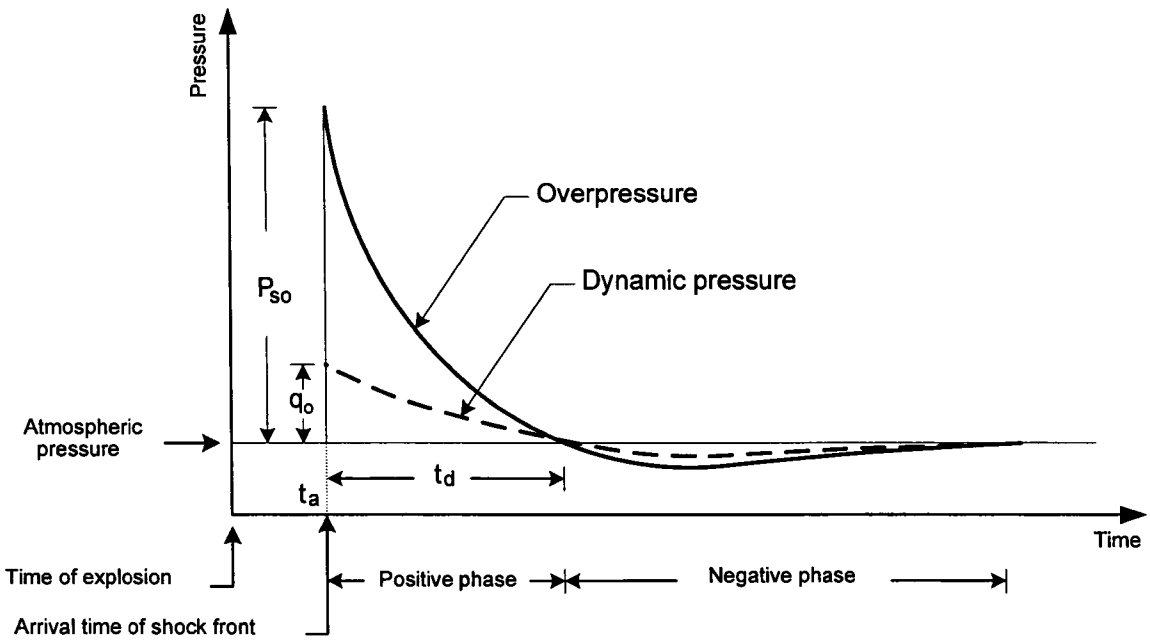

Figure 3.2 Schematic for the variation of overpressure and dynamic pressure with time at a point (from ASCE 1985).

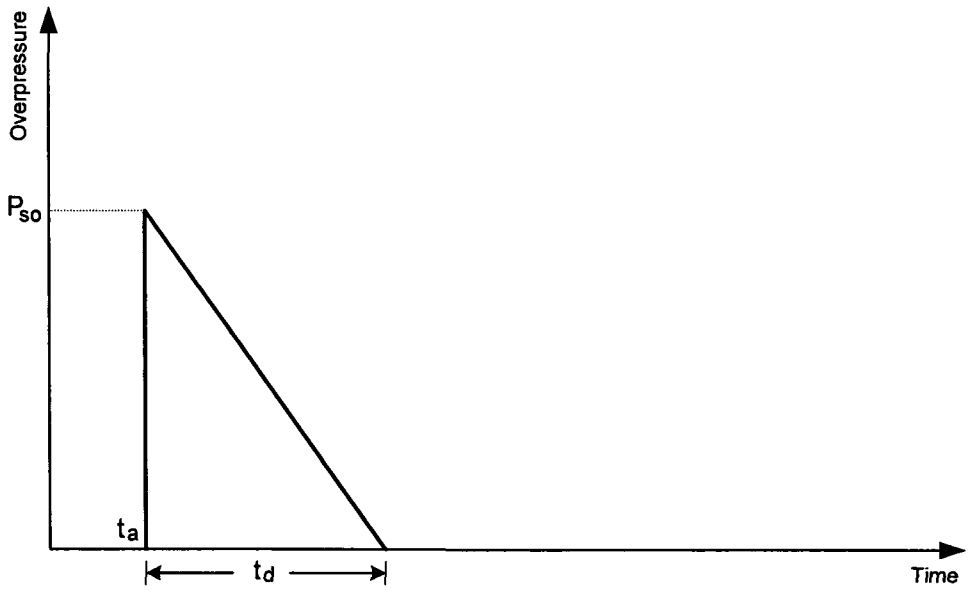

Figure 3.3 Idealized function of blast overpressure vs. time.

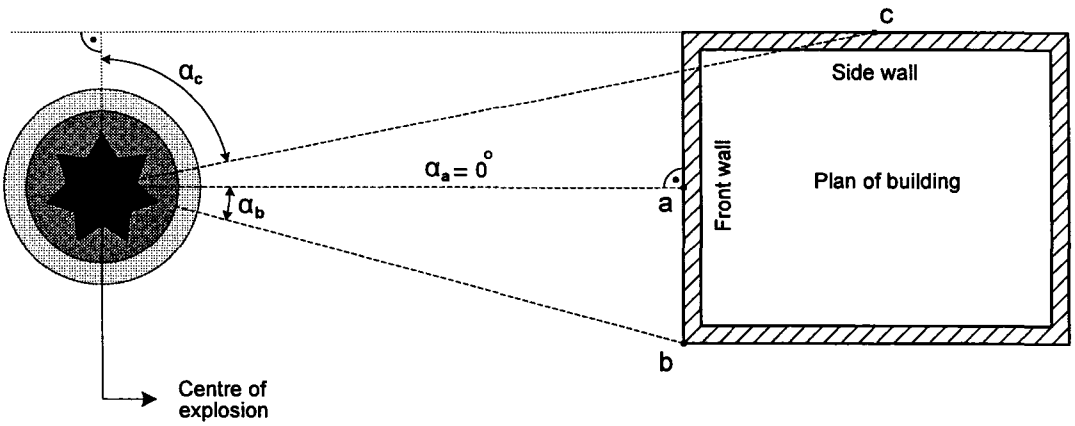

Figure 3.4 Schematic for angles of incidence of blast waves striking a building structure.

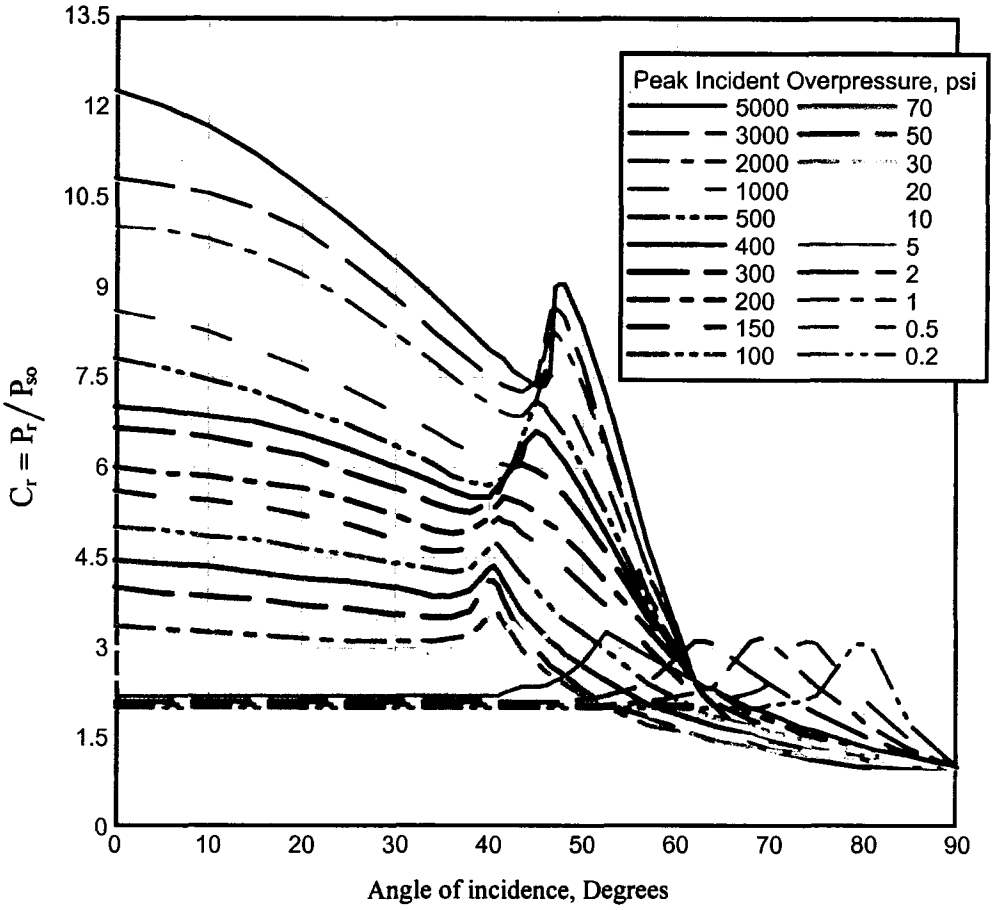

Figure 3.5 Variation of reflection coefficient with incident angle and pressure. (from TM5-1300 manual).

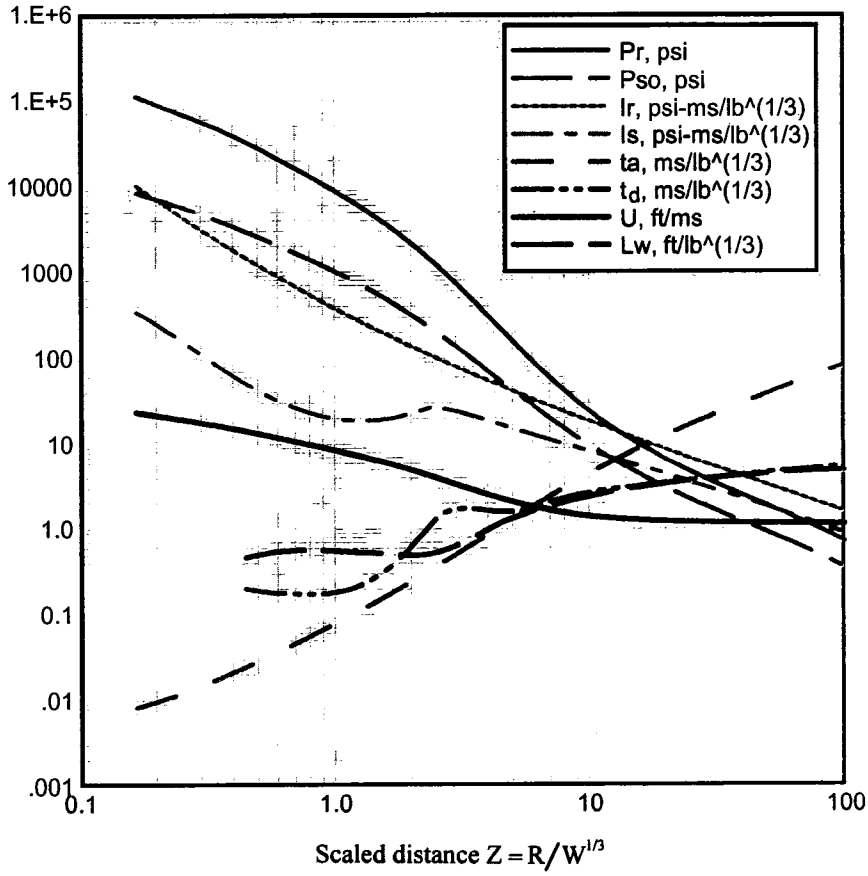

Figure 3.6 Positive phase shock wave parameters for hemispherical TNT detonation on the surface at see level (from TM5-1300 manual).

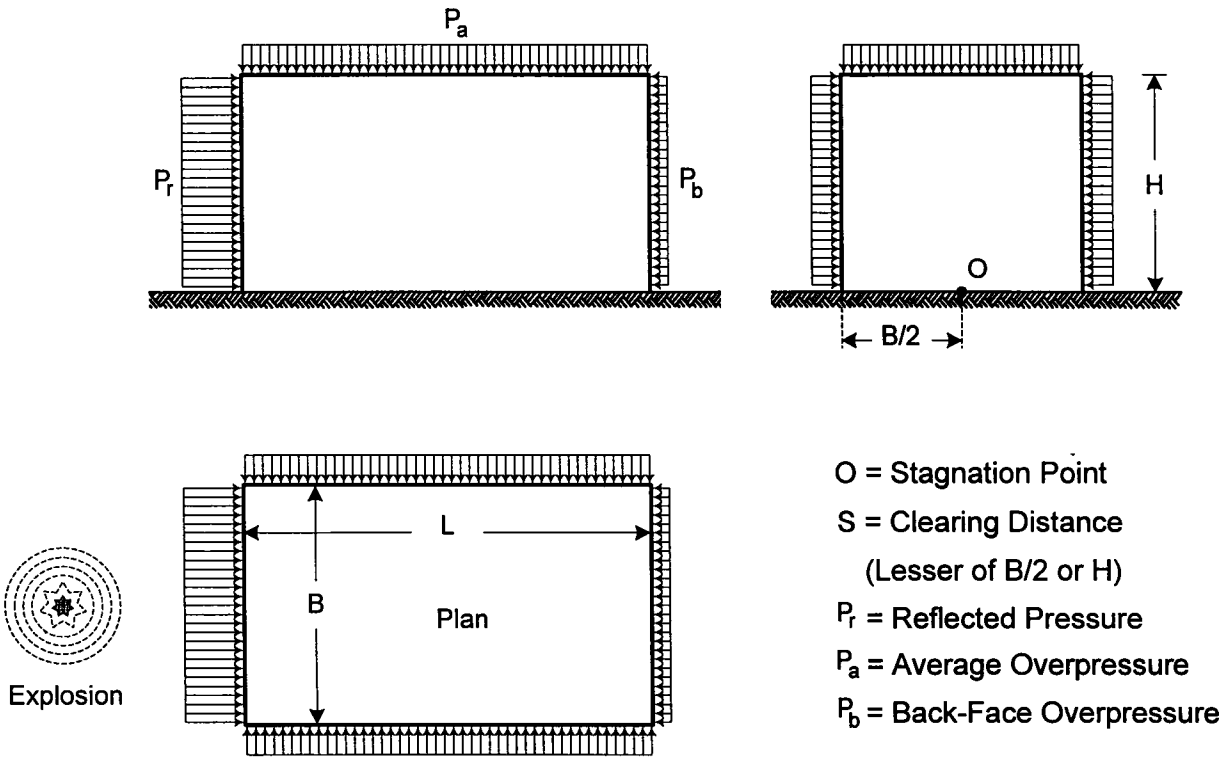

Figure 3.7 Blast loading to a rectangular building (from ASCE 1997).

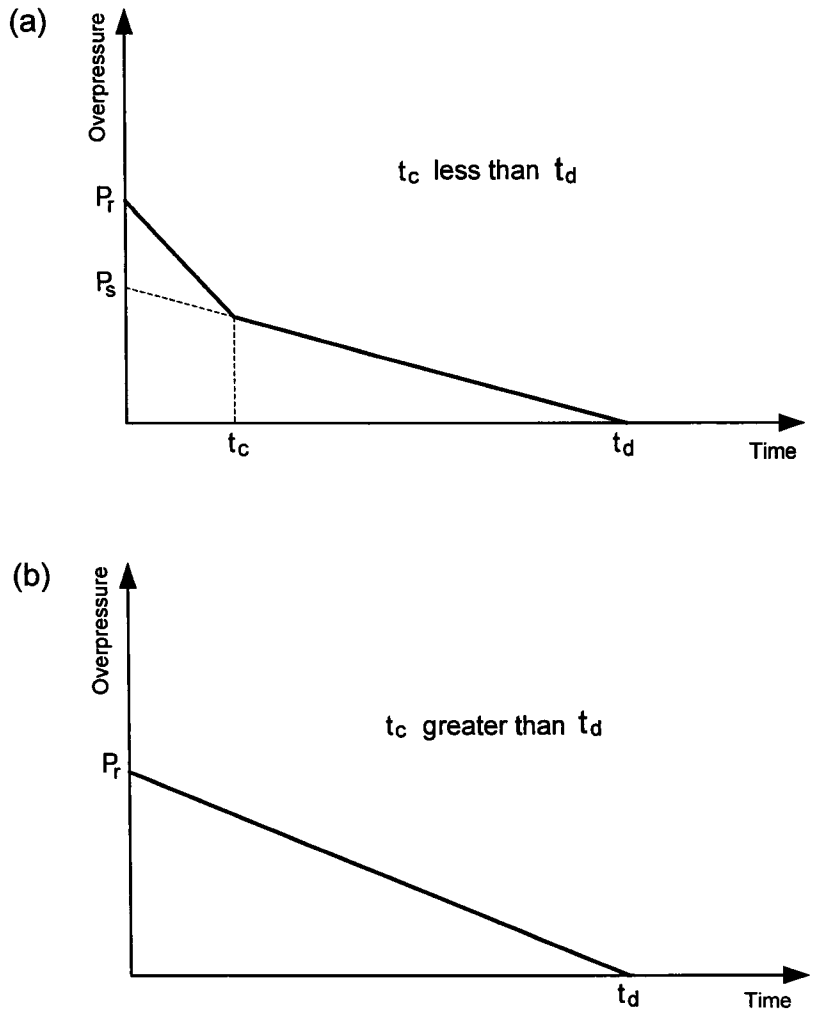

Figure 3.8 Front façade loading; (a) for $t_c < t_d$ and (b) for $t_c > t_d$ (from ASCE 1997).

Chapter 4

Description and Modelling of Building

4.1 Description of Building

The plan and the elevation of the building used in this study are shown in Figure 4.1. It is a ten storey reinforced concrete frame building located in Ottawa. The building is designed as an office building. In plan, there are 6 spans in the longitudinal direction, and 3 spans in the transverse direction. The length of the spans in both the longitudinal and transverse directions is 6 m. The height of the storeys is 4 m.

The lateral load resisting system consists of moment resisting frames. There are 6 frames in the transverse direction, and 4 frames in the longitudinal direction (Fig. 4.1). In Fig. 4.1, Te and Ti indicate transverse exterior and transverse interior frames respectively, and Le and Li indicate longitudinal exterior and longitudinal interior frames respectively.

4.2 Design of Building

The building was originally designed by Dincer (2003) following the seismic provisions of the 2005 edition of the National Building Code of Canada (NBCC 2005). In the original design the building was considered as a *moderately ductile* moment resisting frame building. For the purpose of this study, the building was redesigned. Two designs were conducted: (i) as a moderately ductile moment resisting frame building, and (ii) as a ductile moment resisting frame building. The design of the moderately ductile building was done primarily to check the original design, and as discussed later in this section, the original design was found to be quite accurate.

The gravity loads and the properties of the concrete and reinforcing steel used in the design are shown in Table (4.1). These are the same as those used in the original design conducted by Dincer (2003). As shown in the table, concrete compressive strength $f_c' = 30$ MPa, and reinforcement yield strength $f_y = 400$ MPa were used.

The design was conducted using the equivalent static force procedure. This procedure is appropriate for the building considered, since it is a regular building, its height is less than 60 m, and the fundamental period is less than 2.0 s (Clause 4.1.8.7 of NBCC 2005). The total seismic base shear was computed using the code equation (Clause 4.1.8.11 of NBCC 2005):

$$V = S(T_a)M_v I_e W/(R_d R_o) \quad (4.1)$$

where,

T_a is the fundamental period of the building, which was computed using the equation $T_a=0.075(h_n)^{3/4}$ (Clause 4.1.8.11.(3)(a). Since the total height of the building $h_n=40$ m, the fundamental period is $T_a=0.075 \times 40^{3/4} = 1.2$ s.

$S(T_a)$ is the design spectral acceleration corresponding to the fundamental period of the building, T_a. Using the seismic design spectrum for Ottawa, for site class C (Fig. 4.2), the value for $S(T_a)=S(1.2\text{ s})=0.12$ g.

M_v is the higher mode effects factor, and has a value of 1.0 based on Table 4.1.8.11 for $S_a(0.2)/S_a(2.0) > 8.0$.

I_e is the importance factor, which was taken to be 1.0 since the building is of normal importance (Table 4.1.8.5 in NBCC 2005)

W is the total dead load (i.e., total weight of the building), which was W=32 616 kN.

R_d is the ductility related force modification factor. The values for R_d used in the design were $R_d=2.5$ for moderately ductile reinforced concrete frames, and $R_d=4.0$ for ductile frames (Table 4.1.8.9 in NBCC 2005).

R_o is the overstrength related force modification factor. The values for R_o used in the design were $R_o=1.4$ for moderately ductile reinforced concrete frames, and $R_o=1.7$ for ductile frames (Table 4.1.8.9 in NBCC 2005).

Given the values for R_d and R_o, the total reduction of the elastic base shears is R_dR_o = 2.5 x 1.4 = 3.5 for the moderately ductile building, and R_dR_o = 4.0 x 1.7 = 6.8 for the ductile building.

Note that the foregoing parameters of the base shear formula are the same for both the longitudinal and the transverse directions of the building. Consequently, the total seismic design base shears in the longitudinal and the transverse directions are the same. The values of the total design base shears are:

- $V_{long.} = V_{transv.}$ = 1177 kN for moderately ductile frames, and
- $V_{long.} = V_{trans.}$ = 606 kN for ductile frames.

Having the values for V, the design seismic base shear coefficients, V/W, are:

- V/W = 1177 / 32 616 = 0.037 for moderately ductile frames, and
- V/W = 606 / 32616 = 0.016 for ductile frames.

The total lateral seismic forces, V, were distributed along the height of the building in accordance with Clause 4.1.8.11.(6) of NBCC 2005. An additional concentrated force, F_t, was applied at the top of the building, as required by this Clause for the case when the fundamental period is larger than 0.7 s. The forces at the floor levels were divided by the number of the frames to calculate the forces on each frame. In the transverse direction, the seismic forces were divided by 6, and in the longitudinal direction by 4. The computed seismic forces acting on the frames are shown in Table 4.2.

Two-dimensional (2-D) elastic static analyses were conducted using the computer program SAP 2000 (CSI 2000). In each direction, one exterior and one interior frame were analyzed. The same seismic forces were used in the analyses of the interior and exterior frames of each building. The gravity loads for the interior frames were approximately twice those of the exterior frames. Bending moments, axial forces and shear forces were computed for the beams and columns of the frames. The design was based on the combined effects of: Dead load ± Seismic load + 0.5(Life load), as required by CSA Standard A23.3-94 (CSA 1994). The reinforcement and the dimensions of the beams and columns of the transverse

frames of the moderately ductile building are shown in Table 4.3, and those of the transverse frames of the ductile frame are shown in Table 4.4. The reinforcement and the cross sections of the beams and columns of the longitudinal frames of each building are the same as those of the corresponding (exterior or interior) transverse frames, and these are not shown here in order to avoid repetition (see notes in Tables 4.3 and 4.4). It should be mentioned that the cross sections of beams and columns of both the moderately ductile and the ductile buildings are the same, and the only difference is in the reinforcement in the beams; the reinforcement in the columns of both buildings is the same and corresponds to the minimum reinforcement of 1.0%, as required in the CSA Standard A23.3-94 (CSA 1994). The thickness of the slab is 12.5 cm at all floors.

Figure 4.3 shows the design details for an interior transverse frame of the moderately ductile building. The detailing of the other frames of the moderately ductile building (exterior transverse and longitudinal frames), and the frames of the ductile frames are similar to those in Fig. 4.3, and they are not shown here.

4.3 Modeling of the Building for Blast Analysis

For the purpose of the blast load analysis, the building was modeled for use in the nonlinear program DRAIN-2DX (Prakash et al. 1993). DRAIN-2DX is a general purpose computer program for 2-D static and dynamic analysis of building structures. It is specifically developed for nonlinear time history analysis of buildings subjected to seismic excitations. The dynamic analysis is performed using step-by-step numerical integration method. Among the different elements included in the program, the beam-column element was used in the analysis in this study. Plastic hinges are placed at the end sections of the structural members. The nonlinear behaviour at the plastic hinges follows a modified version of the hysteretic model developed by Takeda et al. (1970) (see Fig. 4.4).

The columns and beams of the frames were modeled by line elements. The parameters required by DRAIN-2DX include the elastic stiffness properties (modulus of elasticity and moment of inertia) and inelastic behaviour parameters (inelastic stiffness, yield moments and yield axial forces at the end sections of structural members). The inelastic behaviour parameters were computed using the program Rc-Section (Saatcioglu 2000). It should be mentioned that the reduced (i.e., cracked) moment of inertia of the structural

members were used in the analysis as required by the CSA Standard A23.3-94 (CSA 1994). This was done by applying a reduction factor of 0.35 to the gross moment of inertia of beams, and a factor of 0.7 to the gross moment of inertia of columns. Dead loads and life loads were included in the nonlinear time-history analysis. The masses were applied at the master joints at the floors. While the program is developed for seismic excitations, it allows application of dynamic loads at the joints, and this option was used in this study. The application of the blast loads is discussed in the Chapter 5.

Table 4.1 Gravity loads and properties of concrete and reinforcing steel used in the design.

Loads/ Strengths	Floor	Roof
Dead load (kN/m^2)	5	3.5
Live load (kN/m^2)	2.4	2.2
Concrete compressive strength (MPa)	30	
Reinforcement yield strength (MPa)	400	

Table 4.2 Seismic forces on frames.

Floor level	W (kN) per floor	Seismic forces per frame			
		Moderalety ductile		Ductile	
		Transverse frame (kN)	Longitudinal frame (kN)	Transverse frame (kN)	Longitudinal frame (kN)
Roof	2484	41.83	62.75	21.53	32.30
9	3348	30.87	46.31	15.89	23.83
8	3348	27.44	41.16	14.12	21.19
7	3348	24.01	36.02	12.36	18.54
6	3348	20.58	30.87	10.59	15.89
5	3348	17.15	25.73	8.83	13.24
4	3348	13.72	20.58	7.06	10.59
3	3348	10.29	15.44	5.30	7.94
2	3348	6.86	10.29	3.53	5.30
1	3348	3.43	5.14	1.76	2.65

Table 4.3 Reinforcement in the transverse frames of the moderately ductile building.

Frame	Floor	Beam section in (mm) and reinforcement	Column sections in (mm) and reinforcement	
			Interior	Exterior
Interior	1-5	300 x 450 3#25 top, 2#20 bottom	500 x 500 12#25	400 x 400 8#25
	6-9	300 x 450 3#25 top, 2#20 bottom	500 x 500 12#20	400 x 400 8#20
	10	300 x 400 3#20 top, 2#15 bottom		
Exterior	1-5	300 x 500 3#25 top, 2#20 bottom	400 x 400 8#25	350 x 350 8#25
	6-9	300 x 450 3#25 top, 2#20 bottom	400 x 400 8#20	350 x 350 8#20
	10	300 x 400 3#20 top,2#15 bottom		

Note: Cross sections of frame members and reinforcement of the interior and exterior longitudinal frames are the same as those of the interior and exterior transverse frames respectively.

Table 4.4 Reinforcement in the transverse frames of the ductile building.

Frame	Floor	Beam section in (mm) and reinforcement	Column sections in (mm) and reinforcement	
			Interior	Exterior
Interior	1-5	300 x 450 2#25 top, 2#15 bottom	500 x 500 12#25	400 x 400 8#25
	6-9	300 x 450 2#25 top, 2#15 bottom	500 x 500 12#20	400 x 400 8#20
	10	300 x 400 2#20 top, 2#15 bottom		
Exterior	1-5	300 x 500 2#25 top, 2#15 bottom	400 x 400 8#25	350 x 350 8#25
	6-9	300 x 450 2#25 top, 2#15 bottom	400 x 400 8#20	350 x 350 8#20
	10	300 x 400 2#20 top, 2#15 bottom		

Note: Cross sections of frame members and reinforcement of the interior and exterior longitudinal frames are the same as those of the interior and exterior transverse frames respectively.

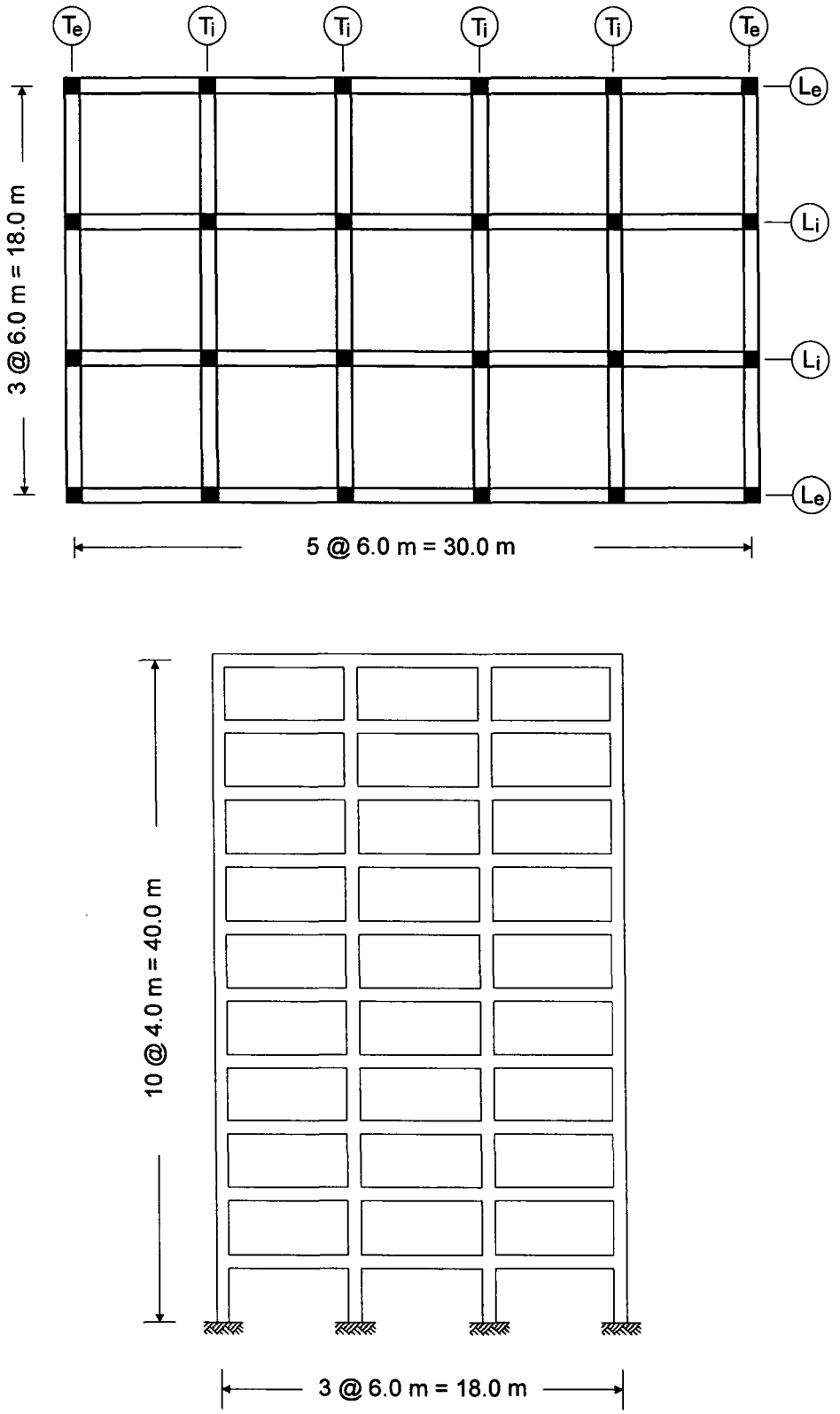

Figure 4.1 Plan of floors and elevation of transverse frames of the building.

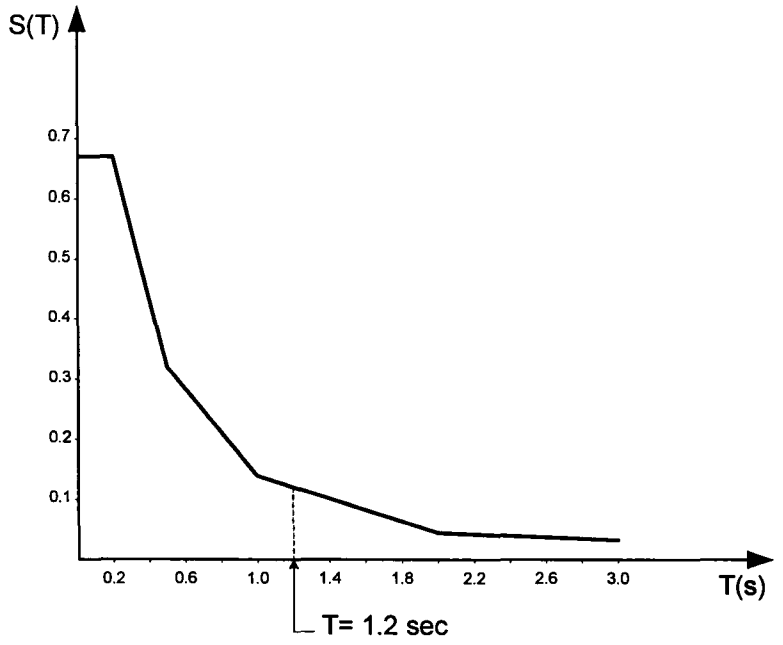

Figure 4.2 Seismic design spectrum for Ottawa, for site class C.

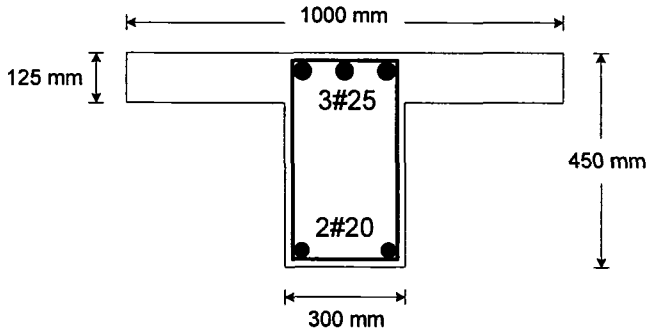

Typical beam section for all levels except the roof

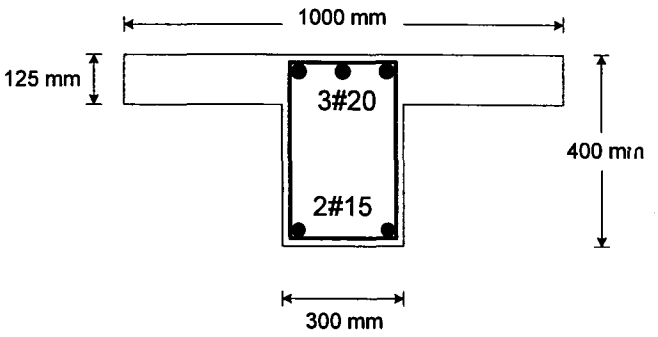

Typical beam section at the roof level

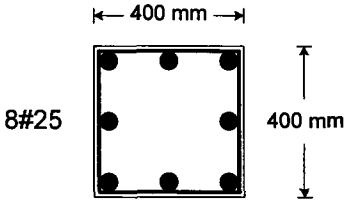

Exterior columns for stories 1-5

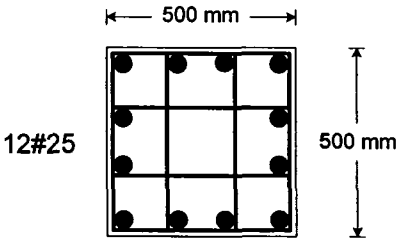

Interior columns for stories 1-5

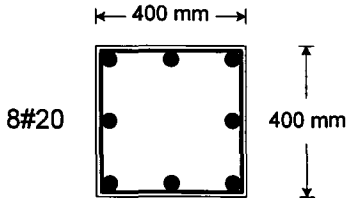

Exterior columns for stories 6-10

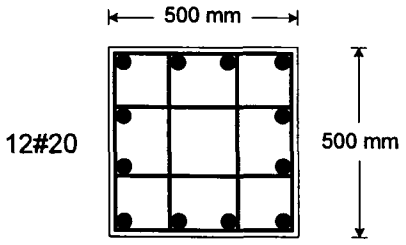

Interior columns for stories 6-10

Figure 4.3 Design details for interior transverse frame members of the moderately ductile building.

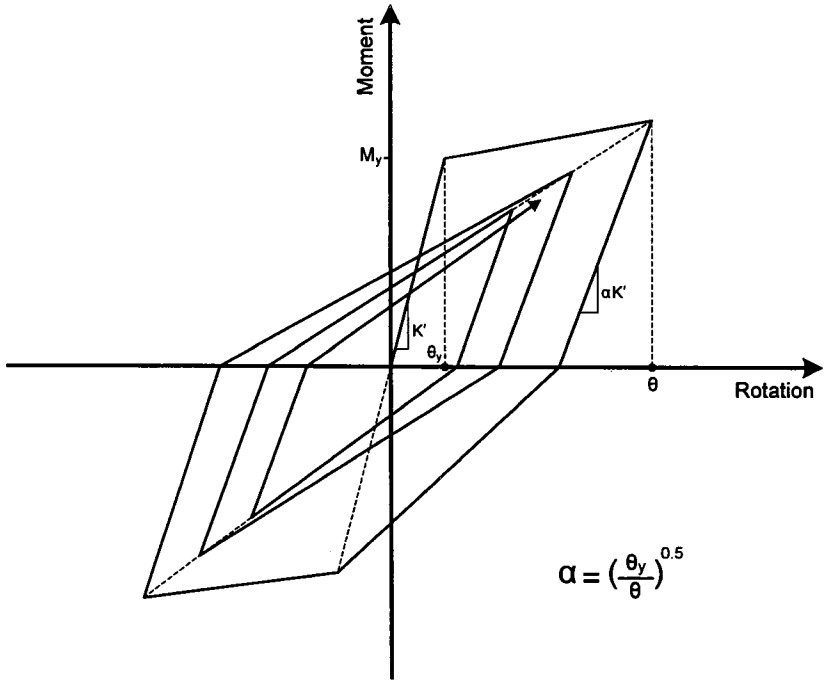

Figure 4.4 Hysteretic moment-rotation model used in DRAIN-2DX.

Chapter 5

Analysis for Blast Loading

5.1 Blast Load Cases and Load Computation

Several scenarios of car bomb explosions were considered in this study to investigate the nonlinear behaviour of the transverse frames of the building designed for moderate ductility. Specifically, one of the interior transverse frames was analyzed in this study. The following loading cases were considered in the analysis:

- Case 1: 125 kg TNT detonation at distances of 5, 10, 15, 20, 25 and 30 m,
- Case 2: 250 kg TNT detonation at distances of 5, 10, 15, 20, 25 and 30 m, and
- Case 3: 500 kg TNT detonation at distances of 5, 10, 15, 20, 25 and 30 m.

The explosions are assumed at the ground level. The distances are measured horizontally at the base of the building. Figure 5.1 shows schematically the plan of the building and the location of explosions. The loads resulting from the explosions were assumed to act horizontally at the floor levels of the frame. This is because the program DRAIN-2DX allows dynamic loads at the floor levels only. The loads along the height of the building are shown in Fig. 5.2. At each floor, the load was calculated for the corresponding distance from the explosion to floor. The exposure area was assumed to be half of the tributary area of the façade, i.e., the exposure area for each floor joint was taken to be A= ½ x (4.0 m x 6.0 m) = 12 m^2, where 4.0 m is the height of the storey, and 6.0 m corresponds to the distance between the transverse frames. It should be noted that the dynamic loads at each floor represent triangular impulsive loads as indicated in Fig. 5.2. In the calculation of the loads it was

assumed that the angles of incidence at all floors are the same as that at the base of the building (i.e., $\alpha = 0^{o}$, Fig. 3.4) and the loads at all floors correspond to normally reflected overpressure.

The reflected overpressures at each floor of the building are given in Tables 5.1, 5.2, and 5.3 for the 125 kg, 250 kg, and 500 kg TNT detonations respectively. Note that the overpressures, P_r, given in the tables were multiplied by the exposure areas at each floor (i.e., A=12 m^2) to obtain the loads F(t) for use in the time-history analysis (See Fig. 5.2). Figure 5.3 shows the overpressures, P_r, at the floor levels for the building, for the 250 kg TNT detonation (referred to as Case 2, above) and all the distances considered in the analysis. These values are the same as those shown in Table 5.2.

Table 5.4 shows the durations of the overpressures, t_d, calculated for the first floor of the building, for the cases considered in the analysis. It can be seen from the table that the duration of the impulsive loads range between approximately 8 and 26 ms. Table 5.4 also shows that, in general, the duration of the overpressures increases with the increase of the distance from the explosion. There are few cases that do not follow this trend. For example the durations for the 125 and 250 kg detonations at 10 m are slightly smaller than those of the same detonations at 5 m. Similarly, the duration for the 500 kg detonation at 15 m is smaller than that of the same detonation at 10 m. This is because of the "non regular" shape of the curve that defines the duration, t_d, as shown in Fig. 3.6. It can be seen from this figure that the t_d curve does not increase steadily with the increase of the distance.

5.2 Nonlinear Dynamic Analysis

Nonlinear time-history analyses of the building were conducted for each of the TNT detonations using the computer program DRAIN-2DX (Prakash et al., 1993). In total 18 time-history analyses were performed [i.e, (3 TNT detonations) x (6 distances each)]. Since the durations of the blast loads are very small, integration time interval of 0.0001 s was used in all analyses. P-Δ effects were taken into account. A damping of 5% of critical was used in the analyses.

For each detonation and distance, the durations, t_d, of the blast loads computed for the first floor (Table 5.4) were used at all floors (i.e., the same durations were used at all floors).

This is because the program DRAIN-2DX accepts the same duration of the forcing functions at the floors.

Response time histories of the displacement at the floor levels, and the bending moments at the end sections of beams and columns were obtained from each analysis. The program also provides maximum inelastic rotations at the ends of beams and columns (i.e., plastic hinge rotations).

For illustration, Figure 5.4 shows roof displacement time history of the building subjected to blast loads resulting from 500 kg TNT detonation at a distance of 10 m. It can be seen from the figure that the response is characterized by one peak that is followed by free vibrations of the building.

Figure 5.5 shows the maximum interstorey drifts of the building due to blast loads resulting from 500 kg TNT detonations at distances ranging from 5 to 100 m. It can be seen from the figure that the maximum drift decreases dramatically with the increase of the distance of detonation, especially within the first 15 m. For example, the drift corresponding to a detonation at 5 m is about 15% and that at 15 m is approximately 2%. For distances larger than 15 m, the drift decreases slowly with the increase of the distance. This figure represents a typical example of the blast effects on building structures, i.e., the largest effects are associated with detonations at small distances (typically smaller than 15 to 20 m).

Figure 5.6(a) shows the response time history of the moment at the base of the interior column of the first storey. As for the roof displacement response (Fig. 5.4), the first peak is the largest and represents the response due to the blast load impulse. The other portion of the response results from the free vibration of the building. Figure 5.6(b) illustrates the hysteretic behaviour (moment vs. storey displacement) of the bottom section of the first storey interior column. It can be seen that the maximum response corresponds to the first peak and it is in the inelastic range.

5.3 Performance Parameters

In this study, the performance of the building was assessed by considering maximum interstorey drifts, displacement ductilities (at storey level), and curvature ductilities at the end sections of beams and columns. These parameters are widely used and are quite appropriate for the assessment of nonlinear response of the buildings. The maximum interstorey drift is a

global response parameter and can be compared by the drift specified in the code. The drifts were computed from the time histories of the displacements resulting from the analyses. The drift, however, does not provide information for the extent of the inelastic response. Displacement ductility, at a storey level, and curvature ductilities at the end sections of beams and columns were computed to assess the inelastic behaviour. The computation of these quantities is described hereafter.

5.4 Computation of Displacement Ductility

In this study, the displacement ductility is calculated for each storey. For a given storey, it represents the ratio of the maximum interstorey drift (in mm) to the yield displacement at that storey:

$$\mu_{\Delta} = \Delta_{storey} / \Delta_y \tag{5.1}$$

where,

μ_{Δ} = displacement ductility,

Δ_{storey} = interstorey drift (in mm), and

Δ_y = yield displacement at the storey (in mm).

The interstorey, Δ_{storey}, is given by the program. Regarding the yield displacement at a given storey, Δ_y, it was taken as the average value of the yield displacements of the interior and the exterior columns of that storey. It is important to mention that the yield displacements of both the interior and exterior columns of each storey are quite close, i.e. the maximum difference is in the range between 2% for the bottom storey to about 7% for the top storey of the building.

The yield displacement, Δ_y, for a given column was calculated as proposed by Paulay and Priestley (1992) (see Fig. 5.7):

$$\Delta_y = \emptyset_y L^2 / 6 \tag{5.2}$$

where:

$\emptyset_y$ = yield curvature, and

L = length of the column.

The yield curvature was calculated using the computer program CURVE (Humar 2000), based on the dimensions of the cross sections of columns, properties of the concrete and reinforcing steel, and axial load.

5.5 Computation of Curvature Ductility

The curvature ductility, μ_Φ, for the end section of a given member (beam or column) represents the ratio of the maximum curvature, $\emptyset_{max}$, to the yield curvature, $\emptyset_y$, at that section, and is expressed by the expression:

$$\mu_\Phi = \emptyset_{max} / \emptyset_y \tag{5.3}$$

where,

$\emptyset_{max}$ = maximum curvature during the response, and

$\emptyset_y$ = yield curvature.

The maximum curvature, $\emptyset_{max}$, at a given section represents the sum of the plastic curvature, $\emptyset_p$, and the yield curvature, $\emptyset_y$, as follows (see Fig. 5.7):

$$\emptyset_{max} = \emptyset_y + \emptyset_p \tag{5.4}$$

where,

$\emptyset_y$ = yield curvature, and

$\emptyset_p$ = plastic curvature.

As mentioned above, the yield curvature was calculated by the computer program CURVE (Humar 2000). The plastic curvature was computed using the equation:

$$\emptyset_p = \theta_p / L_p \tag{5.5}$$

where,

θ_p = plastic hinge rotation, and

L_p = plastic hinge length.

The plastic hinge rotation was obtained from the analysis by DRAIN-2DX. The plastic hinge length was computed using the following equation (Saatcioglu 2004):

$$L_p = 0.5d + 0.005z \tag{5.6}$$

where,

d = depth of column or beam.

z = the distance from the point of contraflexure to the end of column or beam, which was taken to be half of the member length, i.e. z = L/2.

5.6 Discussion of Results

5.6.1 Interstorey Drifts and Displacement Ductilities

The response results for interstorey drift and displacement ductility are shown in Figures 5.8, 5.9 and 5.10 for the detonation of 125 kg, 250 kg, and 500 kg TNT respectively. Six curves are shown in each figure representing the results for the detonations at distances of 5, 10, 15, 20, 25 and 30 m. The figures show that the largest response values correspond to the detonations at a distance of 5 m. The maximum values for both the interstorey drift and displacement ductility for these detonations (at 5 m) are at the first storey.

For the detonation of 125 kg TNT at 5 m (Fig. 5.8), the maximum interstorey drift is 4.5% of the storey height, and the displacement ductility is approximately 7.5. Both these values are quite large indicating that severe damage is expected at the first storey of the building. The maximum drift is approximately twice the design drift of 2.5% allowed by NBCC 2005. The ductility of 7.5 is also quite high compared to the ductility assumed in NBCC 2005; based on the value of R_d=2.5 for moderately ductile frames (specified in Table 4.1.8.9 of NBCC 2005), displacement ductility of approximately 2.5 is considered to be acceptable provided that the overstrength is not taken into consideration in the analysis, as is the case in this study.

The interstorey drifts and displacement ductilities for the 125 kg TNT detonation at distances of 10, 15, 20, 25 and 30 m are all very small. The maximum interstorey drift is about 0.5% and the maximum displacement ductility is approximately 1.0 for distance of 10 m. These results indicate that the structure behaves elastically when subjected to blast loads due to 125 kg TNT detonations at distances larger than 10 m.

Regarding the results for the 250 kg TNT detonations (Fig. 5.9), the maximum values for the detonation at 5 m distance are much larger than those for the 125 kg TNT detonation at the same distance. Maximum drift of 14% and displacement ductility of 23 were obtained at the first storey. These values indicate substantial damage at the first storey, and probably

collapse of the building. This is also observed from the column and beam curvature ductilities discussed below in this section. Maximum drift of 2% and displacement ductility of 3.0 can be observed for the detonation at 10 m distance. Both these values are at the first storey. These values indicate acceptable damage at the first storey. The drifts and displacement ductility for detonations at distances larger than 10 m are quite small indicating elastic behaviour of the building.

The results for the detonation of the 500 kg TNT (Fig. 5.10) show that the building would experience significant damage and possibly would collapse due to detonations at distances of 5 m and 10 m. The maximum interstorey drifts are 15.5% and 10.5% for detonations at 5 m and 10 m respectively (Fig. 5.10(a)), both of which happen at the first storey. The maximum displacement ductilities are also at the first storey and have very large values, i.e., about 27 for a detonation at 5 m and 17 for a detonation at 10 m (Fig. 5.10(b)).

5.6.2 Column Curvature Ductilities

The results for ductilities in columns are shown in Fig. 5.11 for detonation of 125 kg TNT, Fig. 5.12 for detonation of 250 kg TNT , and Fig. 5.13 for detonation of 500 kg TNT. The results are presented only for the distances of the detonations for which ductilities larger than 1.0 were obtained (i.e., the building experienced inelastic response). As can be seen from the figures, ductilities in excess of 1.0 were obtained for the 125 kg TNT detonation at 5 m, and for the detonations of 250 kg and 500 kg TNT at distances of 5 and 10 m.

Ductilities are shown for both the top and the bottom sections of the interior and exterior columns of each storey. Considering Fig. 5.11, for example, the second storey is between floor level 1 and floor level 2 shown on the vertical axis of the figure. The two points slightly above the floor level 1 represent the ductilities at the bottom sections of the interior and exterior columns of the second storey. Similarly, the two points slightly below the floor level 2 represent the ductilities at the top sections of the interior and exterior columns of the second storey.

A general observation from Figures 5.11 to 5.13 is that the largest ductilities are at the bottom of the first storey columns, and the other values are much smaller. This is expected since the largest effects of the blast loads are at the first storey.

The maximum column ductility for the 125 kg TNT detonation at 5 m is about 16 (Fig. 5.11). While damage is expected at the bottom of the first storey columns, this ductility is considered to be acceptable. Heidebrecht and Naumoski (2002) reported that structural members of well designed frame structures could perform satisfactorily at curvature ductilities of 10 to 20.

The maximum column ductility for the detonation of 250 kg TNT at 5 m (Fig. 5.12(a)) is about 50 which indicates that significant damage will occur at the bottom of the first storey columns due to such detonation that could lead to collapse of the building. On the other hand, the maximum ductility due to this detonation at 10 m (Fig. 5.12(b)) is about 6 and is considered acceptable, even though some damage to the columns is expected.

As can be seen in Fig. 5.13, the maximum ductilities resulting from the 500 kg TNT detonation at 5 m is about 56, and that from the detonation at 10 m is about 37. Both these ductilities are for the bottom sections of the first storey columns. These are very large values, and certainly the building could not resist the blast effects due to 500 kg TNT detonations at distances smaller than 10 m.

5.6.3 Beam Curvature Ductilities

The curvature ductilities in the beams are shown in Figures 5.14 and 5.15 for detonation of 125 kg TNT, Figures 5.16 to 5.19 for detonation of 250 kg TNT, and Figures 5.20 to 5.25 for detonation of 500 kg TNT. Beam ductilities are shown only for the distances of detonations for which ductilities larger than 1.0 were obtained. It can be seen in the figures that beam ductilities larger than 1.0 were obtained for the 125 kg TNT detonation at 5 and 10 m, the 250 kg TNT detonation at 5, 10, 15 and 20 m, and the 500 kg TNT detonation at all distances considered in the analysis (i.e. 5 m to 30 m). Ductilities are shown for both the left and the right sections of the exterior and the interior beams at each floor. All the figures are plotted in the same scale, which enables easier comparisons of the ductilities resulting from detonations at different distances.

In can be observed from the figures that in all cases the largest ductilities are in the beams of the first floor. The maximum ductility resulting from the 125 kg TNT detonation at 5 m is about 12 (Fig. 5.14(a)). This value indicates that some damage to the beams at the first floor is expected. As mentioned above, however, curvature ductilities of the order of 10 to 20

are considered acceptable for well designed frame members (Heidebrecht and Naumoski 2002), and ductilities of 12 resulting from the 125 kg TNT detonation at 5 m are not of special concern. The maximum ductility from the detonation at 10 m is about 2, and all other values are of the order of 1.0 and smaller (Fig. 5.15).

The maximum ductility resulting from the 250 kg TNT detonation at 5 m is approximately 43 for the exterior beams (Fig. 5.16(a)), and about 37 for the for the interior beams of the first floor (Fig. 5.16(b)). These values indicate that the beams at the first floor will suffer significant damage when subjected to blast loads due to 250 kg TNT detonation at 5 m. The ductilities from the detonation at 10 m and larger distances are considered acceptable even though some (minor) damage to the beams is expected to occur. The maximum ductility from the detonation at 10 m is about 7 (Fig. 5.17), and the ductilities from the detonations at 15 m and 20 m are 3 and 2 respectively (Figs. 5.18 and 5.19).

The results from the analysis for the 500 kg TNT detonations at 5m and 10 m show very large curvature ductilities for the beams of the first floor. The maximum ductility for the detonation at 5 m is 49 (Fig. 5.20) and that for the detonation at 10 m is 38 (Fig. 5.21), which indicate that these beams would experience substantial damage and probably would collapse. The ductility values for the detonations at 15 m, 20 m, 25 m, and 30 m are approximately 7, 4, 3 and 2 respectively, indicating moderate to minor damage to the beams (Figs. 5.22 to 5.25).

5.7 Summary

Results from the analysis of an interior transverse frame of the moderately ductile building designed for Ottawa are presented in this Chapter. The frame was subjected to blast loads resulting from detonations of 125 kg, 250 kg, and 500 kg TNT at distances of 5, 10, 15, 20, 25 and 30 m from the building. The performance of the frame was assessed by considering interstorey drift, displacement ductility, and curvature ductility in columns and beams. The following are the main observations from the results:

- The effects due to blast loads decreases dramatically with the increase of the distance of the detonation. As an example, interstorey drift resulting from a detonation of 500 kg

TNT at 15 m distance is about 8 times smaller compared to the drift from the same detonation at 5 m distance (Fig. 5.5).

- The largest inelastic deformations for all detonations were obtained for the structural members of the first storey. This was expected because the largest blast loads are at that storey.

- The results from the analysis for the 125 kg TNT detonations showed that significant damage could occur to the building only from the detonation at a distance of 5 m. The interstorey drifts and displacement ductilities obtained from the analysis are much larger than the code specified values. The detonations at larger distances do not have significant effects on the building.

- A detonation of 250 kg TNT at 5 m would cause significant damage to the first storey columns and beams, and might lead even to collapse of the building. This is especially indicated by the interstorey drifts and displacement ductilities obtained from the analyses. Detonations at 10 m would produce much smaller (moderate) damage, and those at larger distances are not considered as a risk to the building.

- Detonations of 500 kg TNT at 5 m and 10m could result in substantial damage to the building, and probably collapse. This is observed from all the response parameters considered in the analysis. Detonations at distances larger than 10 m would cause moderate to minor damage to the building.

- All the results show that providing a standoff distance of about 15 m would lead to the protection of the building from blast loads for detonations of up to 500 kg TNT. Detonations at distances larger than 15 m would cause moderate to minor damage to the structural members of the building, which can be considered acceptable for extreme loads such as the blast loads.

It is important to note that these observations are based on the results for the moderately ductile building analyzed in this study. The findings for another building configuration and design might be somewhat different than those summarized above.

Table 5.1 Overpressures at floor levels of the building for detonation of 125 kg TNT.

Floor	Overpressure, P_r (kPa)					
	R = 5 m	R = 10 m	R = 15 m	R = 20 m	R = 25 m	R = 30 m
1	4287	859	300	153	102	78
2	1283	484	247	138	97	71
3	484	289	189	122	88	67
4	247	193	135	114	78	60
5	145	135	105	84	69	54
6	111	98	84	73	58	50
7	82	82	69	58	51	44
8	69	62	58	51	45	39
9	53	51	49	44	39	36
10	45	44	42	39	36	33

Table 5.2 Overpressures at floor levels of the building for detonation of 250 kg TNT.

Floor	Overpressure, P_r (kPa)					
	R = 5 m	R = 10 m	R = 15 m	R = 20 m	R = 25 m	R = 30 m
1	7681	1884	578	284	156	111
2	2868	890	435	238	148	107
3	994	578	322	203	133	102
4	451	358	234	156	113	95
5	260	230	167	133	102	84
6	179	150	133	105	88	76
7	130	122	105	90	77	69
8	102	95	90	79	69	58
9	85	78	73	65	58	54
10	69	63	62	56	52	48

Table 5.3 Overpressures at floor levels of the building for detonation of 500 kg TNT.

Floor	Overpressure, P_r (kPa)					
	R = 5 m	R = 10 m	R = 15 m	R = 20 m	R = 25 m	R = 30 m
1	13658	3637	1193	492	300	179
2	5437	2303	859	405	270	173
3	2180	1215	598	352	230	150
4	907	631	405	270	203	140
5	496	405	295	218	145	128
6	311	270	222	179	135	109
7	222	199	159	135	119	95
8	150	145	130	109	100	87
9	126	119	115	97	88	79
10	107	92	92	85	78	71

Table 5.4 Duration of overpressures for different detonations and distances.

Weight of TNT (kg)	Duration of overpressure, t_d (s)					
	R = 5 m	R = 10 m	R = 15 m	R = 20 m	R = 25 m	R = 30 m
125	0.0117	0.0102	0.0145	0.0177	0.0198	0.0210
250	0.0133	0.0130	0.0151	0.0188	0.0223	0.0241
500	0.0079	0.0184	0.0155	0.0202	0.0234	0.0261

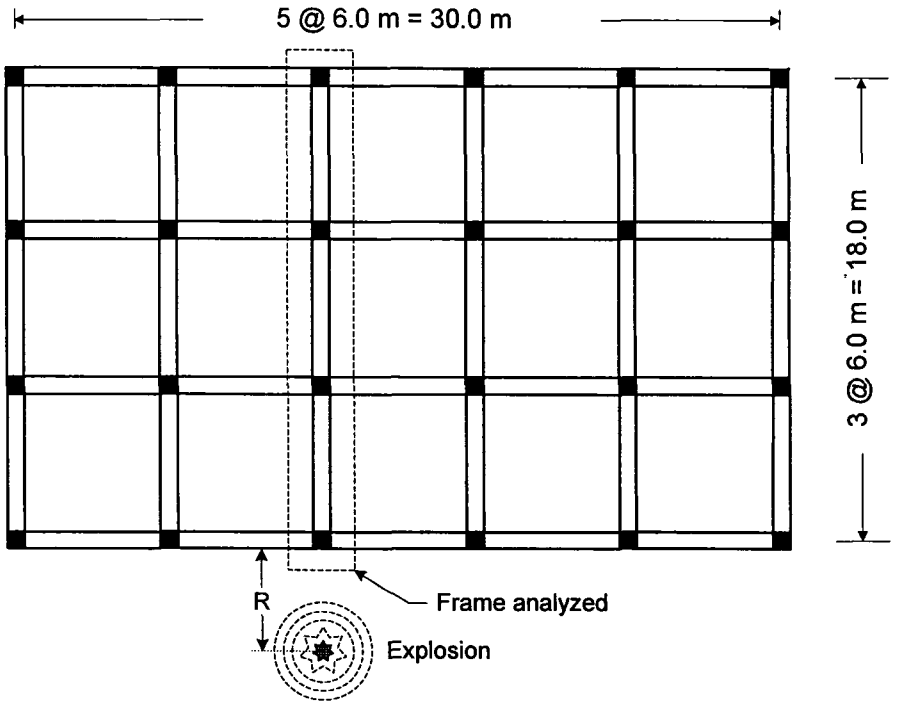

Figure 5.1 Plan of building and location of explosion.

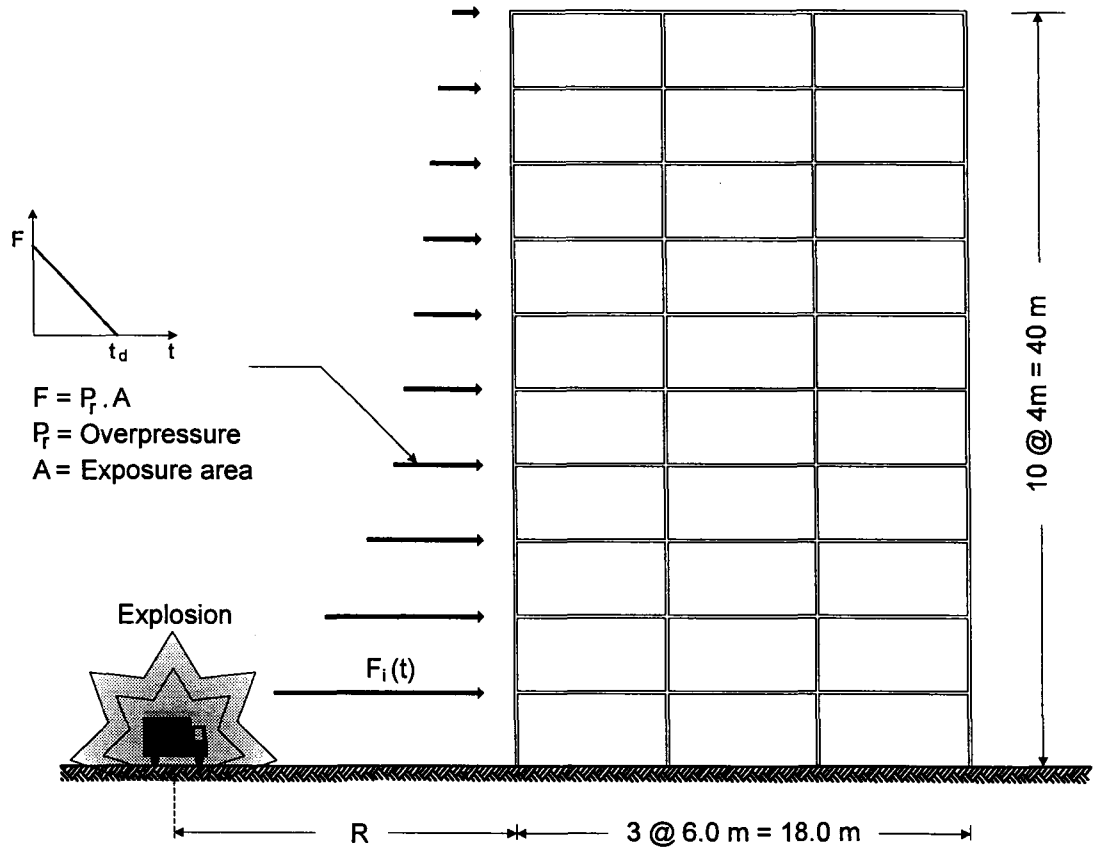

Figure 5.2 Blast loads at floor levels.

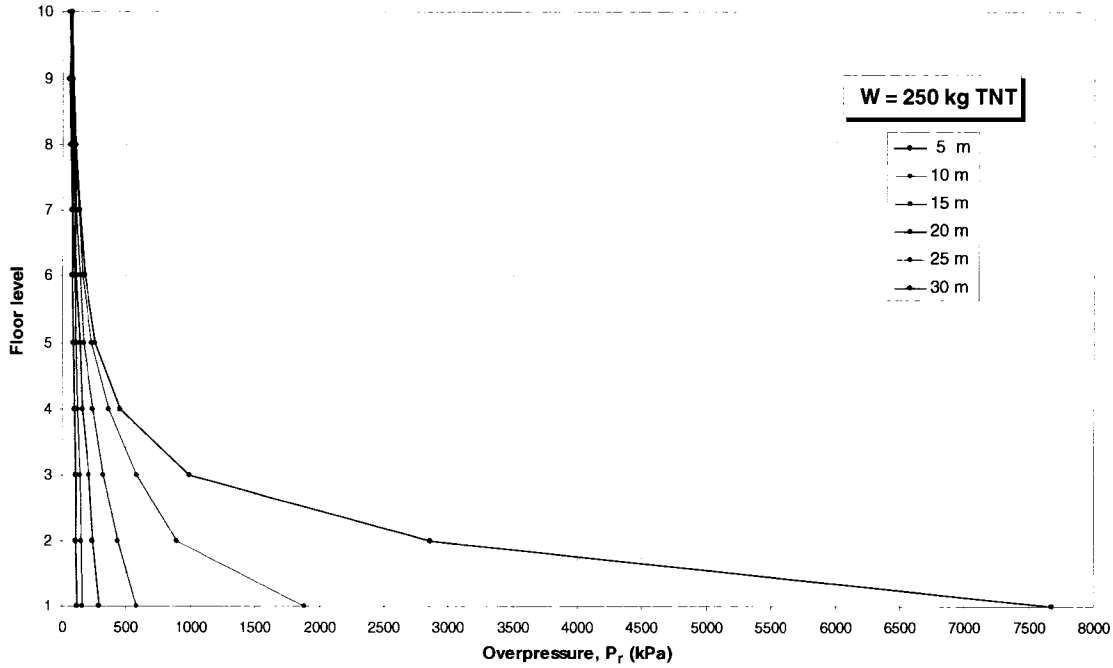

Figure 5.3 Reflected overpressures, P_r, for detonations of 250 kg TNT at different distances.

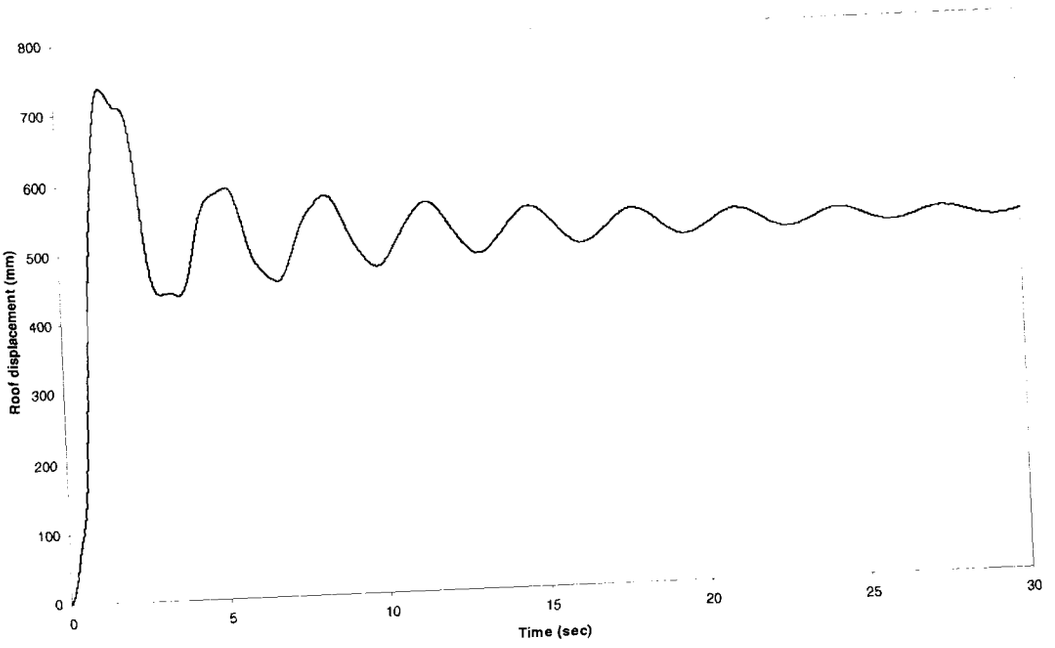

Figure 5.4 Response time history of roof displacement due to 500 kg TNT detonation at distance of 10 m.

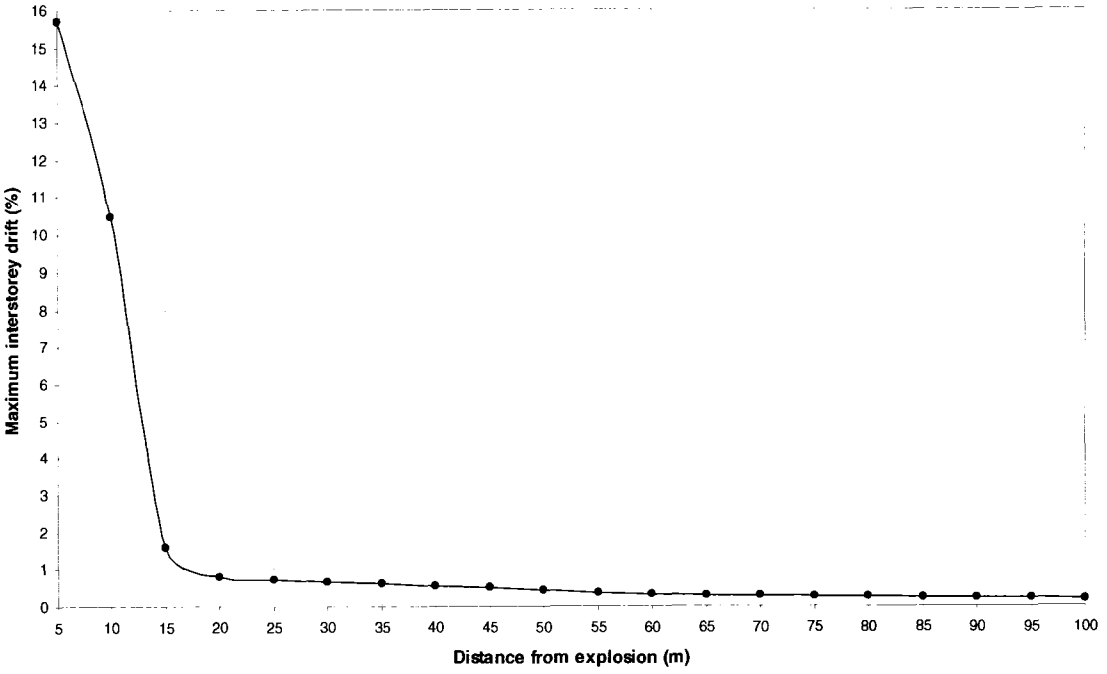

Figure 5.5 Variation of interstorey drift with distance for 500 kg TNT detonation.

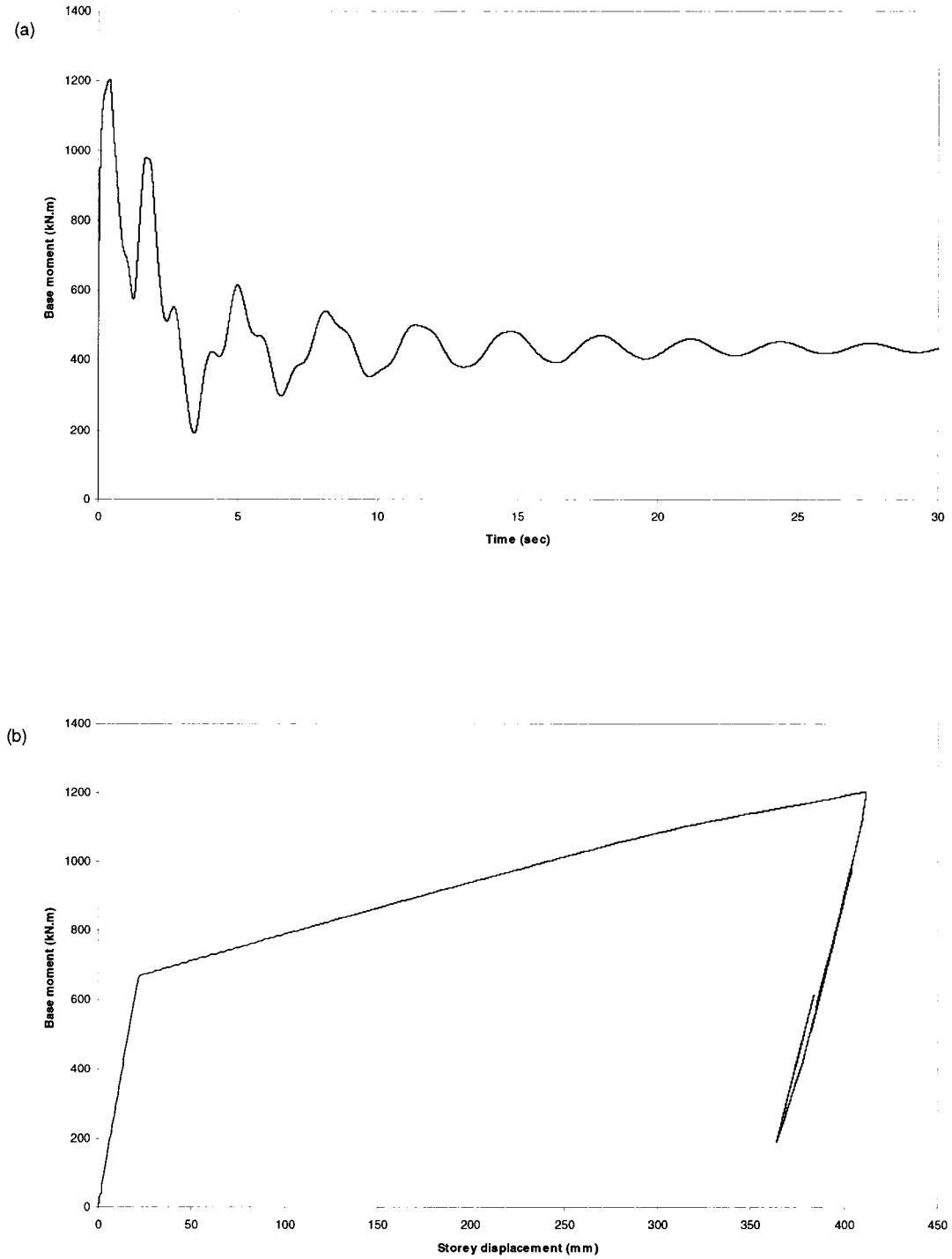

Figure 5.6 Moment response of the first storey interior column due to 500 kg TNT detonation at distance of 10 m; (a) time history of the base moment and (b) base moment vs. storey displacement.

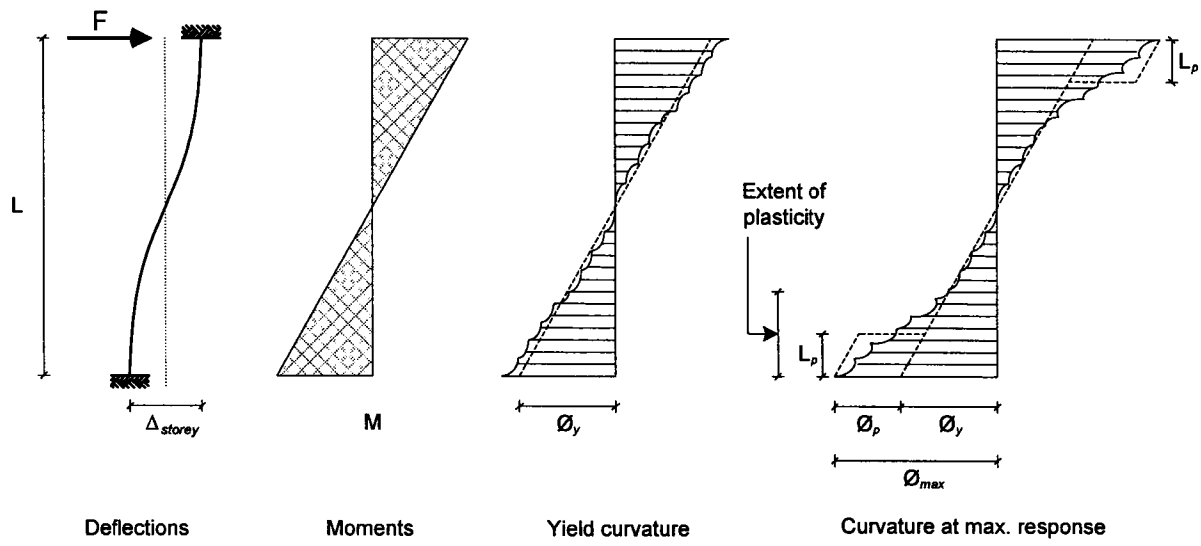

Figure 5.7 Schematic for distributions of moments and curvatures in reinforced concrete structural members (from Paulay and Priestley 1992).

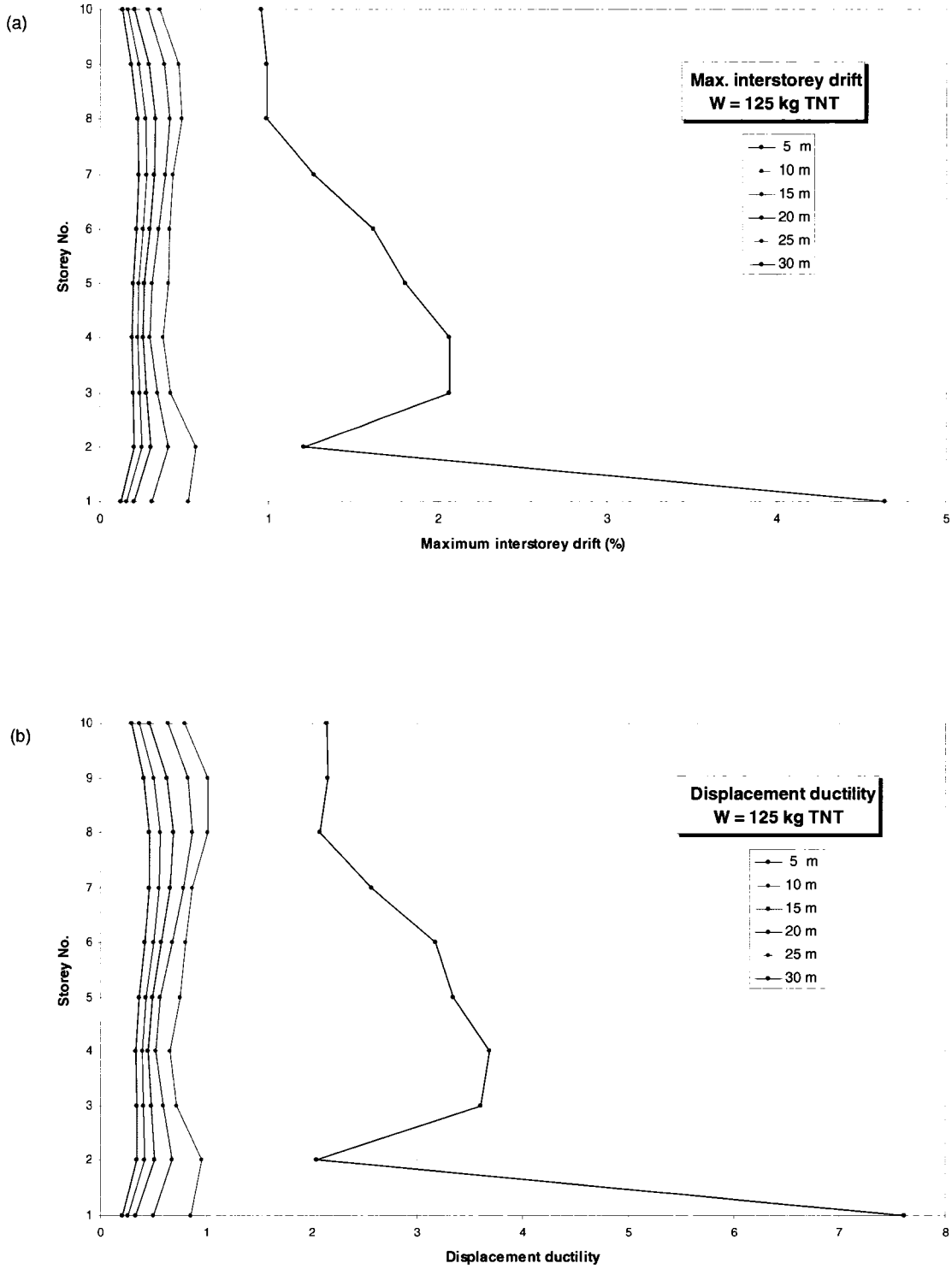

Figure 5.8 Maximum interstorey drifts and displacement ductilities for 125 kg TNT detonation; (a) interstorey drifts and (b) displacement ductilities.

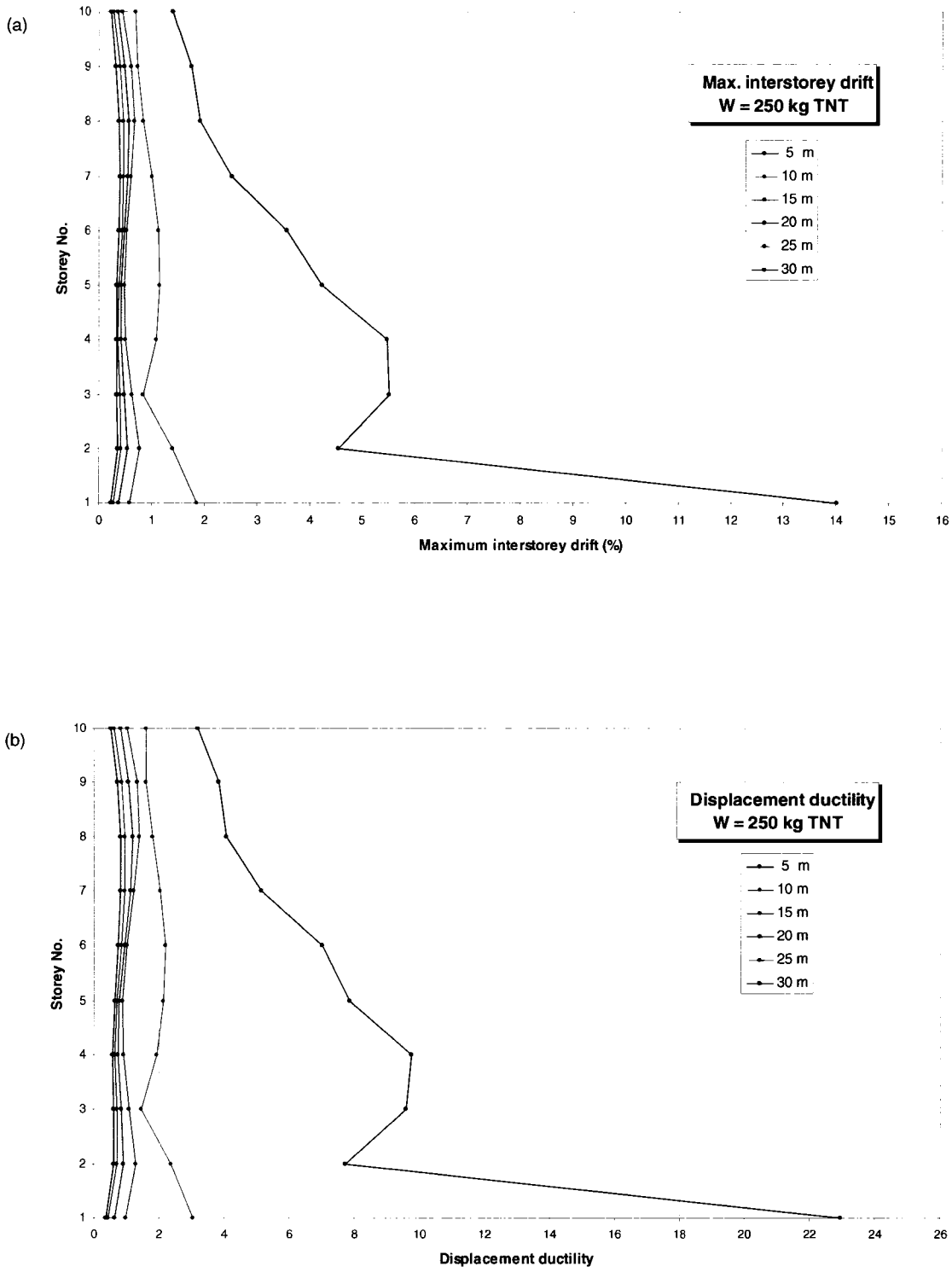

Figure 5.9 Maximum interstorey drifts and displacement ductilities for 250 kg TNT detonation; (a) interstorey drifts and (b) displacement ductilities.

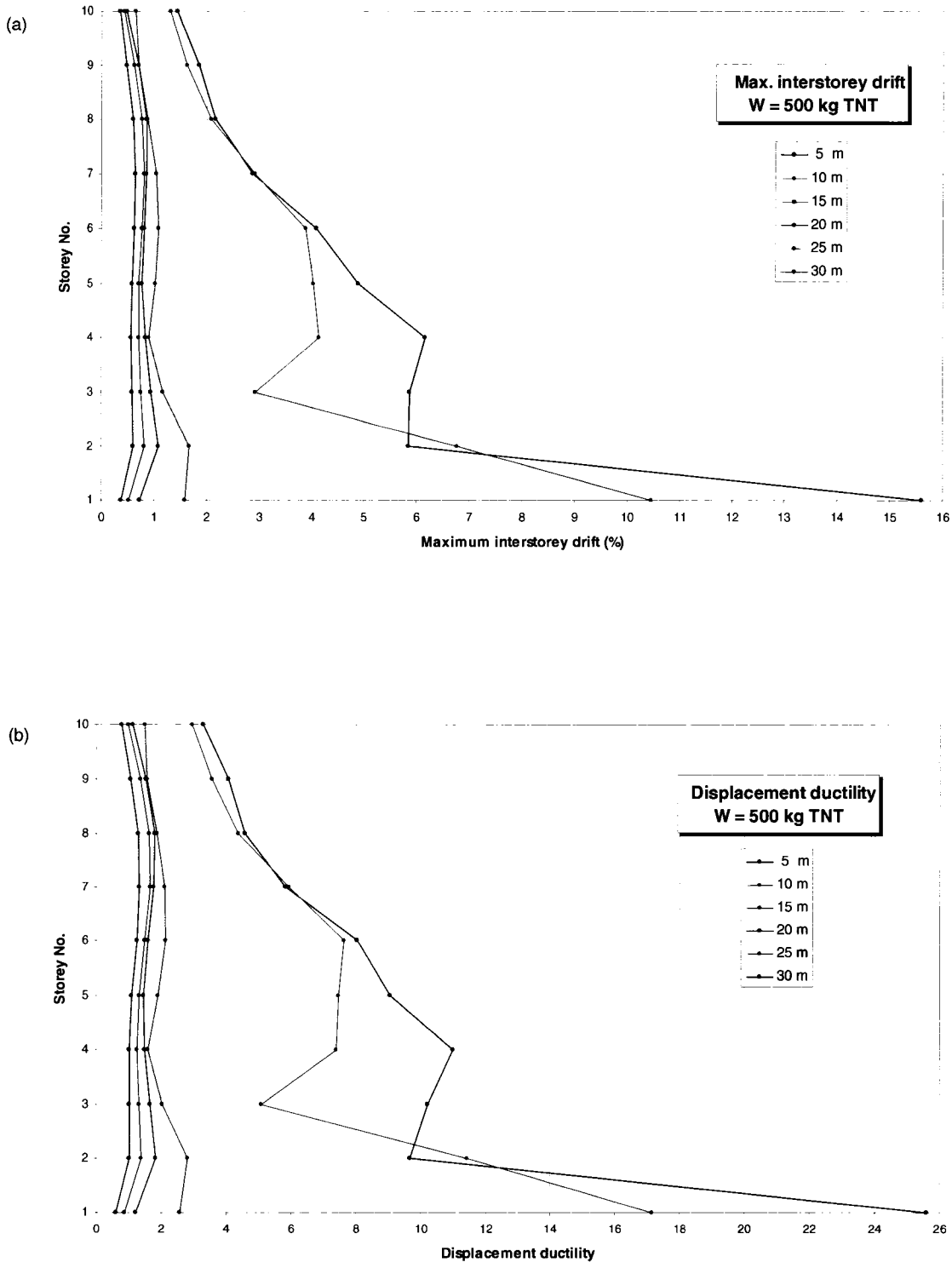

Figure 5.10 Maximum interstorey drifts and displacement ductilities for 500 kg TNT detonation; (a) interstorey drifts and (b) displacement ductilities.

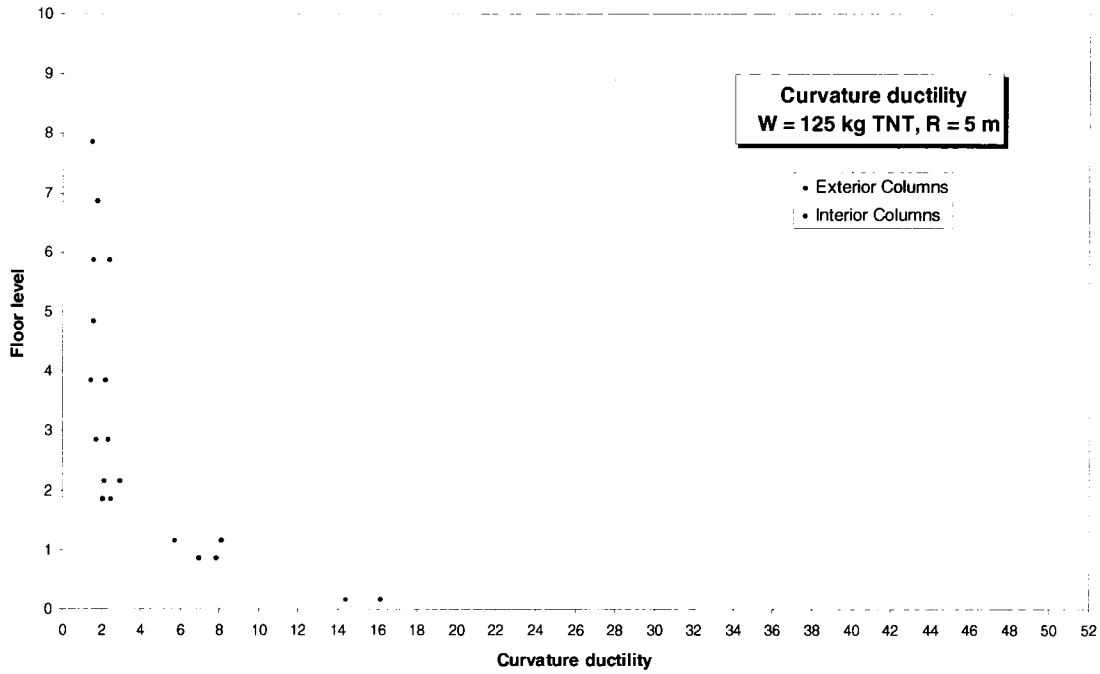

Figure 5.11 Column curvature ductilities for 125 kg TNT detonation at R=5 m.

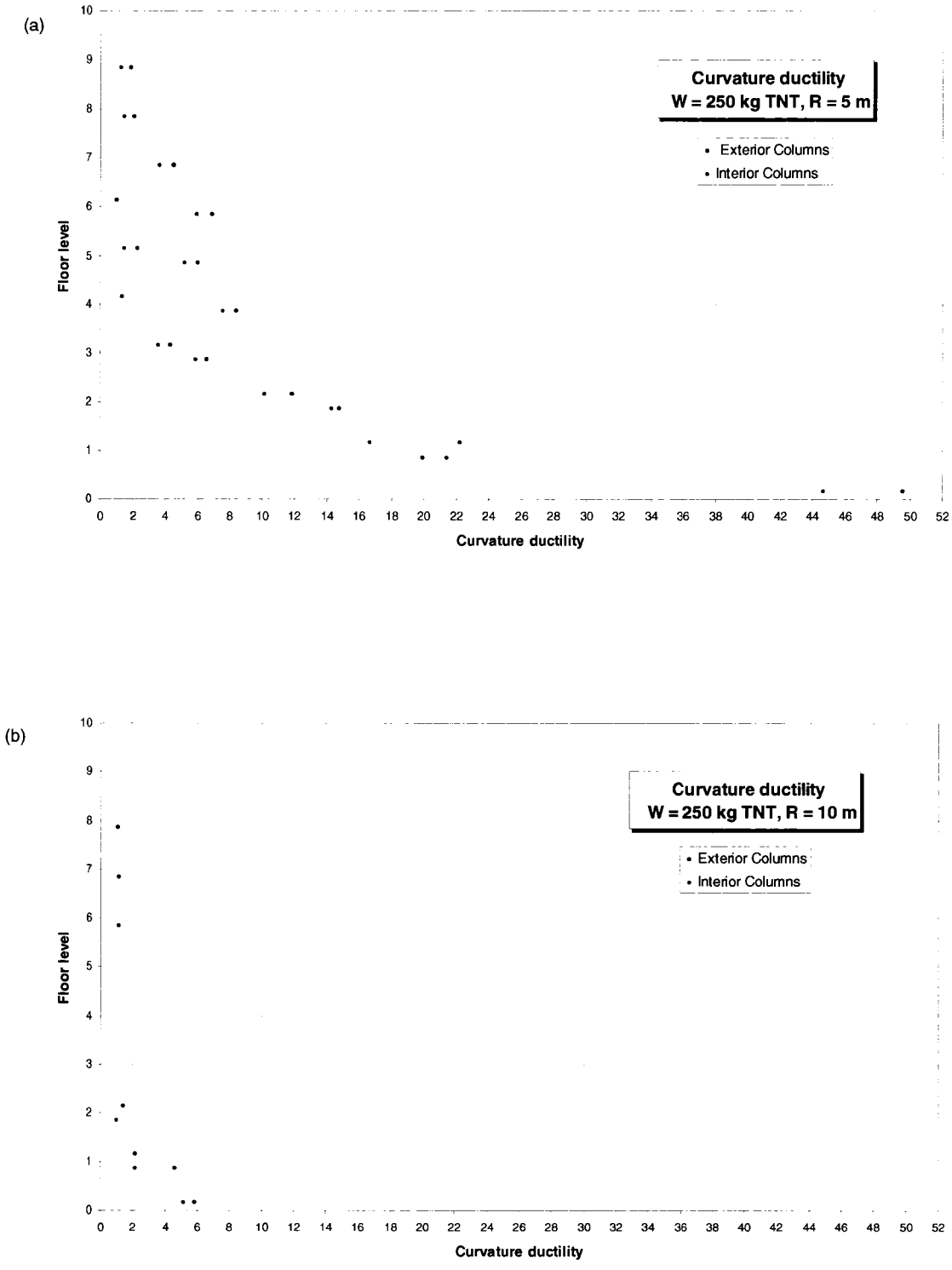

Figure 5.12 Column curvature ductilities for 250 kg TNT detonation; (a) R=5 m and (b) R=10 m.

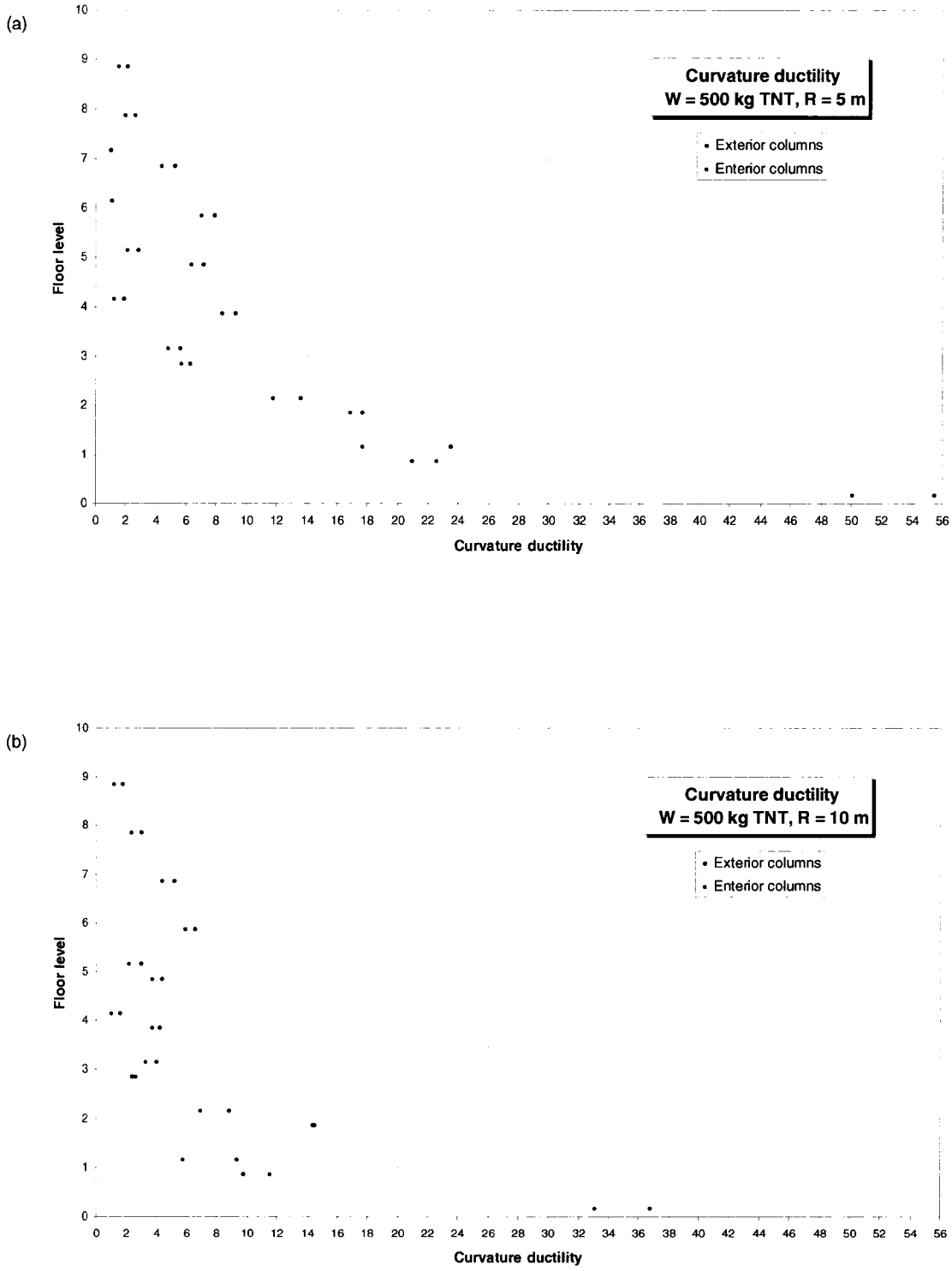

Figure 5.13 Column curvature ductilities for 500 kg TNT detonation; (a) R= 5 m and (b) R=10 m.

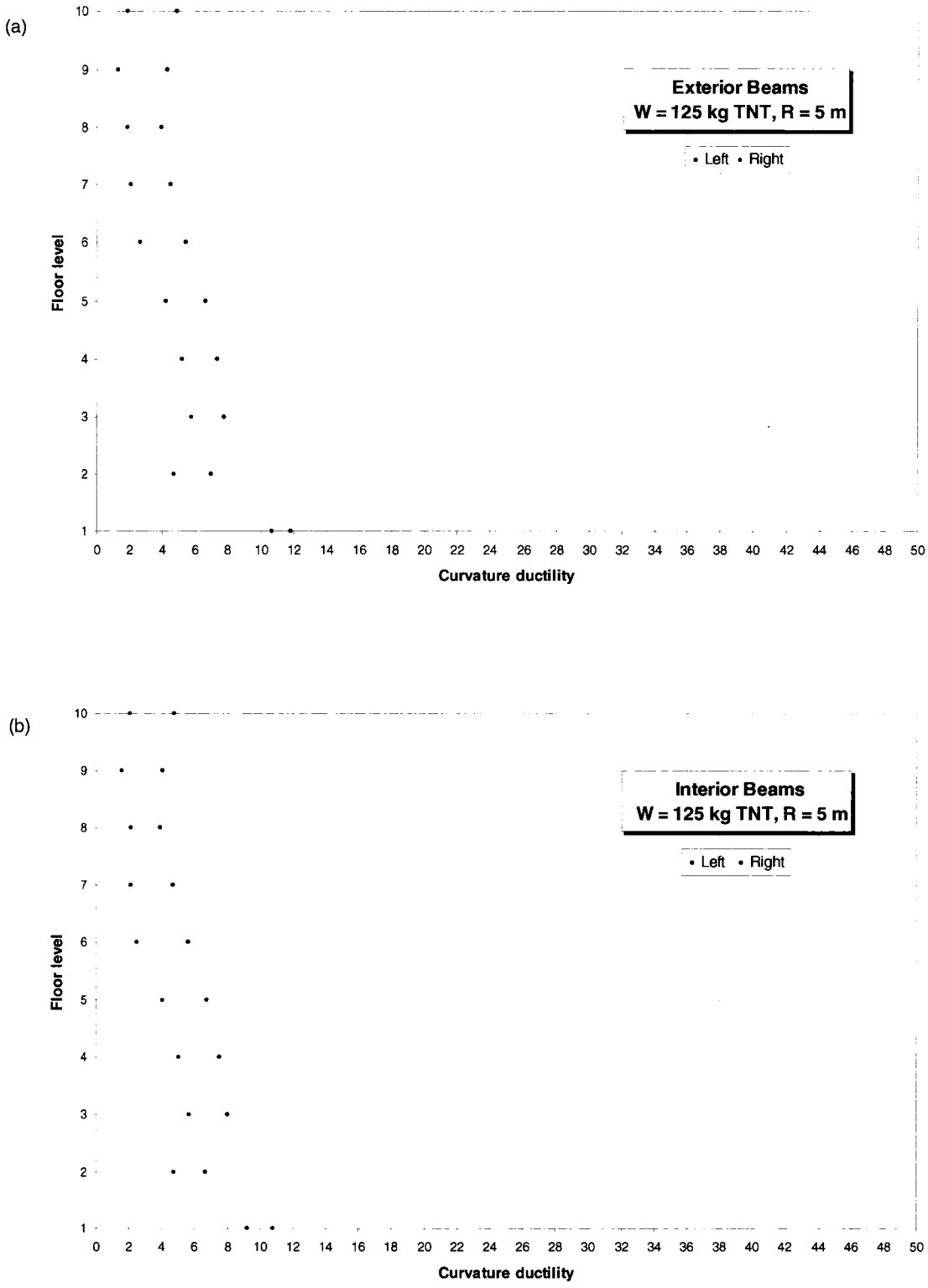

Figure 5.14 Beam curvature ductilities for 125 kg TNT detonation at R=5 m; (a) exterior beams and (b) interior beams.

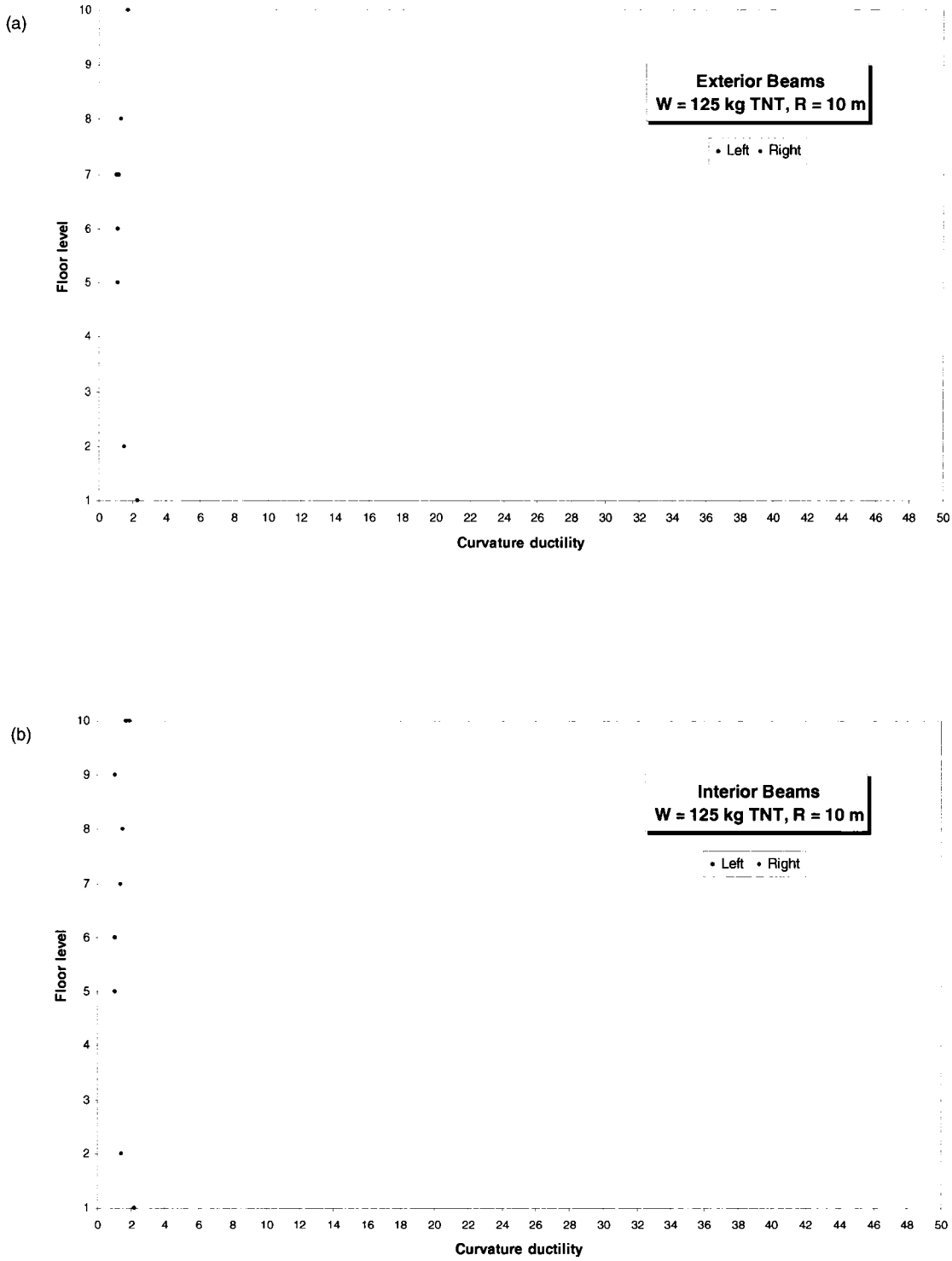

Figure 5.15 Beam curvature ductilities for 125 kg TNT detonation at R=10 m; (a) exterior beams and (b) interior beams.

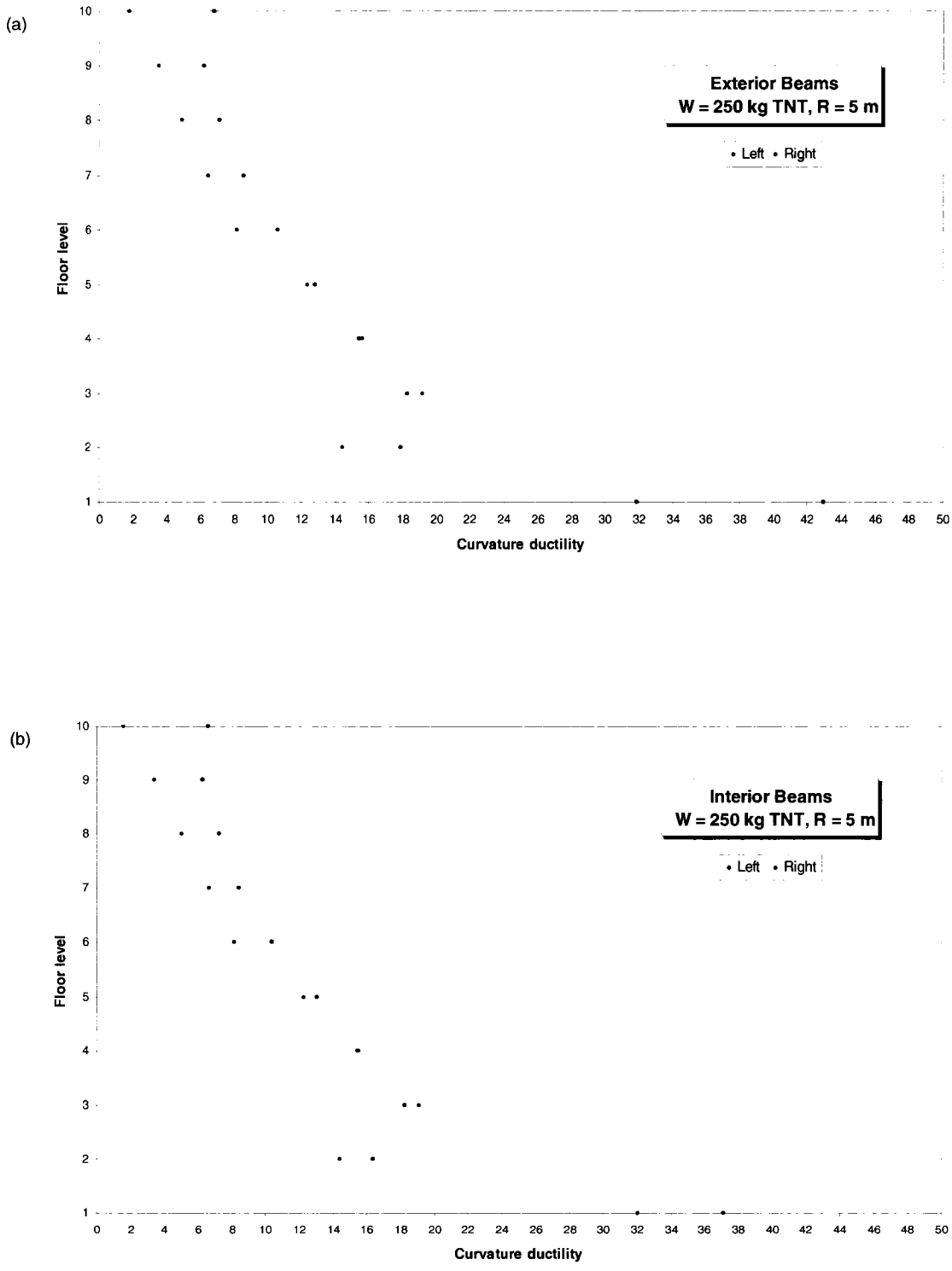

Figure 5.16 Beam curvature ductilities for 250 kg TNT detonation at R=5 m; (a) exterior beams and (b) interior beams.

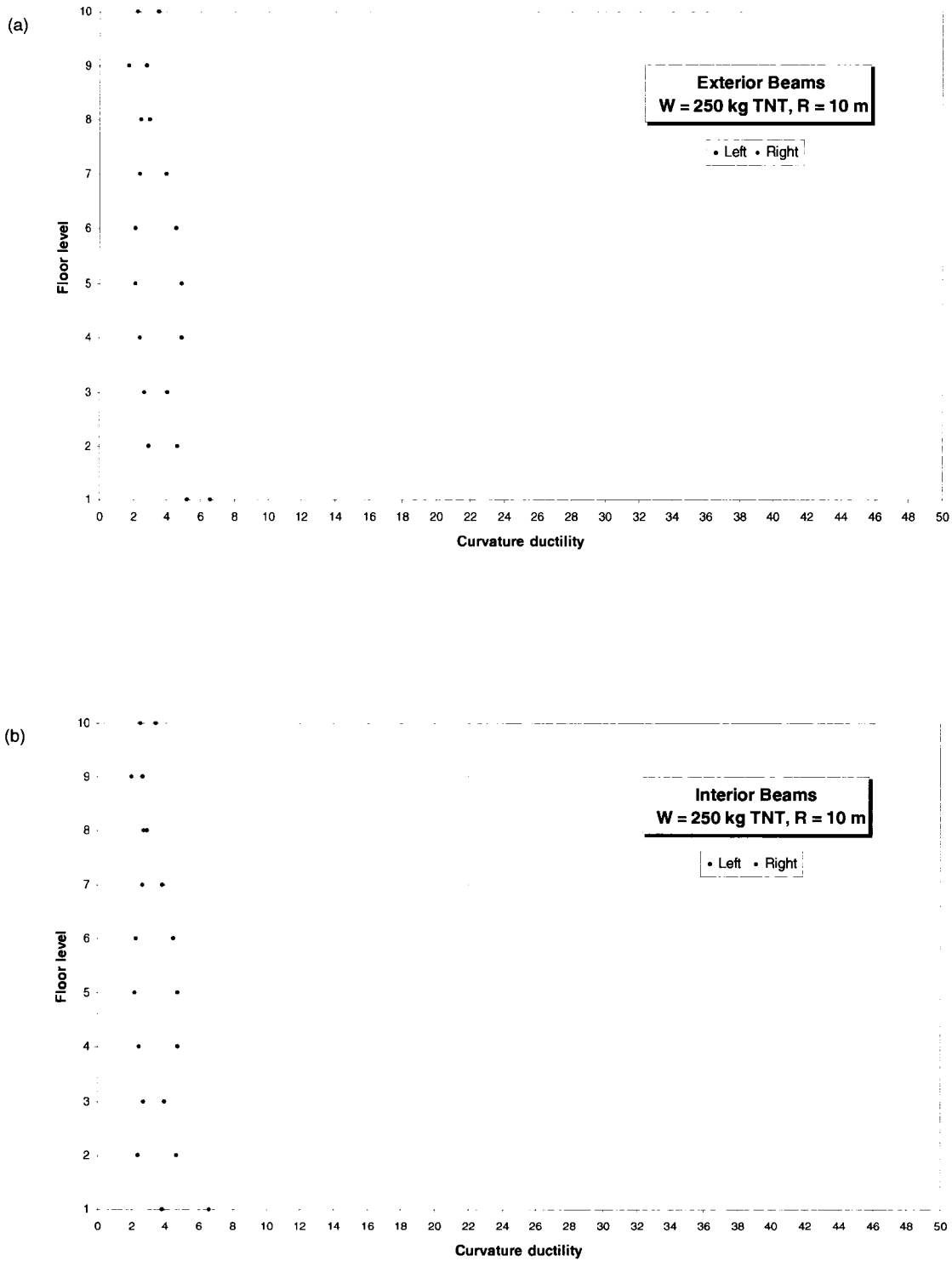

Figure 5.17 Beam curvature ductilities for 250 kg TNT detonation at R=10 m; (a) exterior beams and (b) interior beams.

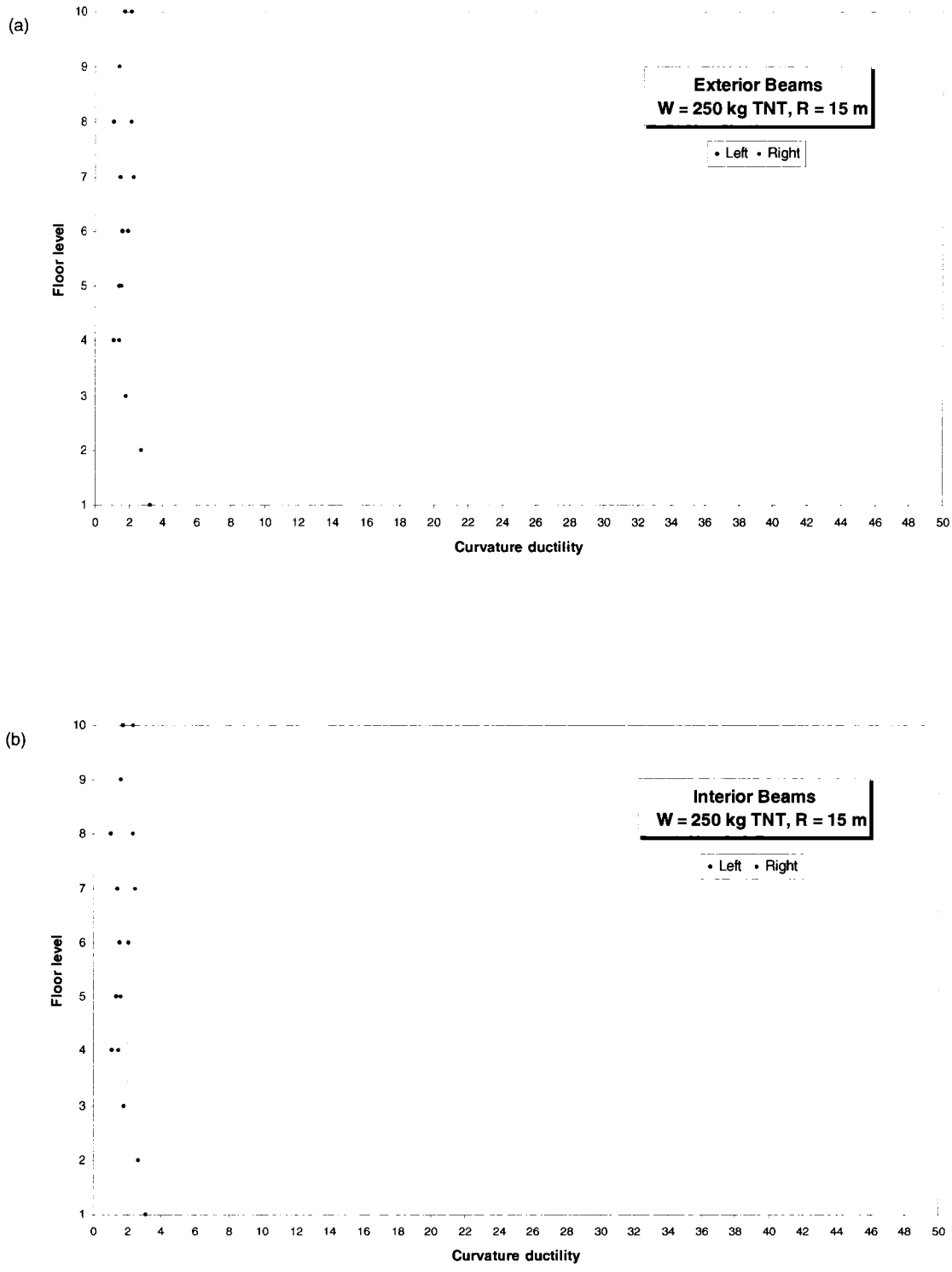

Figure 5.18 Beam curvature ductilities for 250 kg TNT detonation at R=15 m; (a) exterior beams and (b) interior beams.

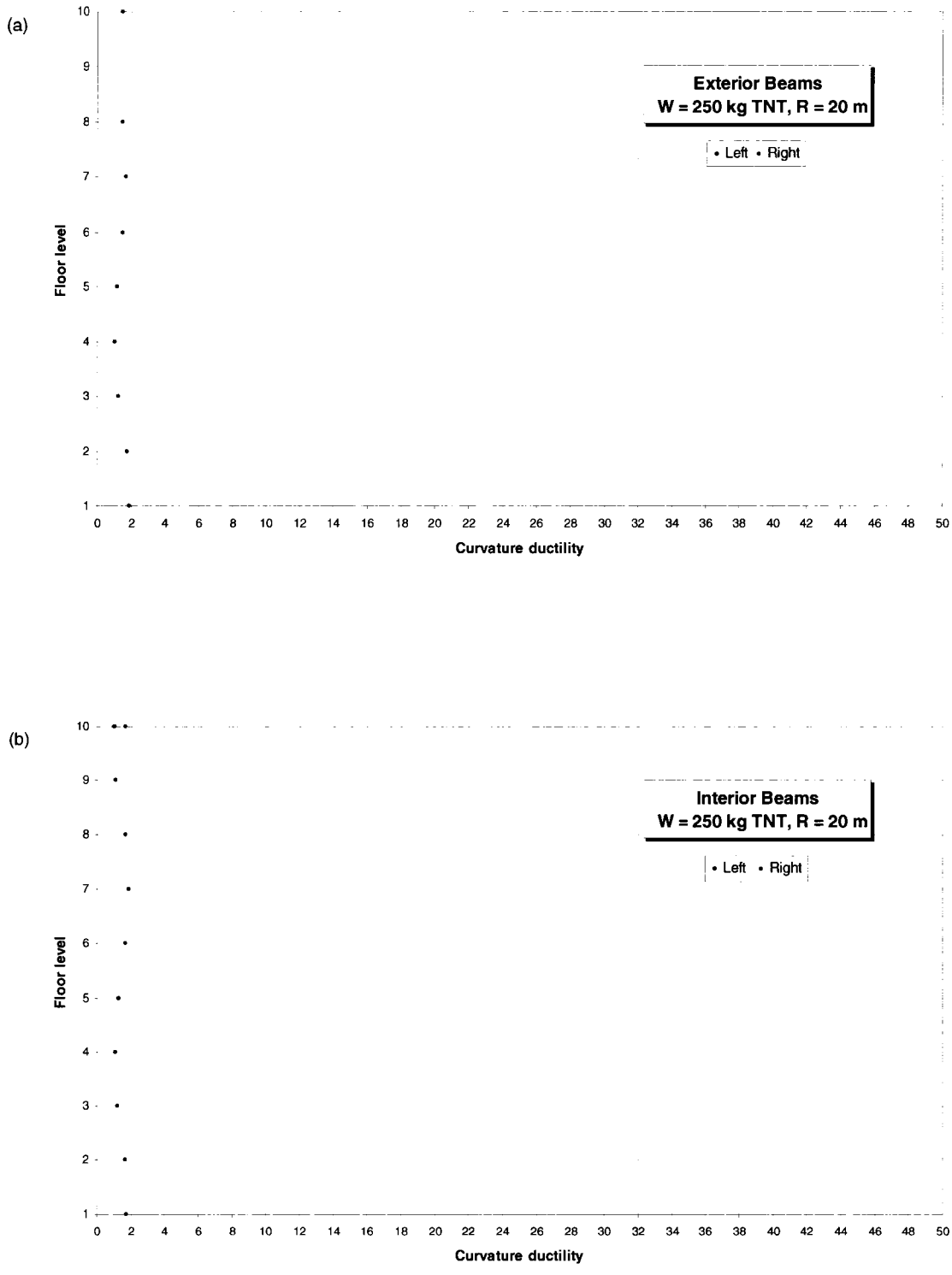

Figure 5.19 Beam curvature ductilities for 250 kg TNT detonation at R=20 m; (a) exterior beams and (b) interior beams.

(a)

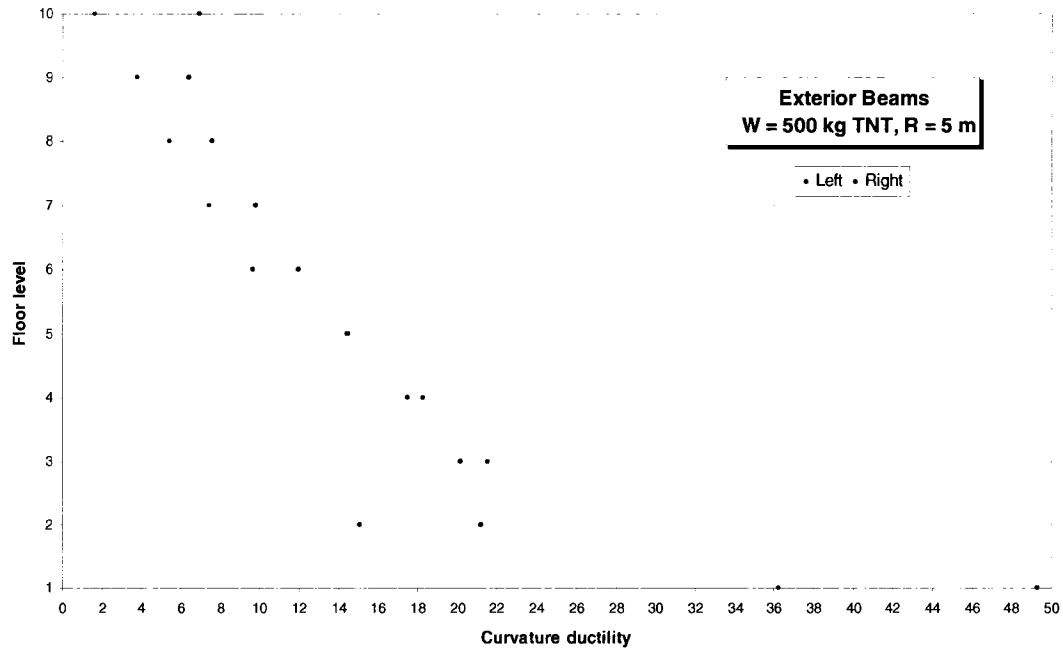

(b)

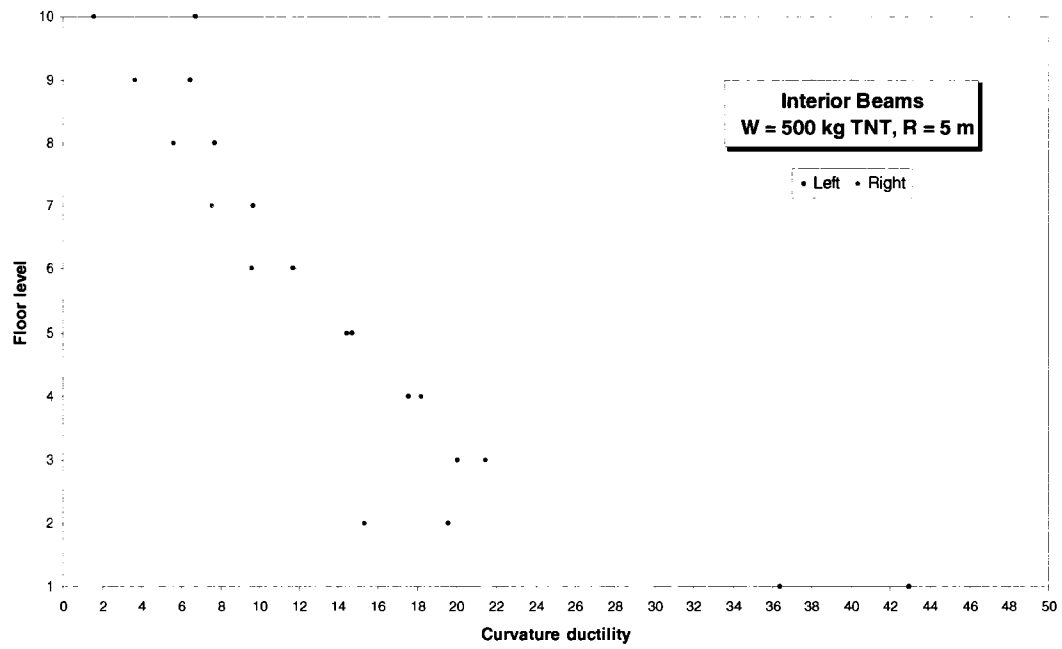

Figure 5.20 Beam curvature ductilities for 500 kg TNT detonation at R=5 m; (a) exterior beams and (b) interior beams.

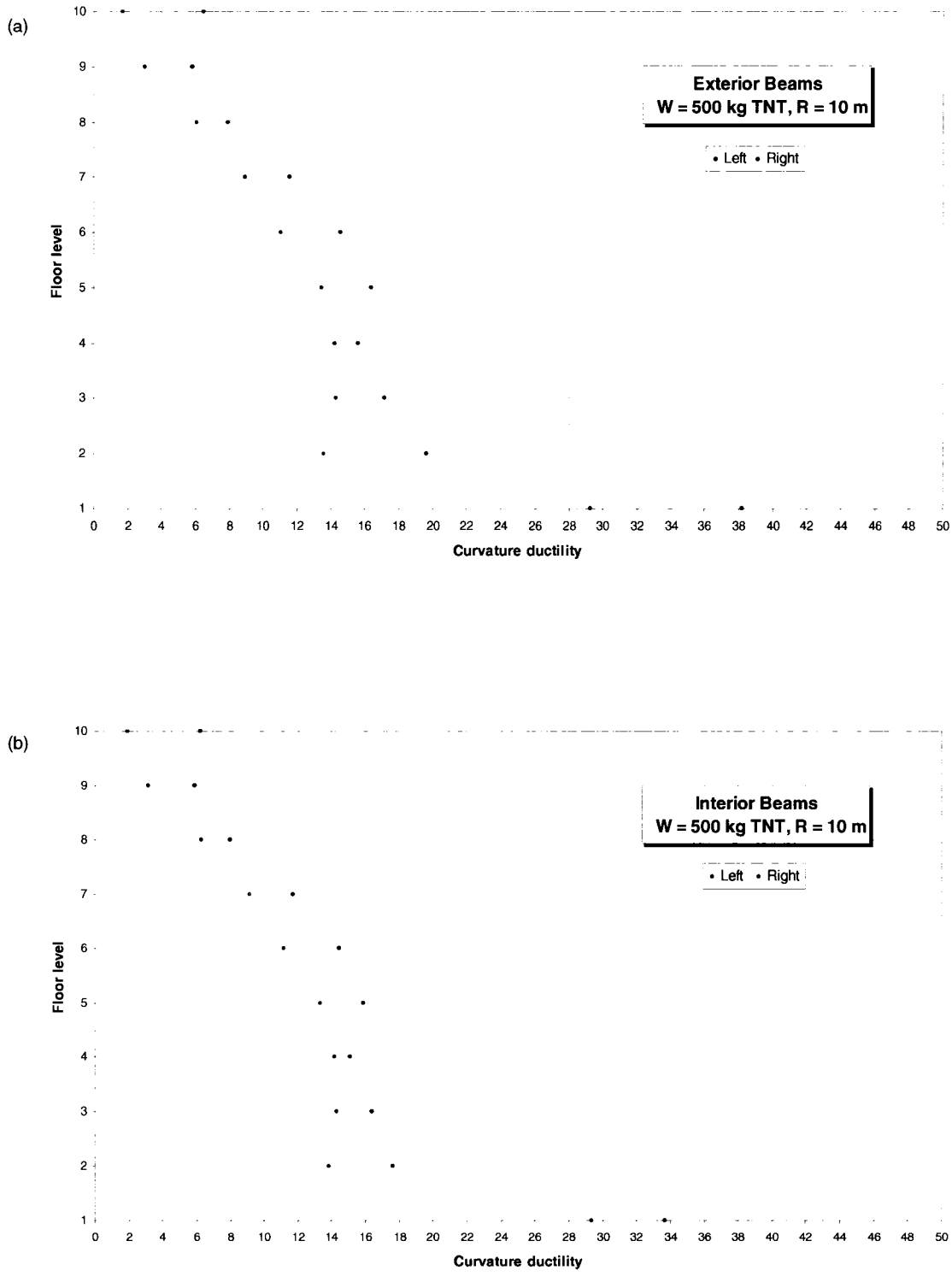

Figure 5.21 Beam curvature ductilities for 500 kg TNT detonation at R=10 m; (a) exterior beams and (b) interior beams.

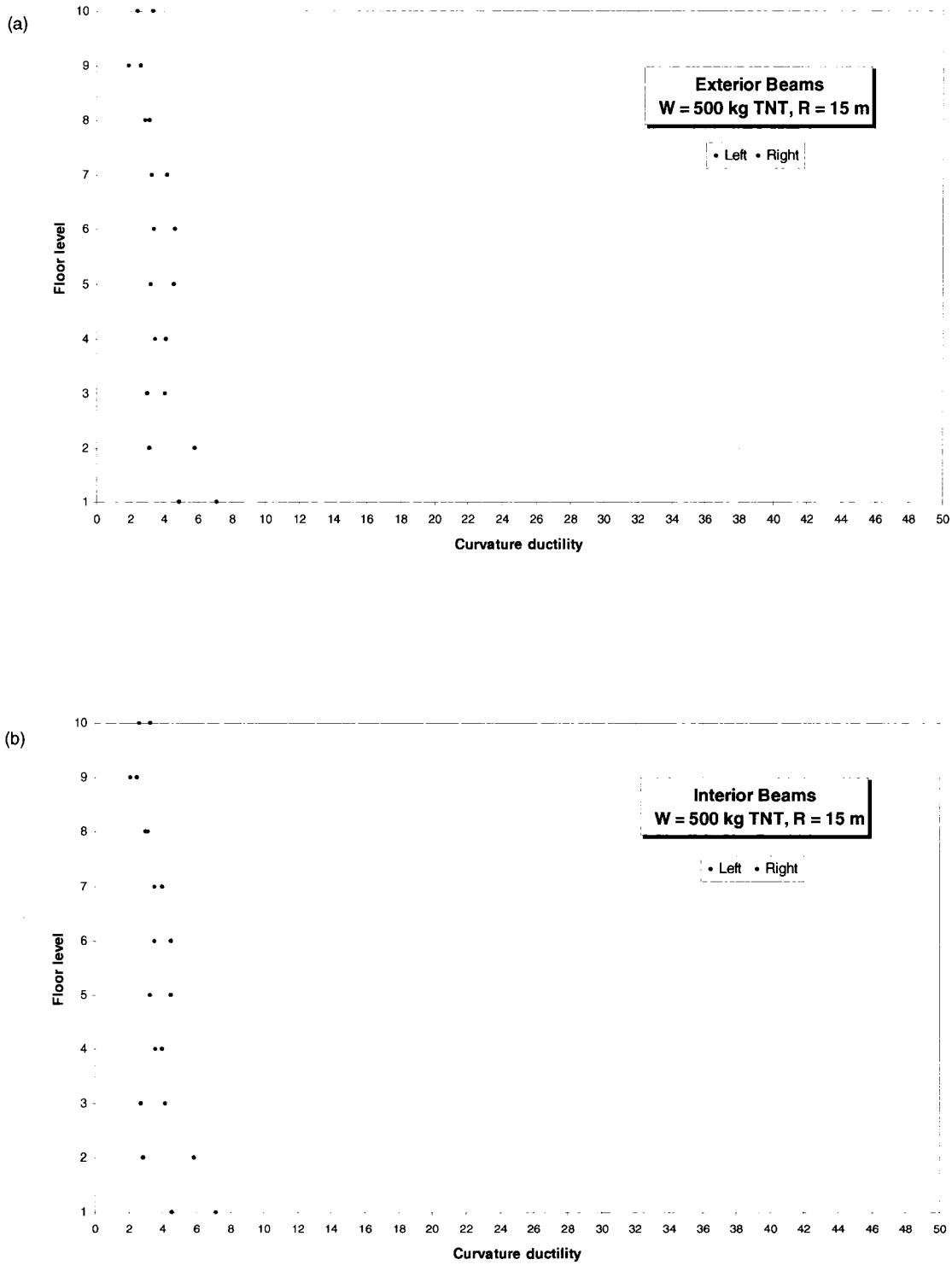

Figure 5.22 Beam curvature ductilities for 500 kg TNT detonation at R=15 m; (a) exterior beams and (b) interior beams.

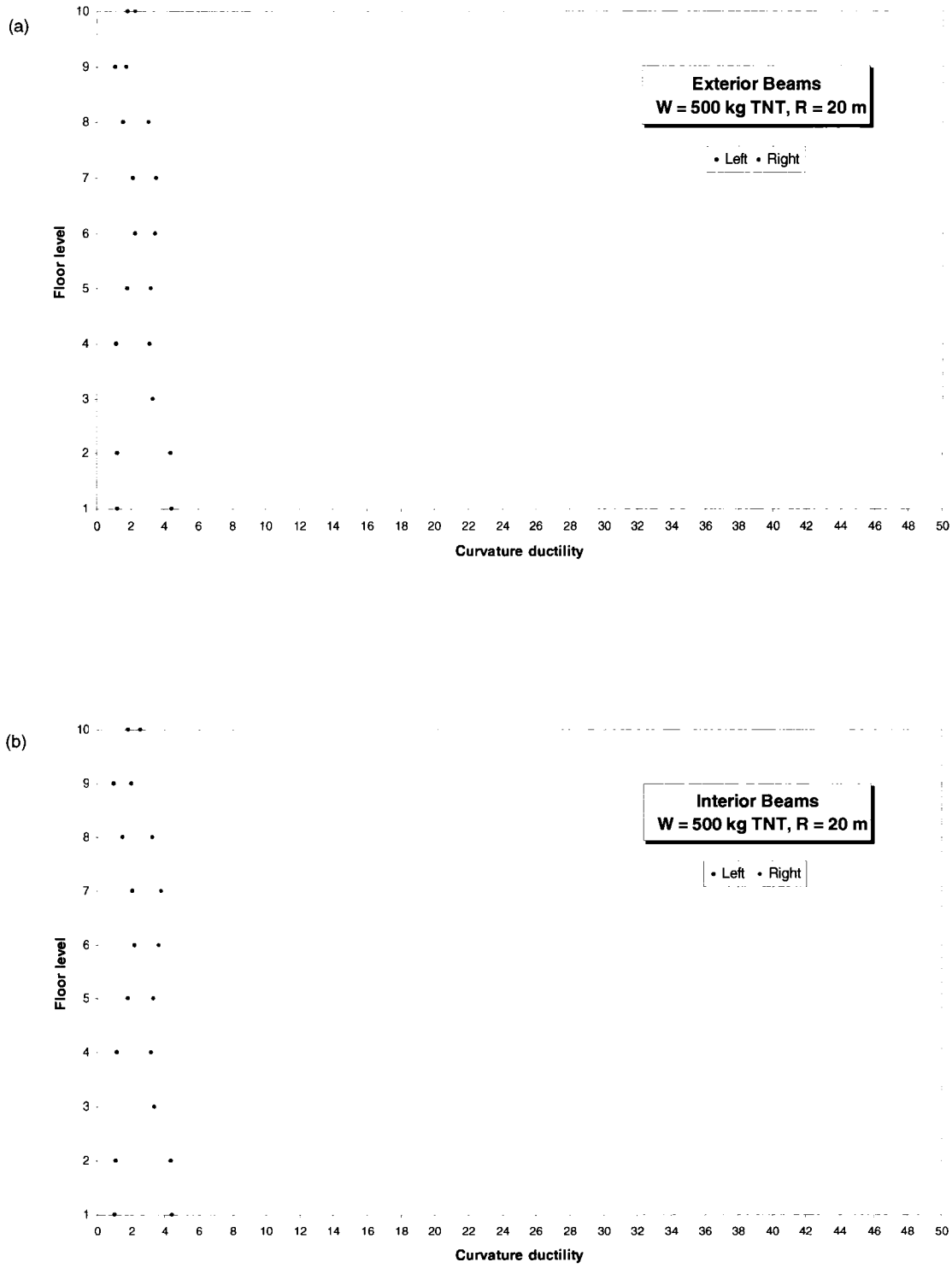

Figure 5.23 Beam curvature ductilities for 500 kg TNT detonation at R=20 m; (a) exterior beams and (b) interior beams.

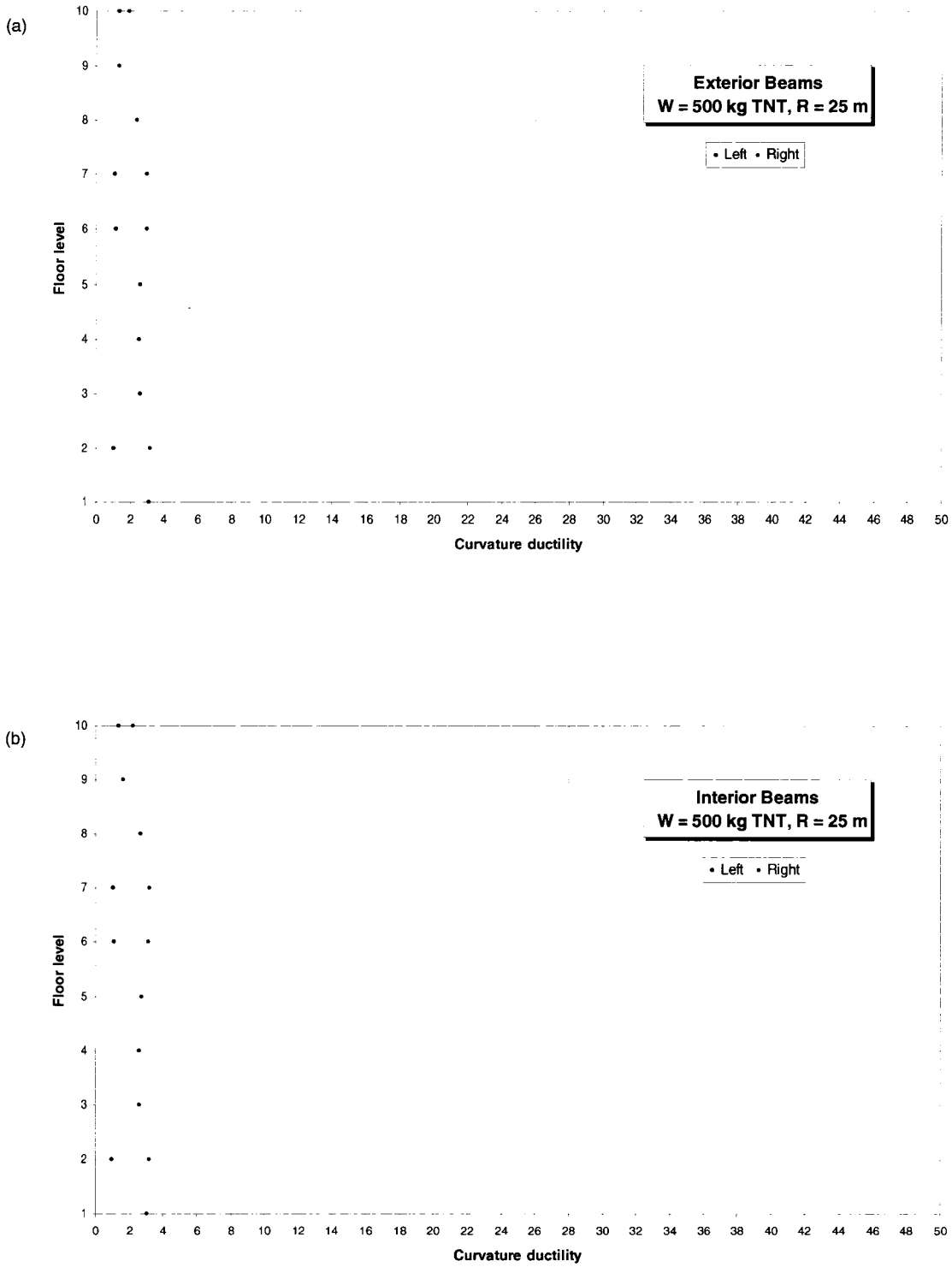

Figure 5.24 Beam curvature ductilities for 500 kg TNT detonation at R=25 m; (a) exterior beams and (b) interior beams.

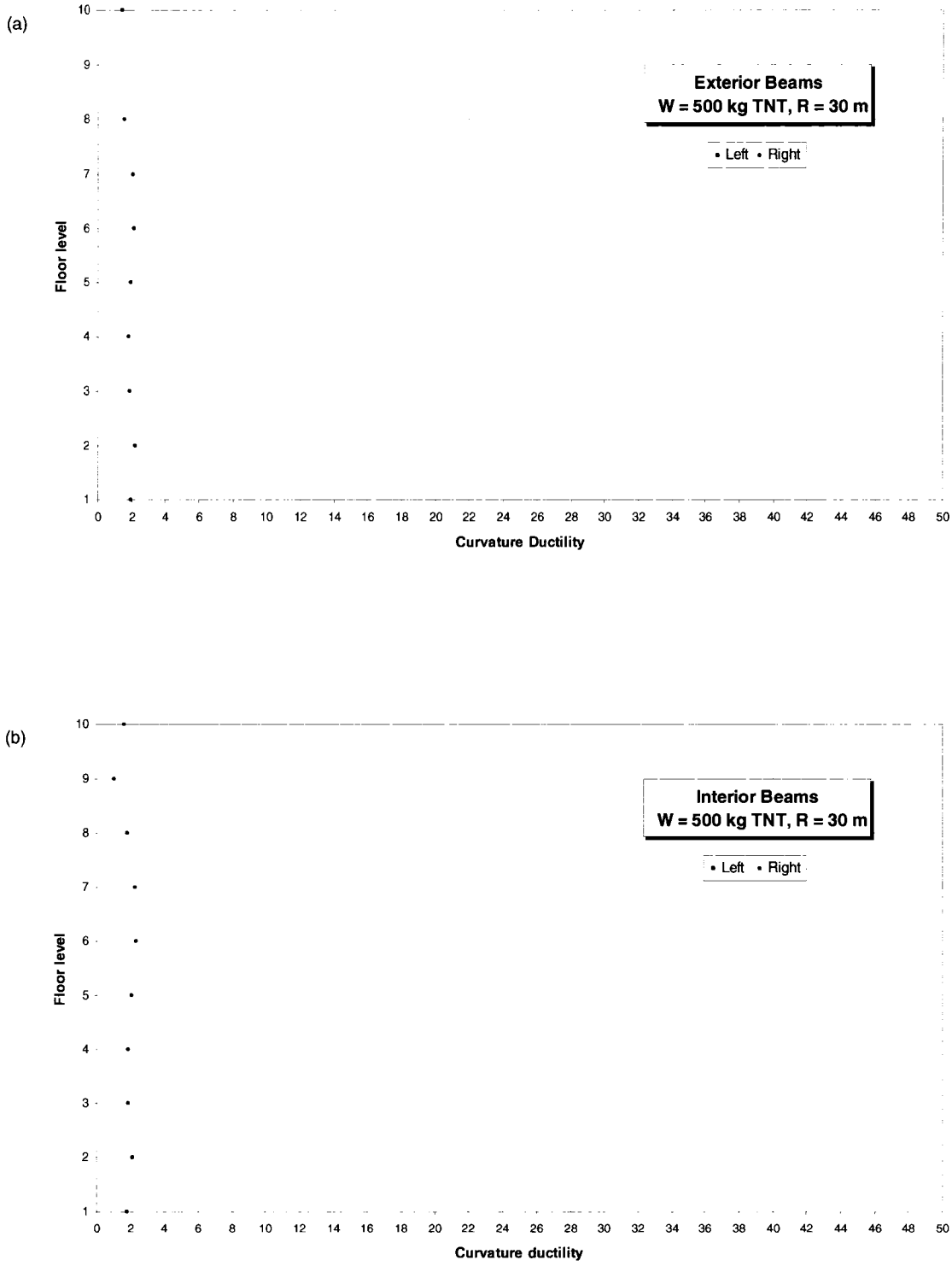

Figure 5.25 Beam curvature ductilities for 500 kg TNT detonation at R=30 m; (a) exterior beams and (b) interior beams.

Chapter 6

Progressive Collapse Analysis

6.1 Introduction

According to the U.S. General Services Administration (GSA 2003), progressive collapse is defined as "a situation where a local failure of a primary structural component leads to the collapse of adjoining members which, in turn, leads to additional collapse. Hence, the total damage is disproportionate to the original cause".

A considerable attention on the protection of building structures from progressive collapse was given by structural engineers following the collapse of a part of the 22 storey Ronan Point apartment building in London, England in 1968 (Shankar 2004). A gas explosion at the 18^{th} floor of the building triggered collapse of the corner slabs at the upper floors (above the 18^{th} floor) that was followed by collapse of all corner slabs of the building (see photograph in the Introduction). A typical example of progressive collapse is the collapse of the Alfred P. Murrah Federal Building in Oklahoma City, in 1995, due to a bomb explosion at the ground level (National Academy of Science 1995). Three columns at the first storey were badly damaged that caused total collapse of almost half of the building (Fig. 1.1, in Introduction).

While the bomb blast is one of the major causes for progressive collapse, it can also be caused by other accidents. For example, a van or truck might hit and damage an exterior column of a building, which can trigger a progressive collapse.

6.2 Guidelines for Progressive Collapse Prevention

Currently, there are two documents that provide guidelines for the design of buildings to resist progressive collapse. These are the GSA document entitled "Progressive Collapse Analysis and Design Guidelines" (GSA 2003), and the document prepared by the U.S. Department of Defence entitled "Design of Buildings to Resist Progressive Collapse" (U.S. Department of Defence 2005). The GSA Guidelines are intended for new federal office buildings and major modernization projects, and those of the U.S. Department of Defence (referred to as DoD for short) are for military building structures. In general, the provisions in both documents are similar. Since the main objective of this section is the analysis for progressive collapse, only the requirements for the analysis, as specified in the GSA and DoD Guidelines, are summarized hereafter.

6.2.1 Structural Configurations for Progressive Collapse Analysis

For moment resisting frame systems as used in this study, GSA requires that separate analyses be conducted for instantaneous loss of a column at the first storey. The following four cases are required to be considered for the removal of columns:

- Column on the perimeter, approximately at the middle of the short side of the building, should be removed.
- Column on the perimeter, approximately at the middle of the long side of the building, should be removed.
- Column at the corner of the building should be removed, and
- Interior column should be removed.

It should be mentioned that the DoD requirements regarding the removal of columns are more stringent than the GSA requirements. While GSA requires removal of columns at the first storey only, DoD requires that removal of columns be considered not only at the first storey, but at all storeys of the building.

6.2.2 Analysis Methods

There are three types of analyses that can be used in the assessment of the potential for progressive collapse of buildings. These include: (i) linear-elastic static analysis, (ii) nonlinear static analysis, and (iii) nonlinear dynamic analysis. The GSA guidelines require the use of the linear-elastic static analysis, and provide detail explanations for the steps involved in the analysis. It is also stated in the GSA guidelines that the other methods (i.e., the nonlinear static and dynamic methods) can also be used.

Both the GSA and DoD guidelines recommend the use of 3-D models in the analysis, in order to account for 3-D effects and to avoid overly conservative solutions. However, 2-D models are also allowed provided that the general response and 3-D effects can be adequately accounted for.

6.2.3 Acceptance Criteria

Acceptance criteria are specified in the GSA and DoD guidelines for the case when elastic static analysis is used. These criteria are expressed in terms of the Demand – Capacity Ratios (DCR), which are defined as

$$DCR = D/C \tag{6.1}$$

where,

D = Demand (i.e., moment, axial force, or shear force acting on the member) resulting from the elastic static analysis, and

C = capacity of the member (i.e., moment, axial force, or shear force that the member can resist).

The allowable DCR values for the structural members are DCR=2.0 for regular buildings, and DCR=1.5 for irregular buildings. Demand-capacity ratios larger than the foregoing values indicate that the building has a high potential for progressive collapse.

It is useful to mention that the GSA guidelines allow the use of increased material strengths in the calculation of the capacities of the structural members. The nominal strengths of the concrete and reinforcing steel may be increased by applying a strength increase factor of 1.25 (Section 4.1.2.5 in GSA guidelines).

6.3 Progressive Collapse Analysis

In this study, progressive collapse analysis was conducted for both the moderately ductile and for the ductile buildings described in Chapter 4. The objective of the analysis was to evaluate the potential for progressive collapse for building structures designed according to NBCC 2005.

A 3-D model was developed as required by the GSA guidelines. Since the geometrical properties of the moderately ductile and the ductile buildings are identical, the 3-D model is the same for both buildings. The model was developed using the structural analysis program SAP 2000 (CSI 2000).

Columns were removed at the first storey. Figure 6.1 shows the cases considered in the analysis. As can be seen in the figure, the following three cases were investigated:

Case 1: Exterior column removed (at the long side of the building),
Case 2: Corner column removed, and
Case 3: Interior column removed.

These three cases are referred to as the "analysis cases" in the further discussion. It should be mentioned that the removal of exterior column at the short side of the building was not considered since it is identical as Case 1. The loads applied at the shaded areas in Fig. 6.1 are 2DL + 0.5LL, where DL represents dead load, and LL represents live load. The loads on the other areas of the floor are DL + 0.5LL. Figure 6.2 shows the elevations of the transverse and longitudinal frames of Case 3 (i.e., the interior column removed) and the corresponding loads at the floors. This loading is as required by the GSA guidelines. It should be mentioned that the uniform loads shown in Fig. 6.2 are only for illustration of the magnitude of the loads acting on the frame members. The actual loads used in the analyses are triangular.

Elastic static analysis using 3-D model was conducted for each of the three cases of removed columns, as required by the GSA guidelines. The program SAP 2000 was used for the analysis. Demands from the applied loads (Fig. 6.2) were computed for beams and columns. These included moments, axial forces, and shear forces. The demands for both the moderately ductile and the ductile buildings are the same. This is because the geometrical properties of both buildings are identical. However, the capacities of the structural members

of the moderately ductile and the ductile buildings are different because they have different reinforcement in the beams.

Moment capacity, axial load capacity, and shear capacity were computed for all structural members of the buildings. Increased strengths of the concrete and reinforcement were used in the computation of the capacities. The nominal strengths of both the concrete and the reinforcing steel were increased by a factor of 1.25, as allowed by the GSA guidelines. Moment (i.e., flexural) capacities and axial load capacities were computed using the longitudinal reinforcement in the structural members. Shear capacities were computed by assuming transverse reinforcement of M10 with spacing of 10 cm representing the minimum transverse reinforcement according to the CSA standard A23.3-94 (CSA 1994).

Demand/capacity ratios (DCR) were computed using the demands and capacities for moments, axial loads, and shear. It was found that the DCR values for axial loads and shear are all well below 1.0, indicating that the axial and shear deformations are not critical for the assessment of the progressive collapse potential for the buildings considered. Given this, only the moment DCR results for the beams are discussed hereafter.

6.4 Discussion of Results

6.4.1 Results for Moderately Ductile Frame Building

The moment DCR results for the moderately ductile frame are shown in Figures 6.3, 6.4, and 6.5 for the three analysis cases (Fig. 6.1). Each figure shows the moment DCR values in the beams of the longitudinal and the transverse frames. The DCR ratios are shown only for the spans where the columns are removed. The values above the beams correspond to the negative moment demand, and those below the beams correspond to the positive moment demand. For example, the DCR values of 1.29 and 1.30 of the first floor beam in Fig. 6.3 are computed using the negative moment demands at the supports and the negative moment capacity corresponding to the yielding of the top reinforcement in the beam. Similarly, the value of 2.04 below the beam (Fig. 6.3) was computed using the positive moment demand at the section (where the column is removed) and the positive moment capacity corresponding to yielding of the bottom reinforcement in the beam at that section.

As required by the GSA guidelines, plastic hinges were placed at the locations where the DCR exceed 1.0, to determine the redistribution of the moments. As an example, consider

the beam at the first floor of the longitudinal frame (Fig. 6.5(a)). The DCR value for the beam is 2.46 at the section where the column is removed. Two hinges were placed at the beam-column joint, one left of the joint, and another one right of the joint. Note that the beam-column joint is not considered as a point, but it is defined by the sizes of the rigid zones of the beam and the column. Moments corresponding to the positive flexural capacity of the beam were placed at the hinges. This was done for all the joints with DCR values larger than 1.0. It was found that this does not affect significantly the redistribution of the moments.

As can be seen in Fig. 6.3, the DCR values from the analysis Case 1 (i.e., when exterior column is removed) are all smaller than the limit value of 2.0 specified by the GSA guidelines, with the exception of the value of 2.04 at the first floor beam which very slightly exceed the limit of 2.0. The DCR values from the analysis Case 2 (Fig. 6.4, for corner column removed) are much smaller than the value of 2.0. The foregoing observations indicate that the building satisfies the GSA progressive collapse acceptance criteria for the analysis Case 1 and Case 2, i.e., no progressive collapse would occur when an exterior column or corner column is removed.

The DCR values for the analysis Case 3 (Fig. 6.5, for interior column removed) indicate that the building is vulnerable to progressive collapse. DCR values larger than 2.0 are obtained for the beams of the 1^{st} to the 4^{th} floor.

For illustration, Figures 6.6, 6.7, and 6.8 show the deflected shapes of the frames for the analysis cases 1, 2, and 3 respectively. The maximum displacements are shown in the figures. It can be seen that the largest displacement of 7 cm was obtained for the analysis Case 3 (i.e., when the interior column is removed).

6.4.2 Results for Ductile Frame Building

The demand/capacity ratios (DCR) for the ductile building are shown in Figures 6.9, 6.10, and 6.11 for the three analysis cases considered (Fig. 6.1). DCR values larger than 2.0 can be observed for all three cases. The DCR values for Case 1 (Fig. 6.9, exterior column removed) and Case 3 (Fig. 6.11, interior column removed) are especially very high, with maximum values above even 3.0. The values for the analysis Case 2 (Fig. 6.10, corner column removed) are smaller than those for the Case 1 and Case 3, but few values exceed the

GSA limit value of 2.0. Based on these results, the ductile building is vulnerable to progressive collapse according to the GSA criteria.

The vertical displacements for the three analysis cases of the ductile building are the same as those of the moderately ductile building (Figs. 6.6 to 6.8). This is because the geometrical properties of both buildings are identical.

6.5 Summary

An overview of the GSA requirements for progressive collapse, and results from progressive collapse analyses of moderately ductile and ductile buildings are presented in this Chapter. The buildings described in Chapter 4 were used in the analysis. Columns were removed at the first storey of each building. The following three cases were considered: (i) exterior column removed (at the long side of the building), (ii) corner column removed, and (iii) interior column removed. Elastic static analysis was conducted for each of these cases using 3-D models, and applying loads as required by the GSA guidelines. Demand/capacity ratios (DCR) obtained from the analysis, and the GSA criteria were used for the assessment of the vulnerability to progressive collapse. The main observations from the results are as follows:

- The moderately ductile building is vulnerable to progressive collapse when an interior column at the first storey is removed. Based on the GSA criteria, no progressive collapse is expected when an exterior or corner column is removed.

- The ductile building has a high potential for progressive collapse when any column at the first storey is removed (i.e., exterior, corner, or interior column).

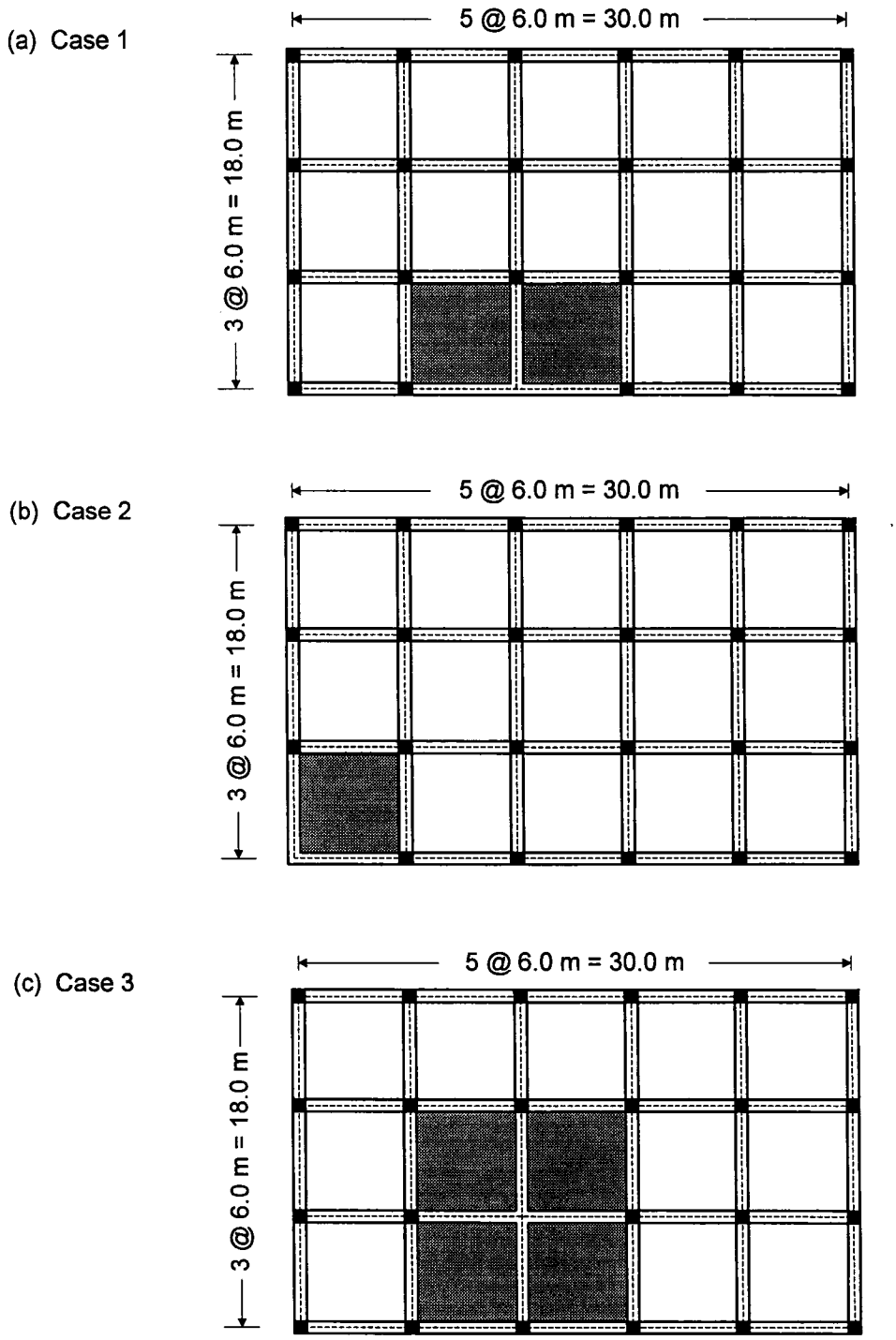

Figure 6.1 Cases considered in the progressive collapse analysis: (a) exterior column removed, (b) corner column removed, and (c) interior column removed.

Note: The loads on the dashed areas are 2DL+0.5LL, and elsewhere are DL+0.5LL

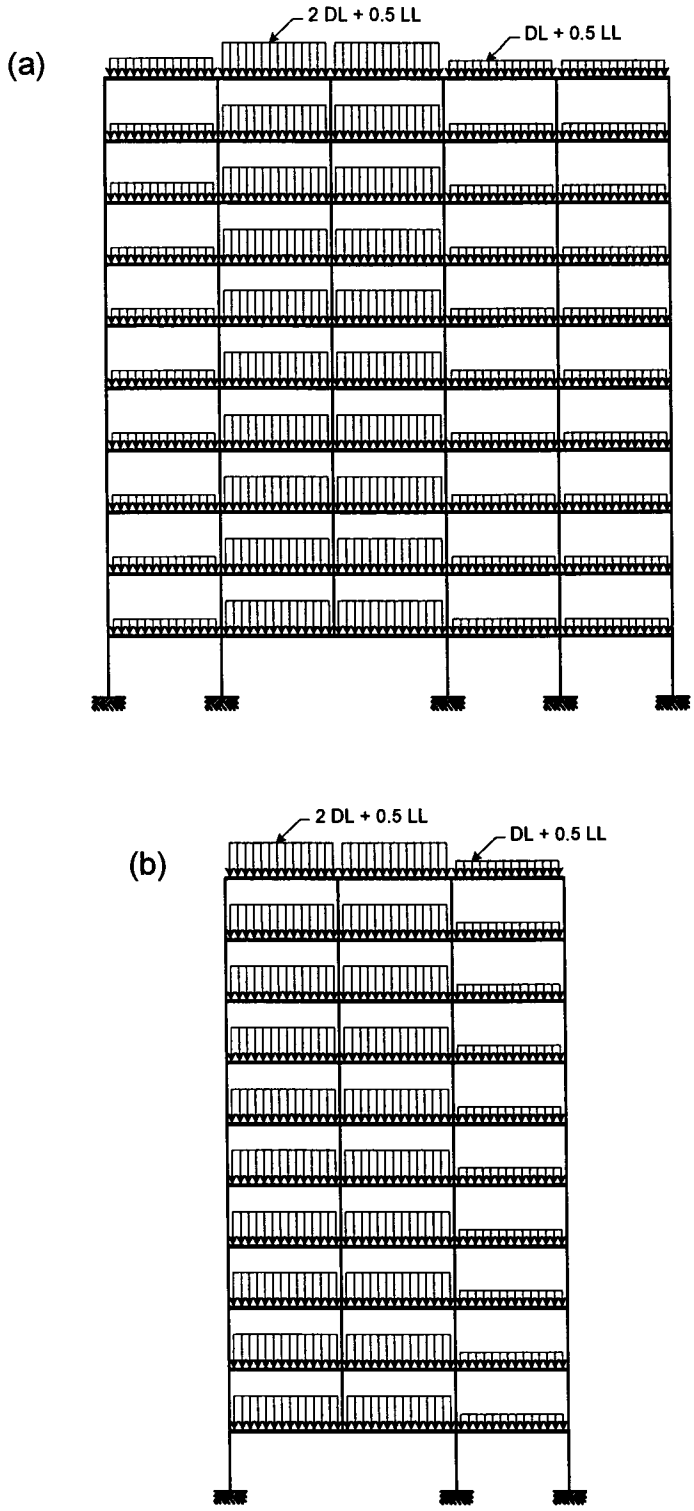

Figure 6.2 Schematic for the loads for Case 3 of the progressive collapse analysis.

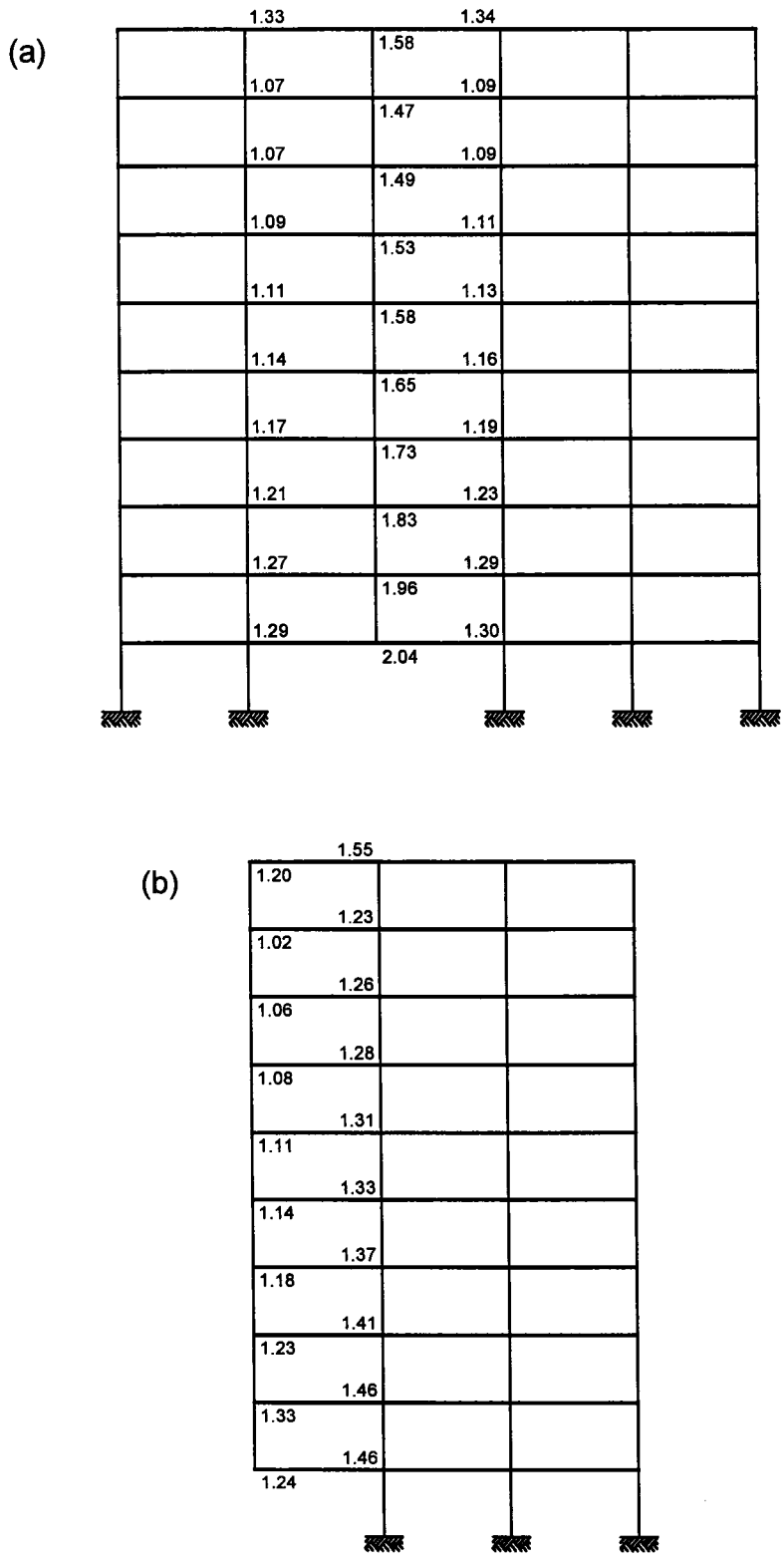

Figure 6.3 Demand/capacity ratios for Case 1 of the progressive collapse analysis of the moderately ductile building: (a) longitudinal frame and (b) transverse frame.

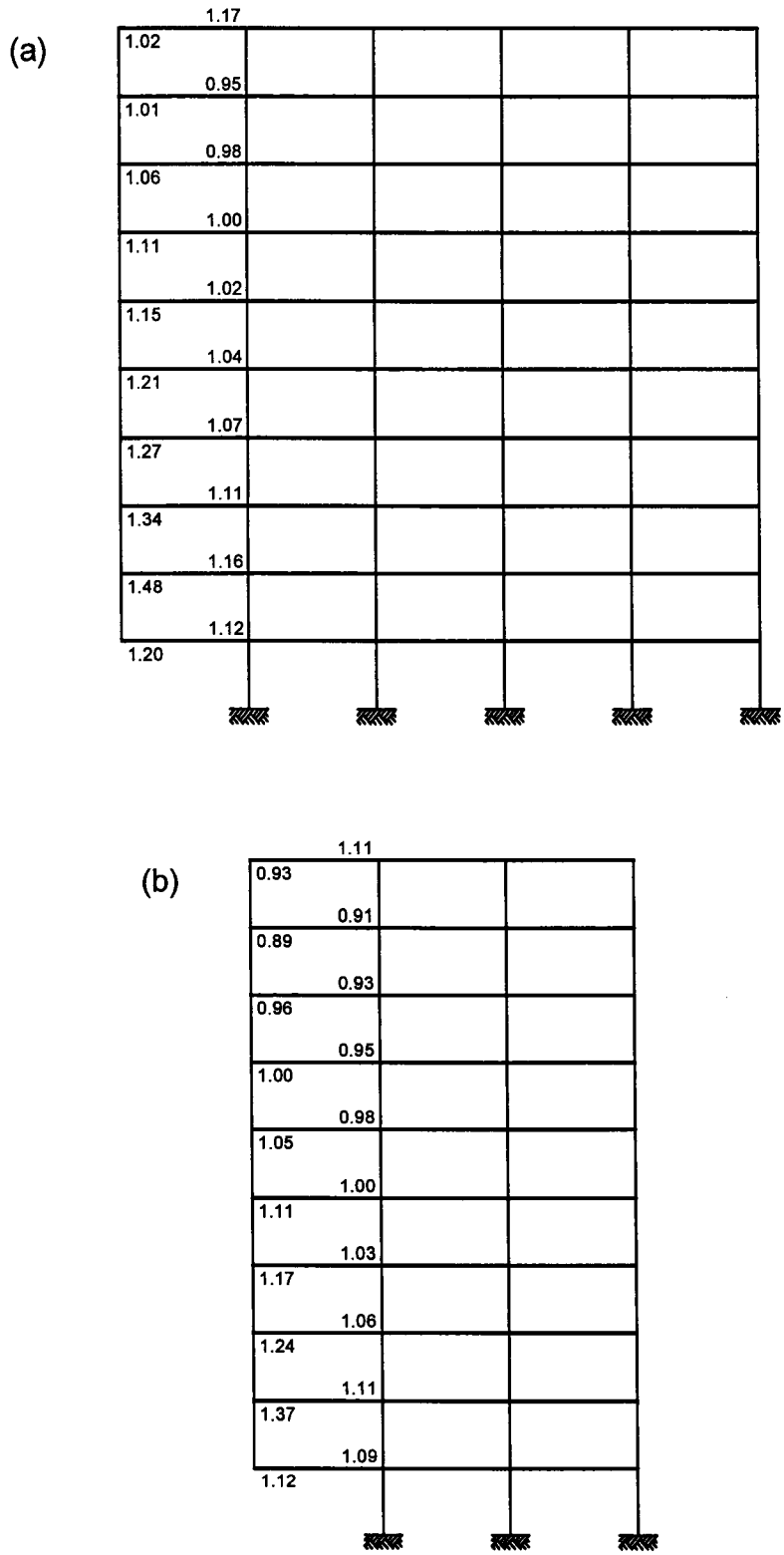

Figure 6.4 Demand/capacity ratios for Case 2 of the progressive collapse analysis of the moderately ductile building: (a) longitudinal frame and (b) transverse frame.

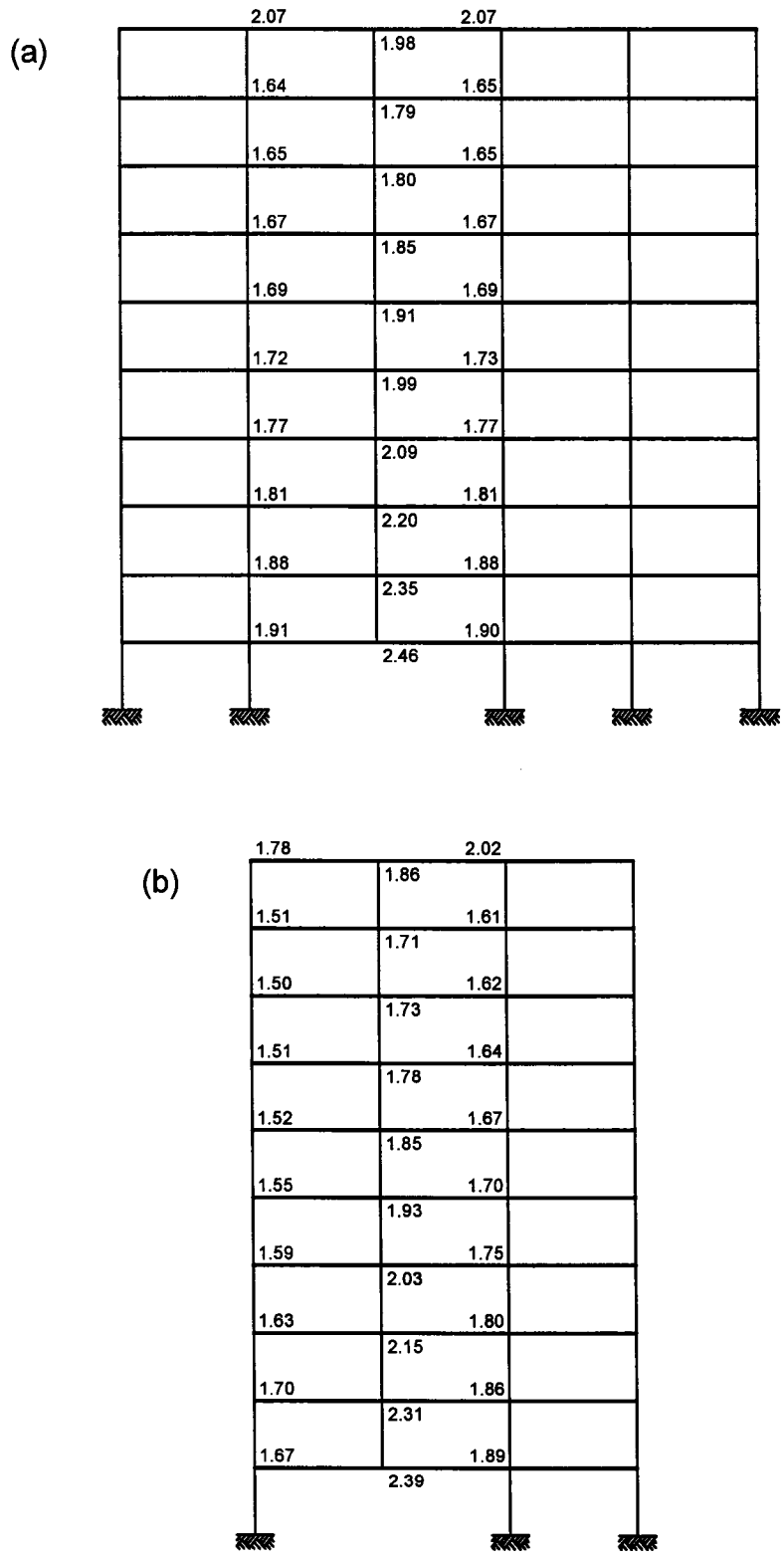

Figure 6.5 Demand/capacity ratios for Case 3 of the progressive collapse analysis of the moderately ductile building: (a) longitudinal frame and (b) transverse frame.

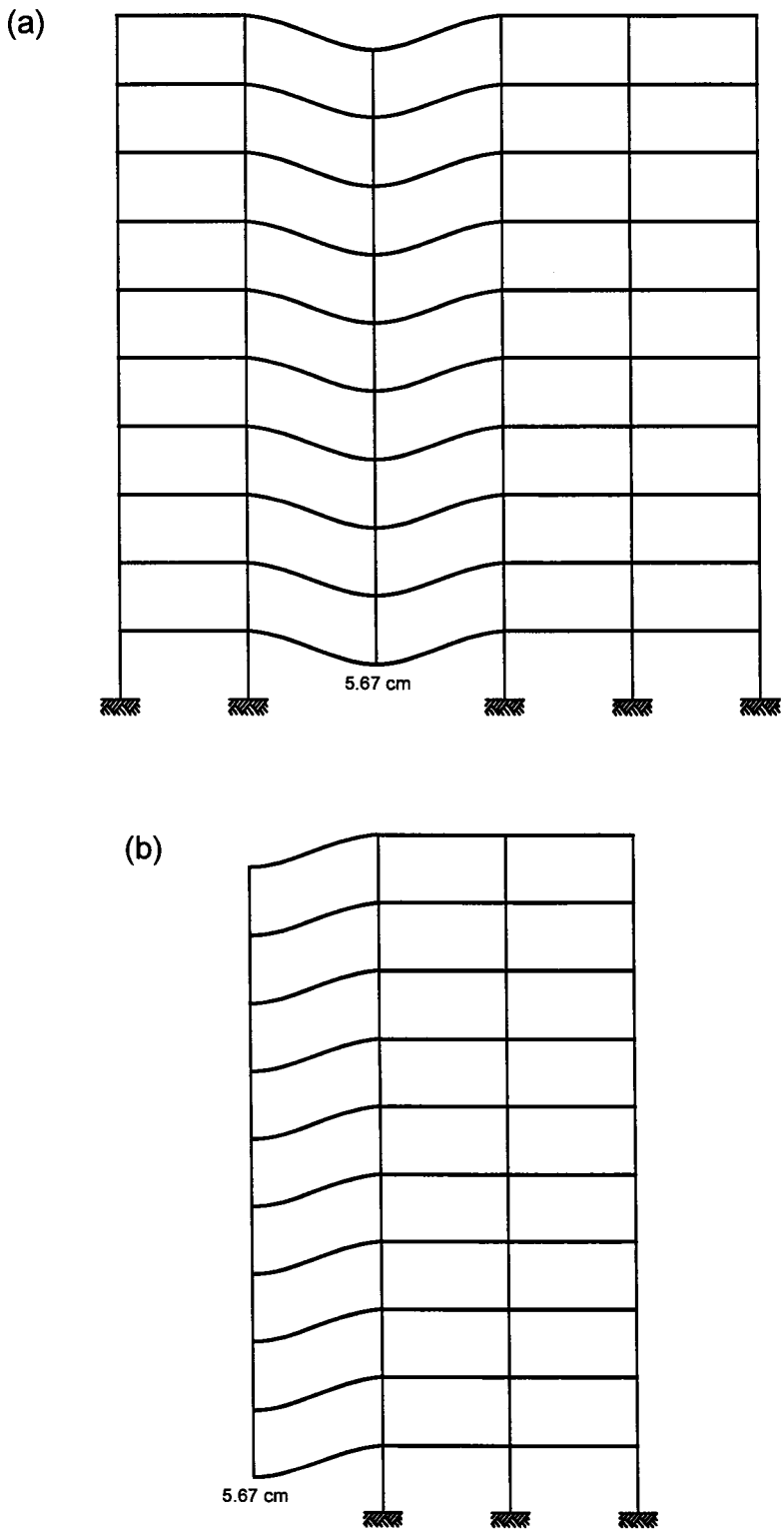

Figure 6.6 Displacements for Case 1 of the progressive collapse analysis: (a) longitudinal frame and (b) transverse frame.

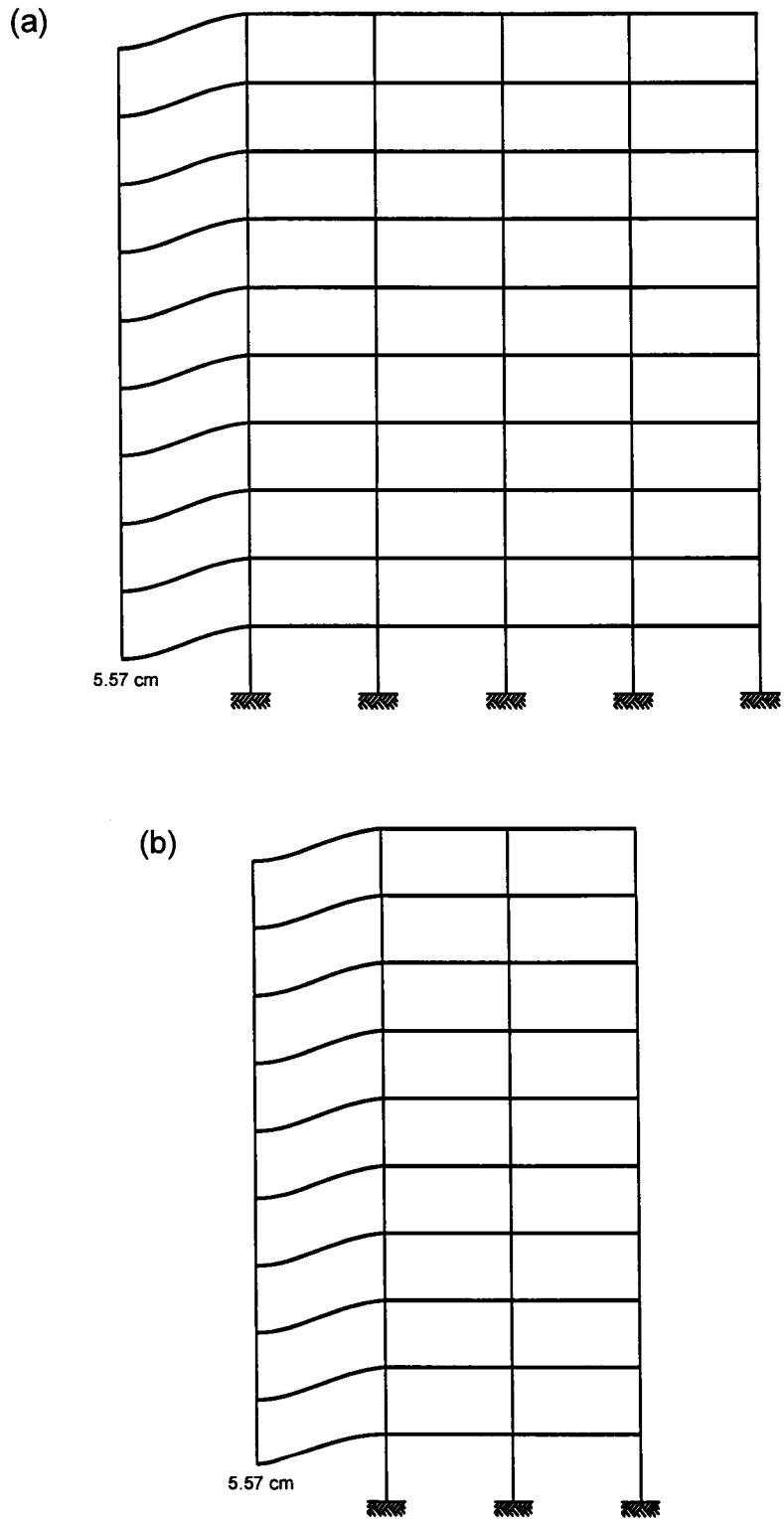

Figure 6.7 Displacements for Case 2 of the progressive collapse analysis: (a) longitudinal frame and (b) transverse frame.

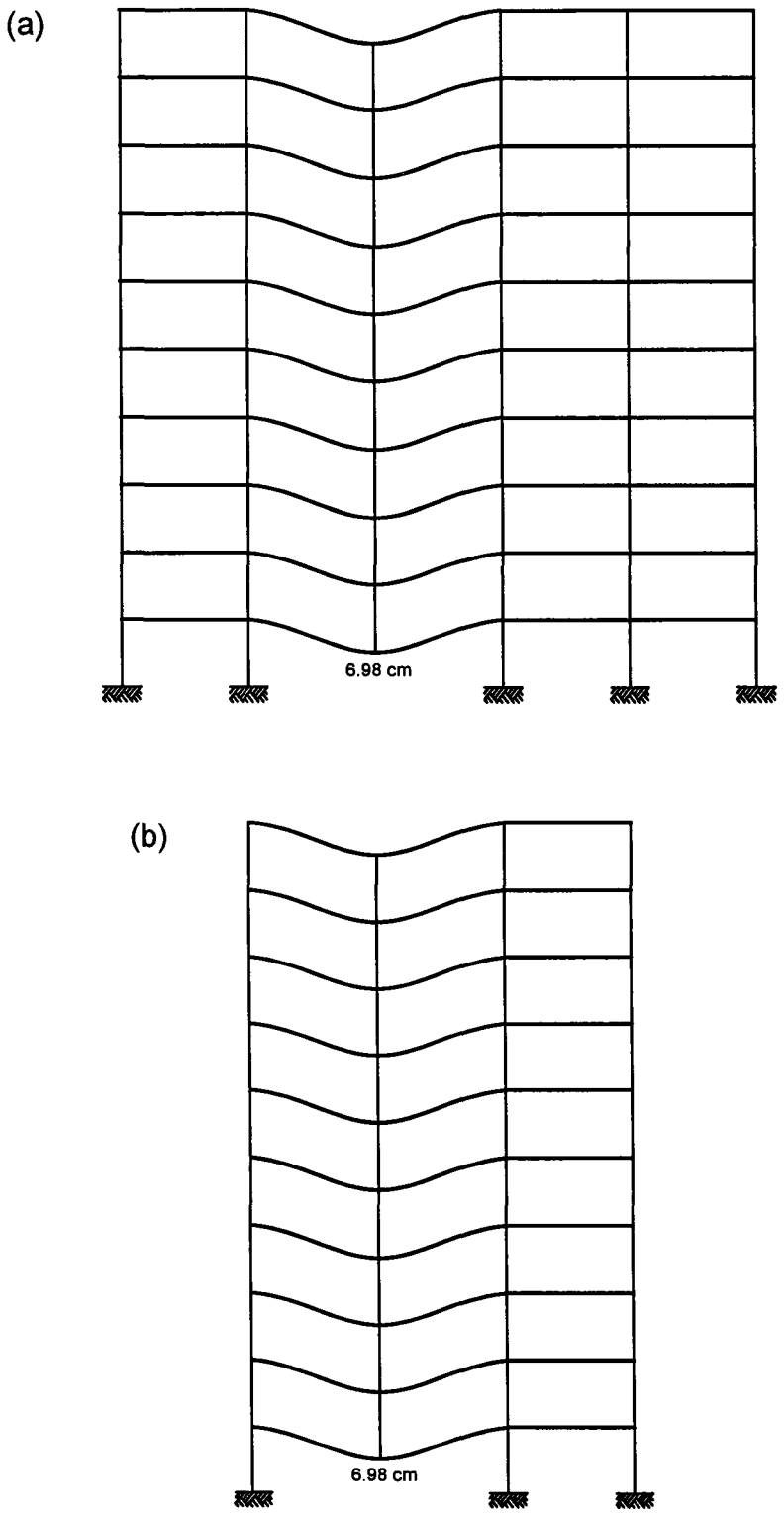

Figure 6.8 Displacements for Case 3 of the progressive collapse analysis: (a) longitudinal frame and (b) transverse frame.

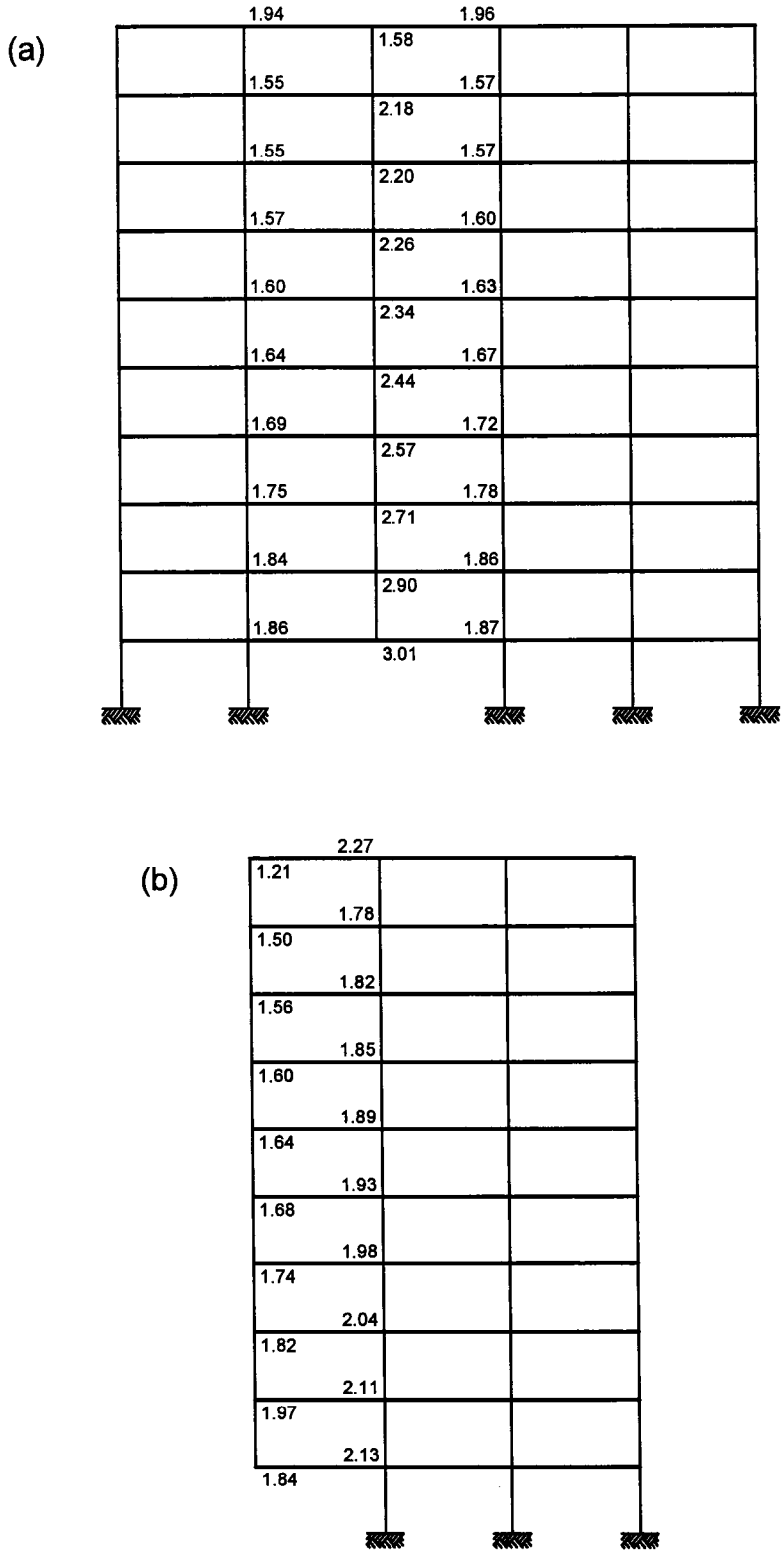

Figure 6.9 Demand/capacity ratios for Case 1 of the progressive collapse analysis of the ductile building: (a) longitudinal frame and (b) transverse frame.

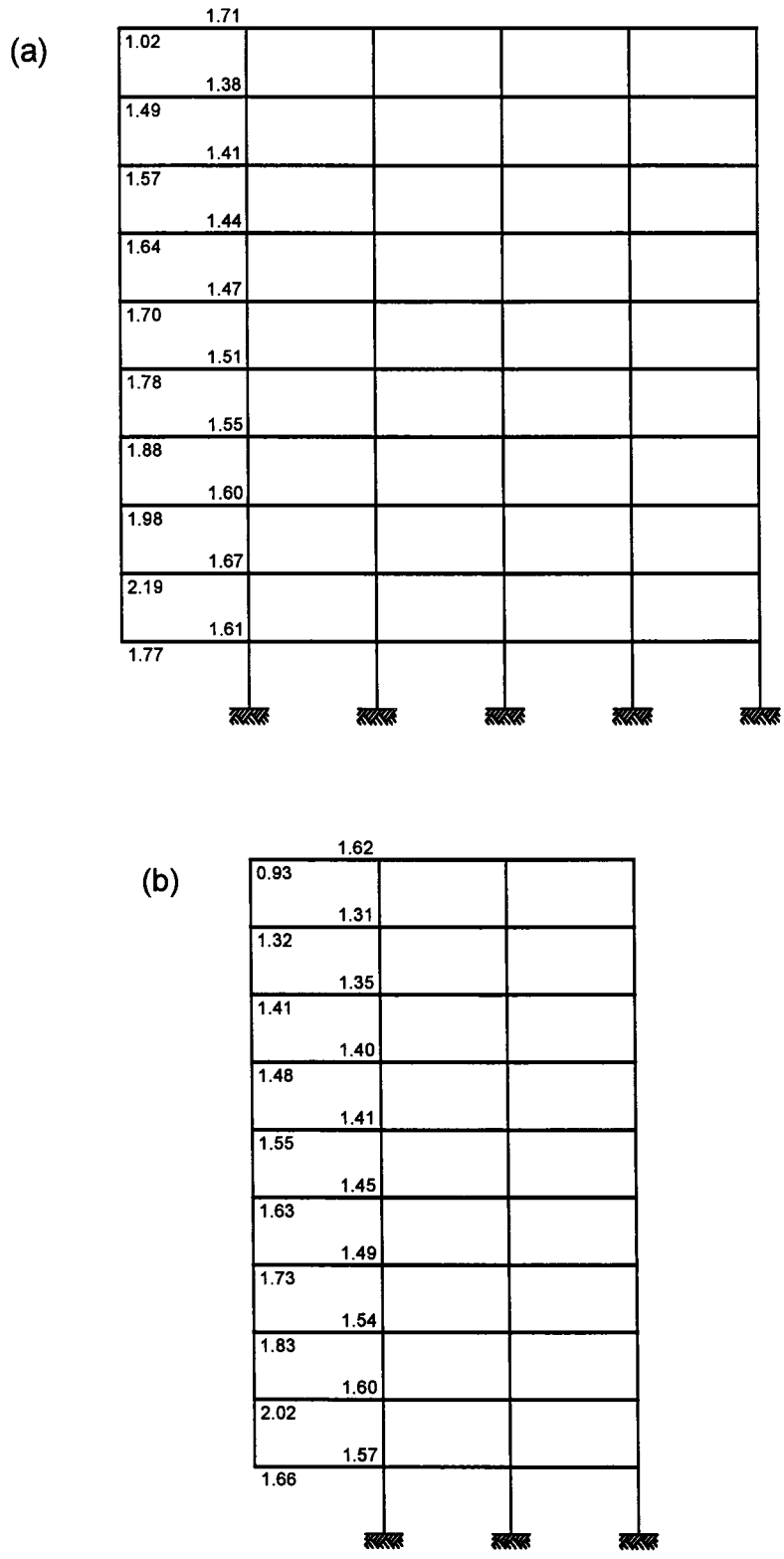

Figure 6.10 Demand/capacity ratios for Case 2 of the progressive collapse analysis of the ductile building: (a) longitudinal frame and (b) transverse frame.

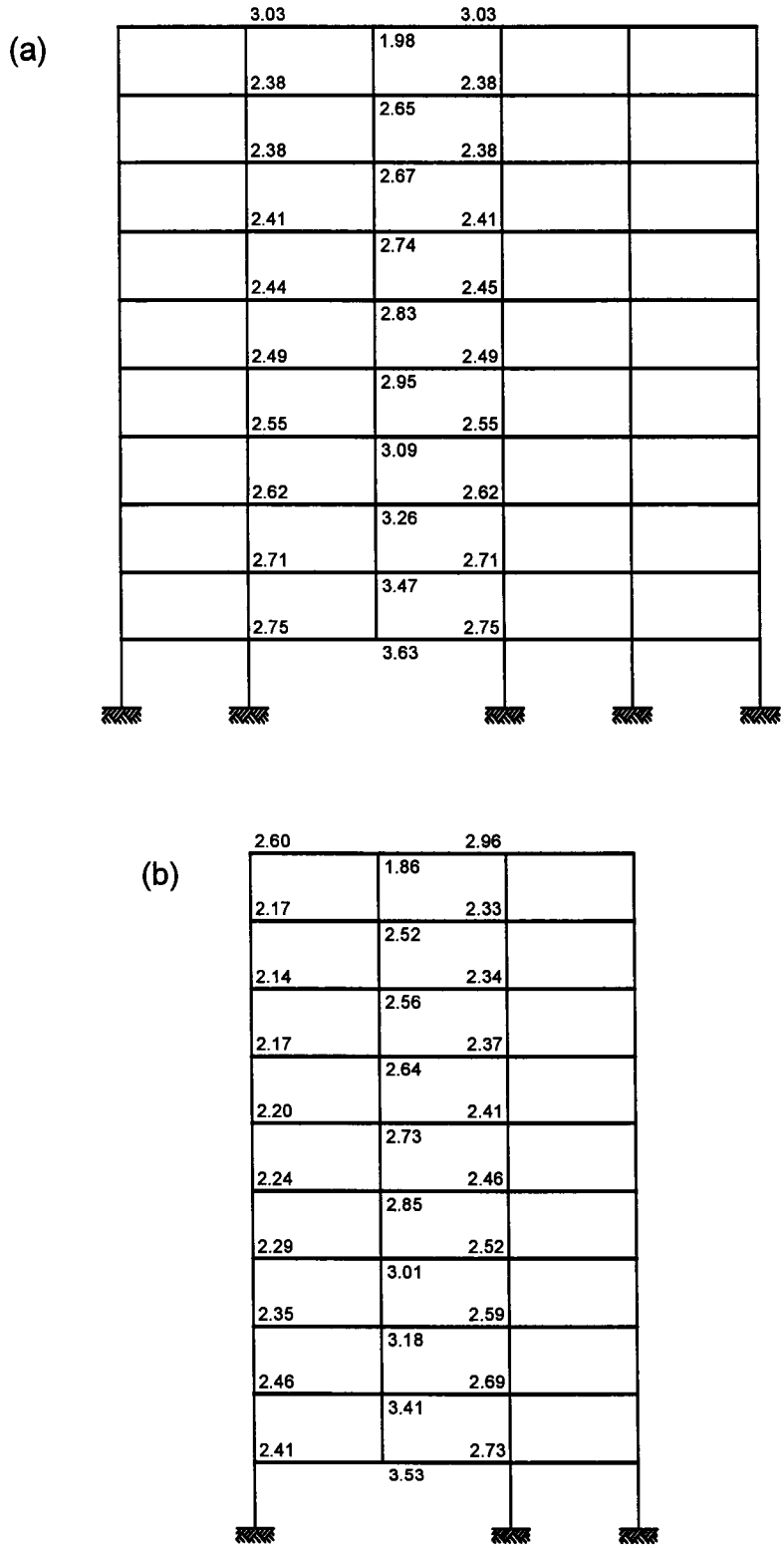

Figure 6.11 Demand/capacity ratios for Case 3 of the progressive collapse analysis of the ductile building: (a) longitudinal frame and (b) transverse frame.

Chapter 7

Discussion and Conclusions

7.1 Discussion

In recent years, the number of terrorist attacks by bombs has increased dramatically around the world. Many buildings have been destroyed and a lot of people have been killed during these attacks. While the issue for the protection from bomb blasts has been considered in the past in the military, no sufficient attention has been paid for civilian structures. Currently, the protection of buildings from bomb blasts is an important topic for the designers, code authorities, and researchers. Substantial work on this issue has been done in the last decade, which resulted in several guidelines for the design and analysis of buildings for blast loads.

The progressive collapse of buildings, which is the most serious consequence of bomb blasts, has also been investigated in recent years. Several guidelines for progressive collapse and analysis are already available. However, much more work is needed in this field.

This study is intended to contribute to the understanding of the behaviour of buildings when subjected to blast loads, and to assess the potential for progressive collapse when columns are lost or severely damaged due to blasts. The objective of this study is:

- to investigate the performance of reinforced concrete frame buildings subjected to blast loads, and
- to assess the vulnerability of such buildings to progressive collapse.

Two buildings designed for Ottawa in accordance with the 2005 edition of the National Building Code of Canada were used to achieve these objectives. One of the buildings was designed as a moderately ductile, and the other one as a ductile frame building. For the purpose of the first objective, nonlinear time history analyses were conducted to the moderately ductile building for a number of bomb blast scenarios. Blast loads resulting from detonations of 125 kg, 250 kg, and 500 kg TNT at distances of 5, 10, 15, 20, 25 and 30 m from the building were used in the analysis. The performance of the building was assessed by considering the interstorey drifts, displacement ductilities, and curvature ductilities obtained from the analysis. The damage levels in this study are defined as significant, moderate, and slight damage. Significant damage is considered to occur when the interstorey drift is larger than 2.5%, and the displacement ductility is larger than 3.5. Moderate damage corresponds to interstorey drifts between 1.0% and 2.5%, and displacement ductility between 1.0 and 3.5. Slight damage is considered when the interstorey drift is less than 1.0% and the displacement ductility is less than 1.0.

Regarding the second objective, both the moderately ductile and the ductile buildings were analysed following the guidelines for progressive collapse analysis and design, prepared by the U.S. General Services Administration (GSA). Columns were removed at the first storey of each building. The following three cases were considered: (i) exterior column removed (at the long side of the building), (ii) corner column removed, and (iii) interior column removed. Elastic static analysis was conducted for each of these cases using 3-D models, and applying loads as required by the GSA guidelines. The demand/capacity ratios (DCR) obtained from the analysis, and the GSA criteria were used for the assessment of the vulnerability to progressive collapse.

7.2 Observations and Conclusions

For clarity, the main observations and conclusions resulting from the analysis of the blast load effects and progressive collapse are summarized separately.

7.2.1 Blast Load Effects

- The effects due to blast loads decreases dramatically with the increase of the distance of the detonation. As an example, interstorey drift resulting from a detonation of 500 kg

TNT at 15 m distance is about 8 times smaller compared to the drift from the same detonation at 5 m distance.

- The largest deformations for all detonations were obtained for the structural members of the first storey. This is expected because the largest blast loads due to hemispherical detonations are at the first storey.

- The results from the analysis for the 125 kg TNT detonations showed that significant damage could occur to the building only from detonations at a distance of 5 m. Detonations at larger distances do not have significant effects on the building.

- A detonation of 250 kg TNT at 5 m would cause significant damage to the first storey columns and beams, and might lead even to collapse of the building. Detonations at 10 m would produce much smaller (moderate) damage, and those at larger distances are not considered as a risk to the building.

- Detonations of 500 kg TNT at 5 m and 10 m could result in substantial damage to the building, and probably collapse. Detonations at distances larger than 10 m would cause moderate to minor damage to the building.

- All the results show that providing a standoff distance of about 15 m would lead to the protection of the building from blast loads for detonations of up to 500 kg TNT. Detonations at distances larger than 15 m would cause moderate to minor damage to the structural members of the building, which can be considered acceptable for extreme loads such as blast loads.

It is important to note that these observations are based on the results for the moderately ductile building analyzed in this study. The findings for another building configuration and design might be different than those summarized above.

7.2.2 Progressive Collapse

- The moderately ductile building is vulnerable to progressive collapse when an interior column at the first storey is removed. Based on the GSA criteria, no progressive collapse is expected when an exterior or corner column is removed.

- The ductile building has a high potential for progressive collapse when any column at the first storey is removed (i.e., exterior, corner, or interior column).

7.3 Recommendations for Future Research

The investigation of the vulnerability of buildings to blast loads and progressive collapse is a new field, and a lot of research is needed. While substantial research has been conducted in the past for military purposes, most of the findings from that research and the software developed are not available for public use. Based on the literature review and the experience during the course of this study, the major topics that should be considered in near future research are as follows:

- Software should be developed specifically for the analysis of structures subjected to blast loads. This is because, as mentioned above, the existing software in the military is not accessible for civilian engineers. The software used in this study, and in general in the engineering community, has been developed for seismic analysis of structures. In order to use this software for blast loads, a number of assumptions need to be made.

- The progressive collapse analysis methods should be evaluated. The General Services Administration Guidelines propose three methods, i.e., linear-elastic static analysis, nonlinear static analysis, and nonlinear dynamic analysis. The most attractive for practical applications is the linear-elastic static method. However, the suitability of the linear-elastic static analysis should be proved by comparing results from that analysis with those from the nonlinear static and the nonlinear dynamic analyses.

- A substantial number of additional analyses on the vulnerability of buildings to blast loads and progressive collapse need to be conducted by considering buildings with

different structural systems and configurations. This would enable making more specific conclusions for a wide range of building structures.

References

ASCE. 1999. Structural design for physical security – State of the practice. American Society of Civil Engineers, Reston, Virginia.

ASCE. 1997. Design of blast resistant buildings in petrochemical facilities. American Society of Civil Engineers. Reston, Virginia.

ASCE. 1985. Design of structures to resist nuclear weapons effects, Manual No. 42. American Society of Civil Engineers, New York.

Baker, W.E. 1973. Explosions in air. University of Texas Press, Austin.

Biggs, J.M. 1964. Introduction to structural dynamics. McGraw-Hill Book Company, New York.

Corley, W.G., Mlakar Sr., P.F., Sozen, M.A., Thronton, C.H.. 1998. The Oklahoma City Bombing: Summary and recommendations for multihazard mitigation. Journal of Performance of Constructed Facilities, Vol. 2, No. 3, American Society of Civil Engineers.

CSA. 1994. CSA Standard A23.3-94 - Design of concrete structures. Canadian Standard Association, Rexdale, Ont.

CSI. 2000. SAP 2000 integrated software for structural analysis and design. Computers and Structures Inc., Berkeley, Calif.

Dincer, E. 2003. Seismic drift demands in reinforced concrete structures. M.A.Sc. thesis, Department of Civil Engineering, University of Ottawa, Ottawa, Ont.

GSA. 2003. Progressive collapse analysis and design guidelines for new federal office buildings and major modernization projects. U.S. General Services Administration, Washington, D.C.

Heidebrecht, A.C., and Naumoski, N. 2002. The influence of design ductility on the seismic performance of medium height reinforced concrete buildings. ACI Special Publication SP-197, American Concrete Institute, Farmington Hills, Mich., pp. 239-264.

Humar, J. 2000. Computer program CURVE – Computation of moment-curvature relations for reinforced concrete members. Department of Civil Engineering, Carleton University, Ottawa, Ont.

Longinow, A., and Mniszewski, K.R. 1996. Protecting buildings against vehicle bomb attacks. Practice Periodical on Structural Design and Construction, Vol. 1, No. 1.

Marchand, K.A., and Alfawakhiri, F. 2005. Facts for steel buildings – Blast and progressive collapse. American Institute of Steel Constructions Inc. (www.aisc.org)

Mays, G.C., and Smith, P.D. (editors). 1995. Blast effects on buildings – Design of buildings to optimize resistance to blast loading. Thomas Telford Services Ltd., London, England.

National Academy of Science, National Research Centre. 1995. Protecting buildings from bomb damage – Transfer of blast-effects mitigation technologies from military to civilian applications. National Academy Press, Washington, D.C.

NAVFAC. 1990. Army Manual TM5-1300 - Structures to resist the effects of accidental explosions. Department of the Army, the Navy, and the Air Force, Washington, DC.

NBCC. 2005. National Building Code of Canada 2005. Institute for Research in Construction, National Research Council of Canada, Ottawa, Ont.

Paulay, T., and Priestley, M.J.N. 1990. Seismic design of reinforced concrete and masonry buildings. John Wiley & Sons, Inc., New York.

Prakash, V., Powell, G.H., and Campbell, S. 1993. DRAIN-2DX, Base program description and user guide. University of California, Berkeley, Calif.

Saatcioglu, M. 2004. Notes of the graduate course "Advanced Reinforced Concrete Design", Department of Civil Engineering, University of Ottawa, Ottawa, Ont.

Saatcioglu, M. 2000. Rc-Section – Computer program for the computation of moment-curvature relationships for reinforced concrete members. Department of Civil Engineering, University of Ottawa, Ottawa, Ont.

Shankar, R. 2004. Progressive collapse basics. American Institute of Steel Construction Inc., 10 pp. (www.aisc.org)

Takeda, T., Sozen, M. A. and Nielsen, N. N., 1970. Reinforced Concrete Response to Simulated Earthquakes, Journal of the Structural Division, ASCE, Vol. 96, No. ST12, pp. 2557-2573.

U.S. Departments of the Army, the Navy, and the Air Force. 1990. Structures to resist the effects of accidental explosions. TM5-1300 Manual, Washington, D.C.

U.S. Department of Defense. 2005. Unified facilities criteria (UFC) – Design of buildings to resist progressive collapse, UFC 4-023-03. U.S. Department of Defense, Washington, D.C.